

# UC Riverside

## UC Riverside Electronic Theses and Dissertations

### Title

Population Genomics of *Phytophthora citrophthora* and *P. syringae* from Citrus in California, Expanded Baseline Sensitivities of These Species to New Fungicides, and Mobility of Mandipropamid in Citrus Plants

### Permalink

<https://escholarship.org/uc/item/5xb7p6f2>

### Author

Riley, Nathan Michigan

### Publication Date

2023

Peer reviewed|Thesis/dissertation

UNIVERSITY OF CALIFORNIA  
RIVERSIDE

Population Genomics of *Phytophthora citrophthora* and *P. syringae* from Citrus in California, Expanded Baseline Sensitivities of These Species to New Fungicides, and Mobility of Mandipropamid in Citrus Plants

A Dissertation submitted in partial satisfaction  
of the requirements for the degree of

Doctor of Philosophy

in

Plant Pathology

by

Nathan Michigan Riley

December 2023

Dissertation Committee:

Dr. James Adaskaveg, Chairperson

Dr. Patricia Manosalva

Dr. Howard Judelson

Copyright by  
Nathan Michigan Riley  
2023

The Dissertation of Nathan Michigan Riley is approved:

---

---

---

Committee Chairperson

University of California, Riverside

## ACKNOWLEDGEMENTS

Chapter I in its entirety is reprinted with permission as it appears in Riley, N.M., Förster, H., Adaskaveg, J.E. 2023. Diversity and clonality in populations of *Phytophthora citrophthora* and *P. syringae* causing brown rot of citrus in California. *Phytopathology. Submitted.* Chapter II in its entirety is reprinted with permission as it appears in Riley, N.M., Förster, H., Adaskaveg, J.E. 2023. Regional comparisons of sensitivities of *P. citrophthora* and *P. syringae* causing citrus brown rot in California to four new and two older fungicides. *Plant Disease. Submitted.* Chapter III in its entirety is reprinted with permission as it appears in Belisle, R.J., Hao, W., Riley, N., Förster, H., Adaskaveg, J.E. 2023. Root absorption and limited mobility of mandipropamid as compared to oxathiapiprolin and mefenoxam after soil treatment of citrus plants for managing *Phytophthora* root rot. *Plant Disease.* 107:1107-1114. Financial support for Chapters I, II, and III was provided by the California Citrus Research Board (CRB). A special thanks to Syngenta Crop Protection, Valent USA, and Luxembourg Industries Ltd. for donating fungicides used in Chapters II and III.

I was honored to receive additional funding through the Dean's Distinguished Fellowship Award (2017) and the Leo J. Klotz Memorial Endowment Fund Travel Grant (2022).

Firstly, I would like to thank my advisor, Dr. James E. Adaskaveg, for his guidance and support throughout my time in the graduate program. I'd also like to thank Dr. Helga Förster, whose expertise and advice was invaluable, especially regarding writing. Their love of science and dedication to the growers and industries that their

research supports have been a constant inspiration to me, and working with Dr. Adaskaveg and Dr. Förster has given me the opportunity to learn from true professionals. I will always be grateful to them for their help and wisdom, and for allowing me to work alongside them.

I'd also like to thank my committee members Dr. Patricia Manosalva and Dr. Howard Judelson for their insight, advice, and guidance throughout their years of serving on both my qualifying and dissertation committees. Thank you to Mark Brandenburg of Helena Agri-Enterprises, LLC for his assistance in orchard sampling. I'd like to acknowledge my collaborators and former Adaskaveg lab members Dr. Wei Belisle and Dr. Rodger Belisle for their assistance with my projects as well as the opportunities I had to learn from them during our time working together. I'd also like to acknowledge our lab supervisor Zayne, whose support and dedication to lab security will always be appreciated. To all other current and former lab members that I've had the pleasure of working with, I will always be grateful for your companionship and advice.

I want to thank my colleague and fellow member of the Fall 2017 cohort Aidan Shands, for his patience and generosity in passing on his knowledge of genomics and bioinformatics to me. In addition to his help at work, I will be forever grateful for his friendship. The days we spent playing disc golf together with our close friend Ryan Pimentel have been a highlight of my time in graduate school, and I look forward to many more rounds in the future.

To my roommate Ben Hoyt and my close friend Valentina Valencia, thank you for your friendship, advice, and kindness. Your support in the final years of my time here has

been truly appreciated, and I can't express my gratitude enough. To my friends Chris Drozd, Colin Todd, Lindsey Pedroncelli-Gietzen, Gabriel Ortiz, Chien-hao Tseng, and Nathan McLain, as well as all of my other colleagues in the PLPA program, thank you for your friendship and the camaraderie we have shared in our time together at UCR. I treasure all the memories we have made, and I am so excited to see what the future has in store for all of us.

I would like to give a special thank you to Annie Montes, who was my first mentor when I began doing research as an undergraduate at the University of Maryland. I will always be grateful for everything you taught me, and for introducing me to the research I have come to love. I'd also like to acknowledge my friend Adam Adaskaveg, for the time he spent working with me as an undergraduate and his assistance with my experiments. I feel that I learned as much from you as you did from me during our time working together, and it has truly been a pleasure seeing you continue to grow as a scientist ever since.

I'd like to thank my parents George and Pamela Riley, my siblings Collin and Kate, as well as my grandparents Alice, Keith, Roseann, and George for their love and support throughout my life, and without whom I would not be the person I am today. Though separated by much distance during my time in graduate school I have always been able to rely on the support of my family, and for that I am eternally thankful.

Finally, to the light of my life, my second half, my partner, Dr. Sara Dorhmi: words cannot adequately express how grateful I am that graduate school brought us together. Your keen intellect and love for science have always further ignited my passion

for the work that we do. Thank you for your patience, support, and love during the times that I have needed it most. You have been an inspiration to me throughout our time together, and I am so proud of everything that we have both accomplished. I am so excited to be starting this next chapter of my life with you, and I cannot wait to see what the future holds for us.

To everyone mentioned in these acknowledgements, I'd like to offer some final words of gratitude: graduate school can be isolating, difficult, and frustrating at times, but thanks to all of you this experience has also been fulfilling, exciting, and fun. With deepest sincerity, thank you!



## DEDICATION

This dissertation is dedicated to my late aunt Meridith Riley, as well as my partner Sara Dorhmi and my friends and family, whose love and support have always been there for me in both the highs and the lows of my time in graduate school.

## ABSTRACT OF THE DISSERTATION

Population Genomics of *Phytophthora citrophthora* and *P. syringae* from Citrus in California, Expanded Baseline Sensitivities of These Species to New Fungicides, and Mobility of Mandipropamid in Citrus Plants

by

Nathan Michigan Riley

Doctor of Philosophy, Graduate Program in Plant Pathology  
University of California, Riverside, December 2023  
Dr. James E. Adaskaveg, Chairperson

*Phytophthora citrophthora* and *P. syringae* are currently the major brown rot pathogens of citrus in California. The diversity and structure of populations of these species have never been characterized using genomic techniques. Recently, ethaboxam, fluopicolide, mandipropamid, and oxathiapiprolin have been registered or are pending registration to manage *Phytophthora* diseases of citrus, whereas others currently used include mefenoxam and potassium phosphite. We evaluated *Phytophthora* populations in three growing regions for fungicide sensitivity and resistance potential using traditional and genomic methods and studied the mobility of mandipropamid in citrus plants. The results of this dissertation are presented in three chapters: 1) genomic characterization of populations of *Phytophthora citrophthora* and *P. syringae* causing brown rot of citrus in California; 2) regional comparisons of sensitivities of these *Phytophthora* spp. to six

fungicides; and 3) mobility of mandipropamid in citrus plants as compared to oxathiapiprolin and mefenoxam. Genomic analyses of isolates of both species in California identified regional differentiation of populations. *P. citrophthora* (heterothallic but unlikely to reproduce sexually) was found to have a clonal to semi-clonal population structure with low levels of diversity within and among sub-groups. In contrast, the population structure of the homothallic *P. syringae* was also clonal to semi-clonal, but isolates were placed into four main clusters of much higher diversity which indicates common sexual reproduction. *P. syringae* isolates collected from non-citrus hosts were found to be distinct from those from citrus, suggesting that isolates from non-citrus hosts are not contributing to brown rot of citrus. Regional comparisons of sensitivities of isolates of both species to new Oomycota fungicides expanded the previously established baselines. Population genomics analyses identified *P. citrophthora* and *P. syringae* isolates from the southern growing regions to have an increased risk for resistance development to mandipropamid and ethaboxam, respectively. Studies on the mobility of mandipropamid showed that it has limited acropetal mobility. The fungicide was absorbed by the roots and translocated at low levels into stem and leaf tissues of young plants, but not back into untreated roots (i.e., no basipetal movement). Oxathiapiprolin had similar acropetal mobility, whereas the previously described limited ambimobile properties of mefenoxam were confirmed.

## TABLE OF CONTENTS

GENERAL INTRODUCTION.....	1
Literature cited.....	9
CHAPTER I: Diversity and Clonality in Populations of <i>Phytophthora citrophthora</i> and <i>P. syringae</i> Causing Brown Rot of Citrus in California	
Abstract.....	13
Introduction.....	14
Materials and Methods.....	16
Results.....	21
Discussion.....	27
Literature cited.....	34
Tables and Figures.....	38
CHAPTER II: Regional Comparisons of Sensitivities of <i>P. citrophthora</i> and <i>P. syringae</i> Causing Citrus Brown Rot in California to Four New and Two Older Fungicides	
Abstract.....	50
Introduction.....	51
Materials and Methods.....	53
Results.....	57
Discussion.....	61
Literature cited.....	66

Tables and Figures.....	70
CHAPTER III: Root Absorption and Limited Mobility of Mandipropamid as Compared to Oxathiapiprolin and Mefenoxam After Soil Treatment of Citrus Plants for Managing Phytophthora Root Rot	
Abstract.....	78
Introduction.....	79
Materials and Methods.....	82
Results.....	90
Discussion.....	94
Literature cited.....	99
Figures.....	103
GENERAL CONCLUSION.....	108

## LIST OF TABLES

### CHAPTER I

<b>Table 1.1</b> Isolates of <i>Phytophthora</i> spp. from California used in this study, their host, geographic origin, and year of isolation .....	38
<b>Table 1.2</b> QUASt output for reference genome assemblies of <i>Phytophthora citrophthora</i> and <i>P. syringae</i> .....	39
<b>Table 1.3</b> BUSCO output for reference genome assemblies of <i>Phytophthora citrophthora</i> and <i>P. syringae</i> .....	40
<b>Table 1.4</b> Average index of association ( $I_A$ ) for simulated and actual datasets for overall and regional populations of <i>Phytophthora citrophthora</i> and <i>P. syringae</i> .....	41
<b>Table 1.5</b> Summary statistics for the genetic diversity of the overall population and geographic sub-populations of <i>Phytophthora citrophthora</i> and <i>P. syringae</i> .....	42
<b>Table 1.6</b> Genetic distance statistics of <i>Phytophthora citrophthora</i> and <i>P. syringae</i> .....	43

### CHAPTER II

<b>Table 2.1</b> Isolates of <i>Phytophthora</i> spp. from citrus fruit with brown rot in California used in this study, their geographic origin, and year of isolation .....	70
<b>Table 2.2</b> In vitro sensitivities of mycelial growth of isolates of <i>Phytophthora citrophthora</i> from three major citrus growing regions in California to six Oomycota fungicides.....	71
<b>Table 2.3</b> In vitro sensitivities of mycelial growth of isolates of <i>Phytophthora syringae</i> from three major citrus growing regions in California to six Oomycota fungicides.....	72

## LIST OF FIGURES

### CHAPTER I

**Figure 1.1. A, B,** Principal component analyses (PCA) and **C, D,** discriminant analyses of principal components (DAPC) visualizing the observed variance of **A, C,** *P. citrophthora* and **B, D,** *P. syringae* isolates grouped by geographic region. CV = Central Valley; IE = Inland Empire; VE = Ventura County.....44

**Figure 1.2. A,** Principal Component analysis (PCA) and **B,** discriminant analysis of principal components (DAPC) to visualize observed variance of *P. syringae* isolates grouped by host. LL = citrus leaf litter (LL\* = all LL isolates are within this cluster).....45

**Figure 1.3.** Population structure of *P. citrophthora* visualized in UPGMA dendrograms that were constructed from observed variants and aligned to bar plots of the fastStructure output for each isolate. In the legend, color codes of the symbols refer to geographic origin of the isolates (CV = Central Valley; IE = Inland Empire; VE = Ventura Co.) In the fastStructure graphs, colors within a given bar represent the posterior membership probability of the isolate to be assigned to the predicted clusters that are color-coded in the squares of the legend.....46

**Figure 1.4.** Population structure of *P. syringae* visualized in UPGMA dendrograms that were constructed from observed variants and aligned to bar plots of the fastStructure output for each isolate. In the legend, color codes of the symbols refer to geographic origin of the isolates (CV = Central Valley; IE = Inland Empire; VE = Ventura Co.) In the fastStructure graphs, colors within a given bar represent the posterior membership probability of the isolate to be assigned to the predicted clusters that are color-coded in the squares of the legend.....47

**Figure 1.5.** Minimum spanning networks visualizing relationships of **A,** *P. citrophthora* and **B,** *P. syringae* isolates grouped by region (CV = Central Valley, IE = Inland Empire; VE = Ventura Co.). Nodes represent individual multilocus genotypes (MLGs). The distance scale represents bitwise distance (connecting lines) over all loci in a MLG. The size differences of the circles represent the number of individuals within that MLG.....48

**Figure 1.6.** Minimum spanning network visualizing relationships of *P. syringae* grouped by host type. Nodes represent individual multilocus genotypes (MLGs). The distance scale represents bitwise distance (connecting lines) over all loci in a MLG. The size differences in the circles represent the number of individuals within that MLG.....49

## CHAPTER II

**Figure 2.1.** Frequency histograms of EC<sub>50</sub> values of *P. citrophthora* to **A**, ethaboxam, **B**, fluopicolide, **C**, mandipropamid, **D**, oxathiapiprolin, **E**, mefenoxam, and **F**, potassium phosphite. Bar height indicates the number of isolates within each bin, and bin width was calculated based on Scott (1979). Bars are color-coded based on the geographic origin of isolates (CV = Central Valley; IE = Inland Empire; VE = Ventura Co.).....73

**Figure 2.2.** Frequency histograms of EC<sub>50</sub> values of *P. syringae* to **A**, ethaboxam, **B**, fluopicolide, **C**, mandipropamid, **D**, oxathiapiprolin, **E**, mefenoxam, and **F**, potassium phosphite. Bar height indicates the number of isolates within each bin, and bin width was calculated based on Scott (1979). Bars are color-coded based on their geographic origin of isolates (CV = Central Valley; IE = Inland Empire; VE = Ventura Co.).....74

**Figure 2.3.** Population structure of *P. citrophthora* visualized in UPGMA dendrograms that were constructed from observed variants and aligned to sensitivity to ethaboxam (Eth), fluopicolide (Flu), mandipropamid (Man), oxathiapiprolin (Oxa), mefenoxam (Mef), and potassium phosphite (Kph). Bootstrap percentages (BP) are shown at the nodes of the dendrogram as BP  $\geq 95$ ,  $70 \leq BP < 95$ , and BP  $< 70$ . fastStructure (fS) cluster membership probability is shown for each isolate with K=2 for *P. citrophthora* and K=4 for *P. syringae*. In the legend, color codes of the circles refer to geographic origin of the isolates (CV = Central Valley; IE = Inland Empire; VE = Ventura Co.). Fungicide sensitivity is color-coded for the new fungicides as below, within, and above baselines and for the older fungicides as sensitive, moderately resistant, and resistant as compared to previously determined values for CV isolates (Gray et al. 2018). In the fastStructure graphs, colors within a given bar represent the posterior membership probability of the isolate to be assigned to the predicted genetic clusters that are color-coded in the squares of the legend.....75

**Figure 2.4.** Population structure of *P. syringae* visualized in UPGMA dendrograms that were constructed from observed variants and aligned to sensitivity to ethaboxam (Eth), fluopicolide (Flu), mandipropamid (Man), oxathiapiprolin (Oxa), mefenoxam (Mef), and potassium phosphite (Kph). Bootstrap percentages (BP) are shown at the nodes of the dendrogram as BP  $\geq 95$ ,  $70 \leq BP < 95$ , and BP  $< 70$ . fastStructure (fS) cluster membership probability is shown for each isolate with K=2 for *P. citrophthora* and K=4 for *P. syringae*. In the legend, color codes of the circles refer to geographic origin of the isolates (CV = Central Valley; IE = Inland Empire; VE = Ventura Co.). Fungicide sensitivity is color-coded for the new fungicides as below, within, and above baselines and for the older fungicides as sensitive, moderately resistant, and resistant as compared to previously determined values for CV isolates (Gray et al. 2018). In the fastStructure graphs, colors within a given bar represent the posterior membership probability of the



isolate to be assigned to the predicted genetic clusters that are color-coded in the squares of the legend.....76

**Fig. 2.5.** Principal component analyses (PCA) of fungicide sensitivity of **A, B, P. citrophthora** to **A**, mandipropamid and **B**, potassium phosphite and **C, D, P. syringae** isolates to **C**, ethaboxam, and **D**, potassium phosphite grouped by fungicide sensitivity (i.e., within or above baseline for mandipropamid and ethaboxam or sensitive, moderately resistant, or resistant for potassium phosphite) as compared to previously determined values for CV isolates (Gray et al. 2018).....77

### CHAPTER III

**Figure 3.1. A,** Inhibition zones of mycelial growth of *Phytophthora citrophthora* in a bioassay with standard amounts of (starting clockwise from the asterisk) 0.01, 0.05, 0.1, 0.25, or 0.4 µg mandipropamid/disk after two days of incubation at 25°C, and **B,** regressions of mean inhibition zones of mycelial growth on amounts of mandipropamid.....103

**Figure 3.2.** Mandipropamid concentrations measured **A**, in a bioassay, and **B**, in the same extracts by high-performance liquid chromatography tandem mass spectrometry (HPLC-MS/MS) in root, stem, and leaf extracts of potted 6- to 7-month-old citrus plants 1, 2, 3, or 4 weeks after soil applications with mandipropamid. The primary vertical axis is used for root extracts, and the secondary vertical axis is used for stem and leaf extracts. Bars followed by the same letter for each sampling time are not significantly different according to a generalized linear mixed model using the PROC GLIMMIX procedure and least square treatment means with the Tukey-Kramer adjustment.....104

**Fig. 3.3.** Regression of log<sub>10</sub>-transformed concentrations of mandipropamid in **A**, root extracts and **B**, stem extracts determined by high-performance liquid chromatography tandem mass spectrometry (HPLC-MS/MS) on those calculated from bioassays. For the bioassays, fungicide amounts were calculated using the standard curve equation  $y = 0.7522x + 1.8249$ .....105

**Fig. 3.4.** Fungicide concentrations in root extracts of 10-month-old split-root-potted citrus plants where soil of one pot of each plant was treated (T) with **A**, mandipropamid, **B**, oxathiapiprolin, or **C**, mfenoxam, and soil in the other pot was not treated (UT). Roots were sampled 4 weeks after fungicide applications. Fungicide amounts were determined based on mean inhibition zones of mycelial growth of *Phytophthora citrophthora* in a bioassay and calculated standard curve equations. Bars followed by the same lowercase letter for each fungicide are not significantly different according to a generalized linear mixed model using the PROC GLIMMIX procedure and least square treatment means with the Tukey-Kramer adjustment.....106

**Fig. 3.5.** Fungicide concentrations in root extracts of citrus trees from a field study where half of each circular basin around the trunk was treated with soil applications of **A**, mandipropamid, **B**, oxathiapiprolin, or **C**, mefenoxam, and the other half was not treated. Roots were sampled 2, 4, and 8 weeks after application. Fungicide amounts were determined based on mean inhibition zones of mycelial growth of *Phytophthora citrophthora* in a bioassay and calculated standard curve equations. Bars followed by the same lowercase letter for each fungicide or by the same uppercase letter for each sampling time in the tables are not significantly different according to a generalized linear mixed model using the PROC GLIMMIX procedure and least square treatment means with the Tukey-Kramer adjustment.....107

## GENERAL INTRODUCTION

Citrus is an important crop in many countries with sub-tropical and tropical environments, and worldwide production was estimated at 143,755,600 metric tons of fruit in 2020 (FAO 2021). In California, citrus production was valued at \$2.5 billion in 2021/22 (Anonymous 2022). The California citrus industry expanded from the first commercial orchard in Los Angeles in 1841 to other southern portions of the state. Following World War II, widespread urbanization and rising property values coupled with the occurrence of Citrus Tristeza Virus gradually pushed most citrus production North (Geisseler and Horwath 2016). Currently, most of the citrus production is in the Central Valley (CV), particularly in Fresno, Kern, and Tulare Co. The remaining production is primarily in the original growing areas of southern California in the Inland Empire (IE - Riverside and San Bernardino Co.), as well in coastal Ventura Co. (VE), San Diego Co. and Imperial Co. (Geisseler and Horwath 2016).

Citrus in California is affected by many diseases, including field diseases such as Huanglongbing, Citrus Tristeza Virus, anthracnose, and Armillaria root rot, as well as postharvest fruit diseases such as green mold, blue mold, and sour rot (Adaskaveg and Förster 2014). Diseases caused by members of the genus *Phytophthora*, organisms in the phylum Oomycota belonging to the Kingdom Stramenopila, present a complex problem for citrus growers due to their ability to affect plants from their propagation in the nursery to tree maturity in the orchard. Newly germinated seedlings may be affected by damping-off, whereas *Phytophthora* root rot can cause reduced growth and even death of plants in the nursery and during orchard establishment, and cause tree decline and reduce

production in mature orchards (Graham and Feichtenberger 2015). Additional *Phytophthora* diseases of citrus include foot rot and gummosis affecting tree crowns and trunks, as well as brown rot of fruit. Brown rot typically infects low hanging fruit of trees, and non-visible infections of harvested fruit may develop during transportation and storage and spread to adjacent non-infected fruit in shipping containers. In California, *P. citrophthora* (R. E. Sm. & E. H. Sm.) Leonian and *P. syringae* (Kleb.) Kleb. are the primary species causing brown rot of citrus (Hao et al. 2018a), while in other growing regions *P. palmivora* (E.J. Butler) E.J. Butler, *P. nicotianae* Breda de Haan (syn. *P. parasitica* Dastur), and sometimes *P. citricola* Sawada are more prevalent (Erwin and Ribeiro 1996; Graham et al. 1998). The two main causal agents of *Phytophthora* root rot of citrus in California are *P. nicotianae* which is mostly active during the warmer months of the year and *P. citrophthora* (Erwin and Ribeiro 1996) that is active year-round (Hao et al. 2018a). The species contributing to brown rot of citrus in California are slightly more varied, with *P. citrophthora* and *P. nicotianae* listed as the major pathogens, whereas *P. syringae* and *P. hibernalis* Carne have been considered of minor importance in the past (Feld et al. 1979; Graham and Menge 2000; Klotz 1978). More recently, however, *P. citrophthora* and *P. syringae* were demonstrated to be the major pathogens (Hao et al. 2018a). In other citrus producing regions such as Florida, additional species such as *P. palmivora* and *P. nicotianae* and sometimes *P. citricola* have been found to be the pathogens responsible for brown rot (Graham and Menge 2000, 1999).

The shift in species composition of brown rot pathogens in California has caused trade restrictions for the California citrus industry by China, a major export country

where *P. hibernalis* and *P. syringae* are quarantine pathogens (Hao et al. 2018a). Export of California citrus fruit to China was closed from 2013 to 2014 and again in 2015 due to the detection of *P. syringae* and *P. hibernalis* in orange fruit shipments, resulting in economic loss to growers, packinghouses, and shippers (Adaskaveg and Förster 2014). The status of *P. syringae* and *P. hibernalis* as quarantine pathogens has elevated brown rot of citrus from a troublesome inconvenience to a serious problem over the past decade, and the factors contributing to the rise of *P. syringae* as a major pathogen causing brown rot are not well understood.

In order to improve our understanding of and ability to manage Phytophthora diseases on citrus in California, characterization of the populations involved is essential. Population genomic analyses have recently been utilized on other *Phytophthora* species such as *P. pluvialis* Reeser, W. Sutton & E.M. Hansen (Tabima et al. 2021), *P. capsici* Leonian (Vogel et al. 2020), and *P. infestans* deBary (Zhang et al. 2021) to investigate population structure, fungicide sensitivity, and pathogen adaptation. This research can be invaluable in identifying populations with greater diversity or clonality and identifying other potential sources of the pathogen, such as other hosts. Further characterization of the sensitivity of these populations to the new chemicals, as performed by Gray et al. (2018) and Hao et al. (2021), can provide yet more information when coupled with genomic analysis. Assessing the sensitivity in previously unsampled IE and VE growing regions would not only give us a more accurate understanding of sensitivity throughout the state of California, but also aid in identifying regions and populations which may be at greater risk for resistance development. Finally, the characterization of the mobility of

mandipropamid within citrus plants would allow us to make better informed decisions regarding how, when, and why mandipropamid is applied to plants.

Management strategies to maintain the productivity of citrus orchards in the presence of *Phytophthora* pathogens include cultural practices and chemical treatments. Integrated management strategies involve the planting of tolerant rootstocks (trifoliolate orange and Swingle citrumelo; Graham 1995), as well as other cultural practices such as proper irrigation and skirting of trees coupled with the application of various Oomycota-targeted fungicide compounds (Adaskaveg and Förster 2022). Fungicides are categorized according to their mode of action by the Fungicide Resistance Action Committee, referred to as FRAC codes (FCs; FRAC 2022). For management of root rot, two fungicide modes of actions have been primarily used in the past, the phenylamides (FC 4) such as metalaxyl and mefenoxam, and the phosphonates (FC P07/33) such as fosetyl-Al and potassium phosphite (Hao et al. 2018b). For preharvest control of fruit brown rot, Bordeaux mixture (copper sulfate and hydrated lime) or other neutral-copper based products (FC M1) have been widely used for many years, and the previously mentioned phosphonates have been used since the 1980s (Adaskaveg and Förster 2014). For postharvest treatment of the fruit, heated potassium phosphite applications are used, sometimes in combination with imazalil and thiabendazole (TBZ) to control not only brown rot but also *Penicillium* decays (Adaskaveg and Förster 2015), however, international maximum residue limits (MRLs) are lacking in many countries that results in limited postharvest use of phosphite compounds.

The compounds that have historically been used to control Phytophthora diseases of citrus are not without their drawbacks. Copper products have become less popular in recent times due to phytotoxicity (Alva et al. 1993; Hippler et al. 2018) and potential environmental contamination of soil and watersheds, while overuse of phosphonates to control infections of the fruit and trunk, as well as overuse of phosphonates and phenylamides to control infections of the roots, have led to the development of resistance in target populations (Adaskaveg et al. 2017; Timmer et al. 1998). Because of this, efforts have been made in recent years to increase the number of compounds with unique modes of action registered for use on citrus in California. Recently registered compounds include the benzamide fluopicolide (FC 43), the carboxylic acid amide mandipropamid (FC 40), and the piperidinyl thiazole isoxazoline oxathiapiprolin (FC 49), whereas registration of the thiazole carboxamide ethaboxam (FC 22) is currently pending (Blum et al. 2010; Gray et al. 2018; Jiang et al. 2015; Pasteris et al. 2016; Uchida et al. 2005).

The registration of these relatively new compounds for use on citrus represents a concerted collaborative effort between fungicide registrants and academic labs with the goal of creating a diverse range of compounds with different modes of action that can be used in multi-year rotations to extend the viable life of each of the compounds involved. Like many other modern fungicides, all four new compounds have single-site modes of action, and therefore, development of resistance in target populations is a constant concern. If a given single-site mode of action compound is adopted too widely and/or too quickly, the risk and rate of resistance development can be very high, similar to the “boom and bust” phenomenon that has been observed in the breeding of plants for R-

gene mediated resistance to pathogens (Pink and Puddephat 1999). Point mutations conferring resistance to mefenoxam, as well as to all four of the newly registered compounds have been identified in *Phytophthora* species or other related organisms in the Oomycota (Blum et al. 2010, Dai et al. 2023 (Preprint), Marin et al. 2023, Peng et al. 2019, Wang et al. 2022) These new compounds have only recently been registered (or are currently pending registration - ethaboxam) on citrus, some have been previously been registered for use on other crops in California. Thus, increased vigilance in assessing potential resistance risk and monitoring target populations for resistance development is warranted. Baseline sensitivities of *Phytophthora* spp. affecting citrus in California to these new chemicals were previously established, and sensitivity to the phenylamide mefenoxam and to potassium phosphite was characterized (Gray et al. 2018; Hao et al. 2021). These latter studies focused on isolates originating from the CV region of California. In the current study, the focus was to collect and evaluate isolates of *Phytophthora* spp. from the IE and VE to expand information on fungicide sensitivity to previously unsampled citrus-producing regions of California.

Due to the ability of *Phytophthora* spp. to attack different parts of citrus plants throughout their life cycle, the properties of a fungicide formulation that allow it to be absorbed into plant tissues and be translocated to other parts of the plant via the vascular system are very important in determining best practices for its use. Acropetal systemic movement of oxathiapiprolin in annual crops (Cohen 2015) and citrus plants (Gray et al. 2020) has been demonstrated previously. For citrus, uptake of the fungicide at low but sufficient concentrations into plant roots provided an explanation for its long-lasting high



activity in the management of Phytophthora root rot. The mobility of mandipropamid in plants has not been studied previously, and this information is important to understand its protective and eradivative activities against diseases caused by *Phytophthora* spp. and to provide information on the best strategies for field usage of this compound.

Thus, the objectives of Chapter I of this dissertation were to: 1) collect isolates of *P. syringae* and *P. citrophthora* from citrus production areas of California not previously surveyed by Hao et al. 2018a; 2) characterize the population structure of these species and determine if populations sampled from different geographic regions are genetically distinct; and 3) determine if isolates of *P. syringae* from non-citrus hosts are genetically distinct from those collected from citrus. For Chapter II, the objectives were to: 1) evaluate selected *P. citrophthora* and *P. syringae* isolates from southern growing regions (i.e., IE and VE) for their sensitivity to the new fungicides ethaboxam, fluopicolide, mandipropamid, and oxathiapiprolin as compared to the older compounds mefenoxam and potassium phosphite; 2) compare them to selected isolates from the CV previously evaluated (Gray et al. 2018; Hao et al. 2021) to establish expanded sensitivity ranges; and 3) utilize population genomic analyses to identify populations and regions with increased potential for development of resistance. The objectives for Chapter III were to: 1) determine whether mandipropamid is taken up by roots and translocated to stems and leaves of citrus plants after soil application; 2) determine if concentrations of the fungicide inside the plant are high enough to be effective against *Phytophthora* species causing root rot; and 3) evaluate if mandipropamid in comparison with mefenoxam is ambimobile and is translocated from treated roots to nontreated parts of the root system at

inhibitory levels to *Phytophthora* spp. so that it could be used in pre- and post-infection applications to manage the disease.

## LITERATURE CITED

- Adaskaveg, J. E., and Förster, H. 2014. Integrated postharvest strategies for management of *Phytophthora* brown rot of citrus in the United States. Pages 123-131 in: Postharvest Pathology, Plant Pathology in the 21st Century. D. Prusky and M. L. Gullino, eds. Springer International Publishing, Cham, Switzerland.
- Adaskaveg, J. E., and Förster, H. 2015. Resistance in postharvest pathogens of citrus in the United States. Pages 449-466 in: Fungicide resistance in plant pathogens: Principles and a guide to practical management. H. Ishii and D. Hollomon, eds. Springer, New York, NY. [https://doi.org/10.1007/978-4-431-55642-8\\_28](https://doi.org/10.1007/978-4-431-55642-8_28)
- Adaskaveg, J. E., and Förster, H. 2022. APS Book. Postharvest diseases of citrus. Pages 403-422 in: Postharvest Pathology of Fruit and Nut Crops – Principles, Concepts, and Management Practices. J. E. Adaskaveg, H. Förster, and D. B. Prusky, eds. American Phytopathological Society Press, St. Paul, MN.
- Adaskaveg, J. E., Förster, H., Hao, W., and Gray, M. 2017. Potassium phosphite resistance and new modes of action for managing *Phytophthora* diseases of citrus in the United States. Pages 205-210 in: Modern fungicides and antifungal compounds, Vol. VIII. H. B. Deising, B. Fraaije, A. Mehl, E. C. Oerke, H. Sierotzki, and G. Stammler, eds. Deutsche Phytomedizinische Gesellschaft, Braunschweig, Germany.
- Alva, A. K.; Graham, J. H.; Tucker, D. P. H. 1993. Role of calcium in amelioration of copper phytotoxicity for citrus. *Soil Sci.* 155:211-218.
- Anonymous. 2022. California Agricultural Statistics Review. [www.cdfa.ca.gov/Statistics/PDFs/2022\\_Ag\\_Stats\\_Review.pdf](http://www.cdfa.ca.gov/Statistics/PDFs/2022_Ag_Stats_Review.pdf).
- Blum, M., Boehler, M., Randall, E., Young, V., Csukai, M., Kraus, S., Moulin, F., Scalliet, G., Avrova, A. O., and Whisson, S. C. 2010. Mandipropamid targets the cellulose synthase-like PiCesA3 to inhibit cell wall biosynthesis in the oomycete plant pathogen, *Phytophthora infestans*. *Mol. Plant Pathol.* 11: 227-243.
- Cohen, Y. 2015. The novel oomycide oxathiapiprolin inhibits all stages in the asexual life cycle of *Pseudoperonospora cubensis* - causal agent of cucurbit downy mildew. *PLoS One* 10:e0140015.
- Cohen, Y., Rubin, E., Hadad, T., Gotlieb, D., Sierotzki, H., and Gisi, U. 2007. Sensitivity of *Phytophthora infestans* to mandipropamid and the effect of enforced selection pressure in the field. *Plant Pathol.* 56:836–842.

- Dai, T., Yang, J., Zhao, C., Zhang, C., Wang, Z., Peng, Q., Liu, P., Miao, J., Liu, X. 2023. Vacuolar H<sup>+</sup>-ATPase subunit a was identified as the target protein of the oomycete inhibitor fluopicolide. bioRxiv. Preprint. <https://doi.org/10.1101/2023.04.22.537907>
- Erwin, D. C., and Ribeiro, O. K. 1996. *Phytophthora Diseases Worldwide*. APS Press. St. Paul, MN.
- FAO. 2021. *Citrus fruit statistical compendium 2020*. Rome. <https://www.fao.org/3/cb6492en/cb6492en.pdf>.
- Feld, S. J., Menge, J. A., and Pehrson, J. E. 1979. Brown rot of citrus: A review of the disease. *Citrograph*. 64:101–107.
- FRAC. 2022. FRAC Code List 2022: Fungicides sorted by mode of action (including FRAC Code numbering). Online publication. <http://www.frac.info>.
- Geisseler, D., and Horwath, W. R. 2016. Citrus production in California. [https://apps1.cdfa.ca.gov/FertilizerResearch/docs/Citrus\\_Production\\_CA.pdf](https://apps1.cdfa.ca.gov/FertilizerResearch/docs/Citrus_Production_CA.pdf).
- Graham, J. H., 1995. Root regeneration and tolerance of citrus rootstocks to root rot caused by *Phytophthora nicotianae*. *Phytopathology* 85: 111-117.
- Graham, J., and Feichtenberger, E. 2015. Citrus *Phytophthora* diseases: Management challenges and successes. *J. Citrus Pathol.* 2. <https://doi.org/10.5070/C421027203>
- Graham, J. H., and Menge, J. A. 1999. Root diseases. Pages 126-135 in: *Citrus Health Management*. L. W. Timmer, and L. W. Duncan, eds. American Phytopathological Society, St. Paul, MN.
- Graham, J. H., and Menge, J. A. 2000. *Phytophthora*-induced diseases. Pages 12–15 in: *Compendium of Citrus Diseases*. L. W. Timmer, S. M. Garnsey, and J. H. Graham, eds. APS Press, The American Phytopathological Society, St. Paul, MN.
- Graham, J. H., Timmer, L. W., Drouillard, D. L., and Peever, T. L. 1998. Characterization of *Phytophthora* spp. causing outbreaks of citrus brown rot in Florida. *Phytopathology* 88:724-729.
- Gray, M. A., Hao, W., Förster, H., and Adaskaveg, J.E. 2018. Baseline sensitivities of new fungicides and their toxicity to selected life stages of *Phytophthora* species from citrus in California. *Plant Dis.* 102:734-742.
- Gray, M. A., Nguyen, K. A., Hao, W., Belisle, R. J., Förster, H., and Adaskaveg, J. E. 2020. Mobility of oxathiapiprolin and mefenoxam in citrus seedlings after root

- application and implications for managing *Phytophthora* root rot. *Plant Dis.* 104:3159-3165
- Hao, W., Förster, H., Adaskaveg, J. E. 2021. Resistance to potassium phosphite in *Phytophthora* species causing citrus brown rot and integrated practices for management of resistant isolates. *Plant Dis.* 105:972-977.
- Hao, W., Miles, T. D., Martin, F. N., Browne, G. T., Förster, H., and Adaskaveg, J. E. 2018a. Temporal occurrence and niche preferences of *Phytophthora* spp. causing brown rot of citrus in the Central Valley of California. *Phytopathology* 108:384–391.
- Hao, W., Gray, M. A., Förster, H., and Adaskaveg, J. E. 2018b. Evaluation of new Oomycota fungicides for management of *Phytophthora* root rot of citrus in California. *Plant Dis.* 103:619-628.
- Hippler, F. W. R., Peten, G., Boaretto, R. M., Quaggio, J. A., Azevedo, R. A., and Mattos, D. 2018. Mechanisms of copper stress alleviation in citrus trees after metal uptake by leaves or roots. *Environ. Sci. Pollut. Res.* 25:13134–13146.
- Jiang, L., Wang, H., Xu, H., Qiao, K., Xia, X., and Wang, K. 2015. Transportation behaviour of fluopicolide and its control effect against *Phytophthora capsici* in greenhouse tomatoes after soil application. *Pest Manage. Sci.* 71: 1008-1014.
- Klotz, L. J. 1978. Fungal, bacterial, and nonparasitic diseases and injuries originating in the seedbed, nursery, and orchard. Pages 1-66 in: *The Citrus Industry*. Vol. IV. W. Reuther, E. C. Calavan, and G. E. Carman, eds. University of -California, Division of Agricultural and Sciences, Oakland, CA.
- Marin M.V., Baggio J.S., Oh Y., Han H., Chandra S., Wang N.Y., Lee S., Peres N.A. 2023. Identification of sequence mutations in *Phytophthora cactorum* genome associated with mefenoxam resistance and development of a molecular assay for the mutant detection in strawberry (*F. × ananassa*). *Sci Rep.* 13(1):7385.
- Pasteris, R. J., Hanagan, M. A., Bisaha, J. J., Finkelstein, B. L., Hoffman, L. E., Gregory, V., Andreassi, J. L., Sweigard, J. A., Klyashchitsky, B. A., Henry, Y. T., and Berger, R. A. 2016. Discovery of oxathiapiprolin, a new oomycete fungicide that targets an oxysterol binding protein. *Bioorg. Med. Chem.* 24: 354-361.
- Peng, Q., Wang, Z., Fang, Y., Wang, W., Cheng, X., Liu, X. 2019. Point Mutations in the  $\beta$ -Tubulin of *Phytophthora sojae* Confer Resistance to Ethaboxam. *Phytopathology.* 109(12):2096-2106.
- Pink, D., Puddephat I, I. 1999. Deployment of disease resistance genes by plant transformation - a 'mix and match' approach. *Trends Plant Sci.* 4(2):71-75.

- Tabima, J. F., Gonen, L., Gómez-Gallego, M., Panda, P., Grünwald, N. J., Hansen, E. M., McDougal, R., LeBoldus, J. M., Williams, N. M. 2021. Molecular phylogenomics and population structure of *Phytophthora pluvialis*. *Phytopathology* 111:108–115.
- Timmer, L. W., Graham, J. H., and Zitko, S. E. 1998. Metalaxyl-resistant isolates of *Phytophthora nicotianae*: Occurrence, sensitivity, and competitive ability on citrus. *Plant Dis.* 82:254-261.
- Uchida, M., Roberson, R. W., Chun, S. J., and Kim, D. S. 2005. In vivo effects of the fungicide ethaboxam on microtubule integrity in *Phytophthora infestans*. *Pest Manag. Sci.* 61:787-792.
- Vogel, G., Gore, M. A., and Smart, C. D. 2021. Genome-wide association study in New York *Phytophthora capsici* isolates reveals loci involved in mating type and mefenoxam sensitivity. *Phytopathology* 111:204–216.
- Wang, Z., Ke, Q., Tao, K., Li, Q., Xia, Y., Bao, J., Chen, Q. 2022. Activity and Point Mutation G699V in PcoORP1 Confer Resistance to Oxathiapiprolin in *Phytophthora colocasiae* Field Isolates. *J. Agric. Food Chem.* 70:14140–14147.
- Zhang, F., Chen, H., Zhang, X., Gao, C., Huang, J., Lü, L., Shen, D., Wang, L., Huang, C., Ye, W., Zheng, X., Wang, Y., Vossen, J. H. and Dong, S. 2021. Genome analysis of two newly emerged potato late blight isolates sheds light on pathogen adaptation and provides tools for disease management. *Phytopathology* 111:96–107.

## **CHAPTER I. Diversity and Clonality in Populations of *Phytophthora citrophthora* and *P. syringae* Causing Brown Rot of Citrus in California**

Reprinted with permission from: Riley, N.M., Förster, H., Adaskaveg, J.E. 2023. Diversity and Clonality in Populations of *Phytophthora citrophthora* and *P. syringae* Causing Brown Rot of Citrus in California. *Phytopathology*. *Submitted*.

### **ABSTRACT**

*Phytophthora citrophthora* and *P. syringae* are currently the primary causal organisms of brown rot of citrus fruits in California. To possibly find an explanation for the prevalence of the previously minor species *P. syringae*, we determined the population structures of both pathogens in California using next-generation sequencing and population genomics analyses. Whole genome sequencing and aligning with newly assembled reference genomes identified 972,266 variants in 132 isolates of *P. citrophthora* and 422,208 variants in 154 isolates (including 24 from non-citrus tree crops) of *P. syringae* originating from three major growing regions. The resulting data sets were visualized using principal component analysis, discriminant analysis of principal components, UPGMA dendrograms, fastStructure, and minimum spanning networks, and we obtained index of association, diversity summary statistics, and the genetic distance statistics values  $G_{ST}$ ,  $G''_{ST}$ , and Jost's  $D$ . Sub-populations of both species were mostly defined by their geographic origin indicating restricted dispersal of inoculum. Except for five isolates, the population structure of *P. citrophthora* (that is heterothallic and unlikely to reproduce sexually) was clonal to semi-clonal with very little genetic diversity within and among sub-groups. In contrast, the population structure of *P. syringae* was also clonal to semi-clonal, but isolates were placed into four main clusters of much higher diversity. Clonality in both species can be explained by a high level of

asexual reproduction. The higher diversity in the homothallic *P. syringae* is likely due to commonly occurring sexual reproduction. One distinct cluster of *P. syringae* consisted solely of isolates from non-citrus hosts; therefore, the origin of *P. syringae* in citrus could not be resolved.

## INTRODUCTION

Citrus is an important crop in many countries with sub-tropical and tropical environments. Total worldwide production was estimated at 143,755,600 metric tons of fruit in 2020 (FAO 2021). In California, citrus production was valued at \$2.5 billion in 2021/22 (Anonymous 2022). The California citrus industry expanded from a first commercial orchard in Los Angeles in 1841 to other southern portions of the state. Currently, most of the citrus production is further North in the Central Valley (CV), particularly in Fresno, Kern, and Tulare Co. The remaining production is primarily in the original growing areas of southern California in the Inland Empire (IE; i.e., Riverside and San Bernardino Co.) as well in coastal Ventura Co. (VE), San Diego Co., and Imperial Co. (Geisseler and Horwath 2016).

Species of *Phytophthora* are responsible for various diseases affecting citrus trees throughout the growing season. These include root rot of young seedlings and mature trees, foot rot causing gummosis of the trunk (i.e., trunk cankers), and brown rot of fruit, all of which may be caused by some of the same species (Graham and Feichtenberger 2015). Fruit brown rot is characterized by tan to brown, leathery lesions that have a distinctive odor. Infected fruit remain firm unless secondary infections occur. In California, brown rot can be caused by *P. citrophthora*, *P. hibernalis*, *P. nicotianae*, or *P.*



*syringae*. *P. syringae* and *P. hibernalis* have been considered of minor importance in the past (Feld et al. 1979; Graham and Menge 2000; Klotz 1978). More recently, however, *P. citrophthora* and *P. syringae* were demonstrated to be the major pathogens, and they can occur within the same orchard (Hao et al. 2018). In other citrus producing regions such as Florida, additional species such as *P. palmivora* and *P. citricola* have been found responsible for brown rot (Graham and Menge 2000).

The shift in species composition of brown rot pathogens in California has caused trade restrictions for the California citrus industry by China, a major export country where *P. hibernalis* and *P. syringae* are quarantine pathogens (Hao et al. 2018). Export of California citrus fruit to China was closed from 2013 to 2014 and again in 2015 due to the detection of *P. syringae* and *P. hibernalis* in orange fruit shipments, resulting in economic loss to growers, packinghouses, and shippers (Adaskaveg and Förster 2014). The status of *P. syringae* and *P. hibernalis* as quarantine pathogens has elevated brown rot of citrus from a troublesome inconvenience to a serious problem over the past decade.

More information is needed as to why *P. syringae* has become a dominant brown rot pathogen in California, and thus, our goal was to study the population demographics of this species in comparison to *P. citrophthora*. The two species differ ecologically: *P. citrophthora* can be isolated year-round, while *P. syringae* is only active during the cooler months. Furthermore, *P. syringae* is homothallic and capable of self-crossing, while *P. citrophthora* is heterothallic but not thought to reproduce sexually in the environment (Erwin and Ribeiro 1996). These characteristics may influence population structure and diversity. Population genomic analyses were recently utilized on other *Phytophthora*

species such as *P. phuvialis* (Tabima et al. 2021), *P. capsici* (Vogel et al. 2020), and *P. infestans* (Zhang et al. 2021) to investigate population structure, fungicide sensitivity, and pathogen adaptation. Our specific objectives were to: 1) collect isolates of *P. syringae* and *P. citrophthora* from citrus production areas of California not previously surveyed by Hao et al. 2018; 2) characterize the population structure of these species and determine if populations sampled from different geographic regions are genetically distinct; and 3) determine if isolates of *P. syringae* from non-citrus hosts are genetically distinct from those collected from citrus. To achieve these goals, reference isolates of *P. syringae* and *P. citrophthora* were sequenced, and sequences were assembled into reference genomes. Subsequently, 132 isolates of *P. citrophthora* and 154 isolates of *P. syringae* from major growing regions in California were sequenced, and sequences were aligned to the reference genomes to identify variant (i.e., single nucleotide polymorphism; SNP) markers to be used for population genomic analyses.

## MATERIALS AND METHODS

**Isolate collection and variant (SNP) identification.** Isolates of *P. citrophthora* and *P. syringae* collected from brown-rotted fruit in the CV of California between 2013 and 2015 were used from a previous study where species identity of isolates was verified by morphology, RAPD fragment patterns, and using a multiplex TaqMan qPCR assay with species-specific probes (Hao et al. 2018). Additional isolates were obtained from VE and the IE region from symptomatic citrus fruit, leaf litter, and soil, as well as from soil of non-citrus hosts between 2018 and 2022. Isolations were done as described by Hao et al. (2018). Colonies resembling *Phytophthora* spp. were sub-cultured onto clarified 5% V8

agar (Ribeiro 1978). Species identification of newly collected isolates was based on morphology, and a subset was subjected to TaqMan qPCR using species-specific probes. For genome sequencing, a total of 132 isolates of *P. citrophthora* (70 from CV, 36 from VE, and 26 from IE) and 130 isolates of *P. syringae* (80 from CV, 14 from VE, 36 from IE) were selected from citrus sources. Additionally, 24 isolates of *P. syringae* were included from orchard soils of non-citrus hosts (19 from almond, 4 from walnut, and 1 from cherry). Isolates used in this study are listed in Table 1.1.

For DNA extraction, isolates were grown for 5 to 10 days in 10% clarified V8 broth at 20°C. Mycelia were rinsed three times with sterile water, and lyophilized. Tissues were homogenized using a stainless-steel grinding ball (Steelball LysingMatrix; MP Biomedicals, LLC, Irvine, CA) using the FastPrep-24 Instrument (MP Biomedicals, LLC) at 6.0 m/s twice for 45 s, and DNA was extracted using the DNEasy Plant Mini Kit (Qiagen, Germantown, MD). DNA quality was assessed by measuring the 260 nm/280 nm ratio of absorbance (NanoDrop ND-1000 UV-Vis Spectrophotometer; Thermo Fisher Scientific, Waltham, MA) and by gel electrophoresis in a 2% agarose gel. Prior to the sequencing of the selected isolates, reference genomes were constructed for *P. citrophthora* isolate 2440 and *P. syringae* isolate 4571. DNA was quantified (Qubit 4 Fluorometer; Invitrogen, Carlsbad, CA) before submission for library prep at the University of California Riverside Genomics Core Facility and subsequent 150-bp paired end sequencing on the Illumina NovaSeq platform. Processing of raw data, creation of reference assemblies, alignment of population data, variant calling, and variant filtering were performed on the UCR High Performance Computing Center cluster. Raw reads

were filtered for a minimum quality score of 30 and Illumina adapters were removed using the fastq-mcf tool (ea-utils v. 1.1.2-537, Aronesty 2013). Filtered raw reads were then used for reference genome assembly using the SPAdes assembly program v. 3.13.1 with default settings (Bankevich et al. 2012). For quality assessment, reference assemblies were analyzed for basic characteristics and quality using QUAST v. 4.6.3 (Gurevich et al. 2013). Assemblies were then assessed for completeness using BUSCO v. 3.0.2 in the “genome” mode with the “Eukaryota Odb9” database (Manni et al. 2021). DNA from the selected isolates was extracted as described above and submitted for library preparation and 150-bp paired-end sequencing on the Illumina NovaSeq platform. Initial processing of data was performed as described above. The reference assemblies for *P. citrophthora* and *P. syringae*, as well as the raw data for all other isolates sequenced have been deposited with links to BioProject accession number PRJNA1010852 in the NCBI BioProject database (<https://www.ncbi.nlm.nih.gov/bioproject/>). The reads from the sequenced isolates were mapped to their respective reference genomes. Using BWA v. 0.7.17 (Li 2013), reference assemblies were indexed using default settings, and alignments were made using the MEM algorithm with the -M setting activated. All other settings were in their default modes. The resulting BAM files were then sorted, mate-fixed, and marked for duplicates using sort, fixmate, and markdup functions (all with default settings except for fixmate, which utilized -m to add mate score tags for use by markdup) of SAMTools v. 1.14 (Danecek et al. 2021; Li et al. 2009). SAMtools was also used to assess mapping percentages with the flagstat function. Genomic variants were predicted using GATK v. 4.2.5.0 (McKenna et al. 2010). For both species, each isolate

was independently genotyped with GATK's haplotype caller in the GVCF mode. Variants were validated using the `ValidateVariants` function before being pooled using the `CombineGVCF` function (both using default settings), and the combined GVCF file was then genotyped using the `GenotypeGVCFs` function, also with default settings. A final combined GVCF file was created for each species using the `GATK SelectVariants` function with `--restrict-alleles-to` set to "BIALLELIC", `--remove-unused-alternates` set to "true", `--select-type-to-include` set to "SNP", and `--exclude-non-variants` set to "true". Variants were then filtered using `VCFTools` v. 0.1.16-18 (Danecek et al. 2011), in which all singletons, all variants with more than 10% missing data, as well as all variants with a read depth of less than 4 and a quality score of less than 10 were removed. Following this, `RepeatModeler` v. 2.0.4 (Flynn et al. 2020) was utilized to identify repetitive regions in the genome (using the `BuildDatabase` and `RepeatModeler` functions), and `RepeatMasker` v. 4-1-4 (Tarailo-Graovac and Chen 2009) was used to perform soft masking and generate a ".gff" file that was then converted into a ".bed" file containing that information. This ".bed" file was then used to filter out variants located in those repetitive regions with the `--exclude-bed` setting of `VCFtools`.

**Population structure.** All analyses were conducted in R v. 4.1.3 (R Core Team 2022) on non-clone corrected data unless otherwise specified. PCA and DAPC analyses were conducted for *P. citrophthora* and *P. syringae* using the *adegenet* package v. 2.1.10 (Jombart 2008) with `nf = 4` and `nf = 5`, respectively. PCA scores were plotted using the *ggplot2* package v. 3.4.2 (Wickham 2016). DAPC scatterplots were plotted using the `scatter.dapc` function of *adegenet*, with `n.pca = 50` and `n.da = 3` for *P. citrophthora* and

n.pca = 20 and n.da = 4 for *P. syringae*. Isolates of both species were grouped by geographic region. Isolates for *P. syringae* were also plotted by host of origin. Unweighted pair-group method with arithmetic mean (UPGMA) dendrograms for each species were generated based on bitwise distance using the `aboot` function of the *poppr* package v. 2.9.4 (Kamvar et al. 2014) with 1000 permutations. These were then plotted using the packages *ggtree* v. 3.7.2 and *ggbreak* v. 0.1.1 to extend the capabilities of *ggplot2* (Xu et al. 2021, 2022). The `gl2structure` function from the R package *dartR* v. 2.7.2 (Gruber et al. 2018) was used to create structure files for use in population structure analyses. The Python program `fastStructure` v. 1.0 (Raj et al. 2014) was then used to analyze population structure for each species, and the `structure.py` function was executed for  $K=1-10$ . The `chooseK.py` function was used to identify  $K$  values that best explained the structure in our data, and  $K=2$  and  $K=4$  were found to be the best fit for *P. citrophthora* and *P. syringae*, respectively. Population structure data for those runs were then plotted using the *pophelper* package v. 2.3.1 in R (Francis 2017), and the results were aligned to the UPGMA dendrograms generated for each species.

**Clonality and minimum spanning networks (MSNs).** To infer the level of clonality in the sampled populations, the index of association ( $I_A$ ) was calculated as described in Shakya et al. 2021 with modifications. The following simulations and actual calculations were performed for each species overall, as well as for subsets containing only citrus isolates from each regional population and for the non-citrus isolates of *P. syringae*. First, the `glSim` function of the *adegenet* v. 2.1.10 package was used to simulate clonal (90% linked SNPs), partially clonal (50% linked SNPs), and sexual (10% linked SNPs)

populations based on each data set. Then, the `samp.ia` function from the *poppr* v. 2.9.4 package (Kamvar et al. 2014) was used to calculate  $I_A$  for each dataset and their simulations from 10,000 randomly sampled SNPs with 100 replicates. Significant differences were identified using ANOVA followed by Tukey's HSD test in R. Due to the presence of clonality, the *poppr* package was then used to generate color-coded MSN plots with distance filters of 0.00375 and 0.04 for *P. citrophthora* and *P. syringae*, respectively. A second color-coded MSN plot was generated for *P. syringae* to reflect the host of the isolates.

**Differentiation statistics.** The `utils.basic.stats` function of the R package *dartR* v. 2.7.2 (Gruber et al. 2018) was used to generate basic summary statistics, including observed heterozygosity ( $H_o$ ), within population gene diversity ( $H_s$ ), total genetic diversity ( $H_T$ ), gene diversity among samples ( $D_{ST}$ ), and fixation index ( $F_{ST}$ ,  $D_{ST}/H_T$ ). The pairwise `Gst_Nei`, `pairwise_Gst_Hedrick`, and `pairwise_D` functions from the R package *mmod* v. 1.3.3 (Winter 2012) were used to calculate Nei's  $G_{ST}$  (a multi-allelic measure of  $F_{ST}$ ) (Nei 1973; Nei and Chesser 1983), Hedrick's  $G''_{ST}$  (a version of  $G_{ST}$  that accounts for sample size) (Meirmans and Hedrick 2011), and Jost's  $D$  (a measure of allele frequency difference among populations), respectively (Jost 2008).

## RESULTS

**Variant (SNP) identification.** Quality and structure metrics of reference genome assemblies for *P. citrophthora* and *P. syringae* including size, number of contigs, N50, L50, and error rate are listed in Table 1.2. BUSCO outputs for the genome assemblies of both species can be found in Table 1.3. Results show the proportions of orthologous

genes to the 303 genes that were searched for as a metric for assembly completeness. Reads of all sequenced isolates of both species aligned more than 90% to their respective reference genomes. A total of 945,881 variants were identified in *P. syringae* before filtering and repeat masking, while 1,531,374 variants were identified in *P. citrophthora*. After filtering out singletons and variants with more than 10% missing data, a read depth of less than 4, or a quality score of less than 10, and singletons and variants occurring in repeated regions, the final data set for *P. syringae* contained 422,208 variants, while the final data set for *P. citrophthora* contained 972,266 variants.

**Population structure.** The PCA for isolates of *P. citrophthora* from citrus by geographic region of origin resulted in three distinct clusters, and 85.51% of the observed variance was captured by PC1 (Fig. 1.1A). The majority of isolates was placed into two large closely-related clusters to the right of the y axis, whereas five CV isolates were found more distant to the left of the y axis. The large cluster above the x axis primarily consisted of VE and IE isolates, while the one below the x axis primarily consisted of CV isolates. Still, both of these clusters contained isolates from all three geographic regions.

The PCA for *P. syringae* isolates grouped by geographic origin revealed three clusters, and 47.07% of the observed variance was captured by PC1 (Fig. 1.1B). A large cluster in the lower left of the plot consisted almost entirely of citrus isolates from CV and IE, except for three isolates from VE. A smaller cluster in the lower right comprised 21 non-citrus CV isolates. Eleven citrus VE isolates were loosely clustering along the y axis on the upper left of the plot, whereas one citrus CV and three almond CV isolates were not clearly associated with any cluster.



In the DAPC analyses where differences between groups are maximized and similarities are minimized, isolates of the two main PCA clusters for *P. citrophthora* were separated into three distinct clusters in the scatterplot (Fig. 1.1C). Each of these three clusters contained isolates mostly from one of the regional groups (CV, IE, VE), except for one VE isolate within the CV cluster. The DAPC scatterplot of *P. syringae* based on geographic origin of isolates also formed distinct clusters for each regional group, but the CV isolates grouped closely to IE isolates and several CV individuals plotted within the IE cluster. The cluster of 12 VE isolates was more distant, indicating higher differentiation of this population (Fig. 1.1D). One individual from VE was plotted within the IE cluster and a second one (hidden behind the orange triangles of IE isolates in Fig. 1.1D) just outside of it.

In the second PCA for *P. syringae* isolates with categorization by host, the large cluster in the lower left of the plot and the looser cluster of 11 isolates in the upper left both consisted entirely of isolates from citrus fruit or leaf litter (Fig. 1.2A). A cluster of 21 isolates in the lower right originated entirely from non-citrus hosts (i.e., almond, cherry, and walnut). Three isolates from almond and one citrus CV isolate were not associated with any cluster.

The DAPC scatterplot of *P. syringae* with grouping by host reflects the distinctness of citrus isolates (except for one) from those collected from non-citrus hosts (Fig. 1.2B; green circles representing citrus leaf litter isolates are hidden behind the orange circles of the citrus fruit isolates). The 19 almond isolates formed a less tight cluster, and one

isolate from walnut is closely associated. The remaining non-citrus isolates (three from walnut, one from cherry) were scattered more distantly from the almond isolates.

UPGMA dendrograms of *P. citrophthora* (Fig. 1.3) and *P. syringae* (Fig. 1.4) provided additional information on the population structures of the two species. Isolates of *P. citrophthora* exhibited relatively low genetic distances among individuals throughout the geographic populations sampled, except for five CV isolates (at the top of the dendrogram). The genetic diversity among these five isolates was much higher than that among the remaining majority of CV, IE, and VE isolates that were mostly found within distinct portions of the dendrogram, and thus, grouped based on their geographic origin. CV isolates were distinct, were located on a major lower branch of the dendrogram and were separated from IE and VE isolates. In comparison, the *P. syringae* dendrogram showed much greater genetic distances among individuals, both within and between sampled geographic populations. The non-citrus isolates formed their own distinct cluster (at the top of the dendrogram in Fig. 1.4) separate from the other sampled populations. Isolates from VE clustered mostly on a branch in the upper parts of the dendrogram, whereas CV and IE isolates were not clearly separated.

When UPGMA dendrograms were aligned with fastStructure bar plots, similar groupings of isolates of both species were observed in the clusters generated by both types of analyses. Thus, for *P. citrophthora* the majority of isolates grouped together (cluster 2 in Fig. 1.3). The exception again was five CV isolates that were assigned to their own cluster (cluster 1). This separation was observed for a range of K values from 2 to 10, indicating no mixture with the other populations. For *P. syringae*, isolates from

non-citrus hosts again formed a distinct cluster (cluster 3 in Fig. 1.4). Similar to the UPGMA dendrogram, VE isolates from citrus were primarily assigned to their own unique cluster (cluster 2). Most CV and IE citrus isolates were assigned to two distinct clusters (clusters 4 and 1, respectively), although many isolates showed partial assignment to both clusters.

**Clonality and minimum spanning network (MSN).** Calculated values for  $I_A$  across all loci indicated partial clonality ( $I_A > 0$ ) in all sampled geographic populations of both species (Table 1.4). Replicates for each dataset had very low deviation from the mean, and Tukey's HSD found all actual datasets to be significantly different ( $P < 0.05$ ) from the simulated data sets. For *P. citrophthora*, the overall and CV datasets had  $I_A$  values much greater than the simulated clonal dataset, indicative of clonal reproduction, whereas the IE and VE datasets had  $I_A$  values closest to the semi-clonal datasets. For *P. syringae*, the overall and VE datasets had  $I_A$  values greater than the simulated clonal dataset, whereas the IE and non-citrus datasets had  $I_A$  values closest to the simulated clonal dataset. The CV dataset had the lowest  $I_A$ , and this was closest to the simulated semi-clonal dataset.

After distance filtering, the 132 *P. citrophthora* isolates and 154 *P. syringae* isolates were assigned to 38 and 70 multilocus genotypes (MLG) respectively. The generated MSN for *P. citrophthora* revealed three large MLGs and smaller MLGs, each primarily consisting of isolates from one of the three sampled regions (Fig. 1.5A). The thick and dark connecting lines between nodes indicate small genetic distances as shown by the scale bar in the figure. The MSN for *P. syringae* was comparatively more dispersed and

included more nodes and a larger number of mostly smaller MLGs (Fig. 1.5B). One of the larger MLGs consisted of only IE isolates, whereas the other two were mostly associated with IE isolates but also were represented at relatively high incidence by one or two of the other geographic populations. The smaller groups of MLGs were mostly associated with CV isolates, although three represented isolates from VE, and they were connected by more gray and thinner lines, indicating larger genetic distances based on the scale bar. The genetic distances between MLGs of CV isolates at the “tail” trailing off the top of the network were greater than in the rest of the network. When isolates of *P. syringae* were color-coded by host, it is evident that the nodes of the “tail” all represented non-citrus host isolates and the remaining network all comprise isolates from citrus (Fig. 1.6). All except four of the 24 non-citrus isolates possessed their own unique MLG, and two each of these four originated from the same orchards.

**Differentiation statistics.** The summary statistics for *P. citrophthora* indicates relatively low within-population diversity  $H_S$  that was highest for the CV population (Table 1.5). The summary statistics for *P. syringae* indicates higher overall within-population diversity  $H_S$  and  $F_{st}$  fixation index values as compared with *P. citrophthora*; for citrus isolates,  $H_S$  was highest for the VE population but was even higher for the non-citrus isolates. Analysis of pairwise Nei’s  $G_{ST}$ , Hedrick’s  $G''_{ST}$ , and Jost’s  $D$  values provided additional insight into the differentiation of populations of *P. citrophthora* and *P. syringae* (Table 1.6). *P. citrophthora* exhibited lower levels of differentiation based on all metrics than *P. syringae*. For *P. citrophthora*, differentiation was lowest between VE and IE populations and highest between VE and CV populations. For isolates of *P.*

*syringae* from citrus, differentiation was lowest between CV and IE populations and highest between VE and IE populations. Differentiation between isolates of *P. syringae* from non-citrus hosts and any of the three regional citrus populations was all higher than among the citrus populations.

## DISCUSSION

Extensive population genetic analyses were conducted to characterize isolates of *P. citrophthora* and *P. syringae* from citrus in three major growing regions of California: the CV, VE, and IE. New insights were gained into population structures, and we characterized distinct differences between the two brown rot pathogens that relate to their lifestyles. Isolates of *P. syringae* from non-citrus tree crops separated from citrus populations and therefore, we found no evidence for the origin of this species on citrus and its emergence as a primary citrus brown rot pathogen.

Genomic variants in isolates were identified by aligning short-read sequences with our newly assembled reference genomes of the two species. No reference genomes were available at the time these studies were initiated. Recently published genomes of *P. syringae* with assembly sizes of 74.9 Mb or 57 Mb (GenBank accessions 19064958 and 35224038), however, are of a similar size range as our genome of this species (i.e., 52 Mb). We conducted no genetic comparisons of these genomes including gene annotations because our reference genomes were solely used to identify sequence variants (i.e., SNPs) for comparisons of regional populations of *P. citrophthora* and *P. syringae*.

Our analyses indicate that genetically distinct populations of both *P. citrophthora* and *P. syringae* are present in California. Sub-populations of both species, mostly defined by

their geographic origin, were clearly identified by UPGMA, PCA, DAPC, fastStructure, and MSN analyses. FastStructure did not resolve the major cluster of *P. citrophthora* isolates but identified sub-populations in *P. syringae*. There was limited overlap between geographic sub-populations, indicating restricted airborne dispersal of inoculum or possible anthropogenic movement of these soilborne *Phytophthora* species. Sampling regions were separated by distances of more than 150 km and by major urban regions or mountainous areas without agriculture. The limited overlap in clustering of geographic populations that was more pronounced in *P. syringae* could be explained by movement of harvested fruit to distant packinghouses that may be located in a different growing area. Decayed fruit including those with brown rot are sorted out in the packinghouse and are sometimes dumped in land fill areas or in orchards where they can become a source of inoculum.

Overall, the population structure of *P. citrophthora* across three main citrus growing regions of California can be described as to consist of closely related but distinct regional populations with relatively low intra-group diversity. This finding is consistent with the heterothallic nature of this species that requires the presence of two mating types. Additionally, oogonia, antheridia, and oospores have not been observed in nature, and it is assumed that the sexual stage is not a common part of the life cycle (Erwin and Ribeiro 1996). Oospores of *P. citrophthora* have been produced only in laboratory matings of certain isolates or in matings with other species (Erwin and Ribeiro 1996). Asexual reproduction in this species can explain the observed similarity among isolates and groups in our study. Still, a more diverse cluster of five CV isolates was identified, and

these isolates possibly originated by hybridization as has been described for a number of *Phytophthora* species (Van Poucke et al. 2021) or by introductions from different hosts or from other citrus growing areas.

In contrast to the mostly closely related sub-populations of *P. citrophthora*, *P. syringae* exhibited much more variation with clonal lineages existing within sub-populations. Similar as for *P. citrophthora*, sub-populations of *P. syringae* were often associated with specific growing regions, and some MLGs were present in two or all three regions. A higher variation in *P. syringae* can be expected because sexual reproduction likely occurs readily. Higher variability may have been responsible for this species becoming prevalent in citrus during the last 40 years. *P. syringae* is homothallic but capable of outbreeding; still, this limits the possibility of generating new genotypes as compared to an outcrossing species if both mating types are present in a single population.

Both species reproduce mostly asexually by formation of sporangia with zoospores that are the main infective propagules. This asexual reproduction can explain the clonality ( $I_A$  values of  $>0$ ) that was inferred in all sampled geographic populations of both species. The overall  $I_A$  for both *P. citrophthora* and *P. syringae* was found to be greater than their respective simulated clonal datasets. Sub-populations of both species exhibited a range of calculated  $I_A$  values. For *P. citrophthora*,  $I_A$  values for IE and VE populations were closest to the simulated semi-clonal dataset; whereas the  $I_A$  value for the CV population was clearly above the simulated clonal dataset. For *P. syringae*, the  $I_A$  value for the CV population was closest to semi-clonal, whereas those of IE and non-citrus populations

were closest to the simulated clonal dataset and that of the VE population was above the simulated clonal dataset. These results reflect our current understanding of the reproduction and lifestyle of the homothallic *P. syringae* where both sexual and clonal reproduction are thought to readily occur in the environment. The MSN generated for *P. syringae* reflected the expected structure, with VE isolates belonging to the fewest MLGs and CV (and non-citrus) isolates being the most diverse and fragmented into the most unique MLGs. Still, sample size may have some impact on these results, as only 14 VE isolates were available for analyses as compared to 80 and 36 isolates for CV and IE regions, respectively. *P. syringae* is more prevalent in colder environments, and therefore, is expected to be more common in the inland areas of California (i.e., CV and IE regions) where most of the isolates were obtained.

In contrast, the comparatively low  $I_A$  values calculated for the IE and VE populations of *P. citrophthora* are more difficult to explain because *P. citrophthora* is not thought to reproduce sexually in the environment. Our UPGMA dendrogram depicting these populations (Fig. 1.3) shows extremely little genetic distances among individuals belonging to the IE and VE populations. Furthermore, the MSN plot generated for *P. citrophthora* using a distance threshold produced MLGs that we believe are accurate depictions of the clonal structure within these populations. It is possible that factors not considered may impact this method of simulating  $I_A$  values for a dataset. Additional investigations are needed to assess and characterize the mode of reproduction in natural populations of *P. citrophthora*.



An important finding of our study is that citrus isolates of *P. syringae* were clearly differentiated from those from non-citrus tree crop hosts. This is especially noteworthy for isolates from the CV where growing areas of different tree crop hosts often overlap. In rainy winter seasons, *P. syringae* can be a serious almond pathogen causing trunk and crotch cankers (i.e., aerial Phytophthora disease; Browne and Viveros 1999), and there has been concern that the extensive almond cultivation contributed to the emergence of *P. syringae* as a major citrus brown rot pathogen. This hypothesis, however, is not supported by our data with a relatively limited sampling of non-citrus isolates, and the source of citrus *P. syringae* inoculum remains unknown. Non-citrus isolates were genetically diverse. They grouped on distinct branches of the UPGMA dendrogram and represented multiple MLGs in the MSNs. More sampling is warranted to describe population structures of non-citrus isolates of *P. syringae*.

Several measures were calculated to characterize differentiation within species and regional populations. For *P. citrophthora*, a low overall  $F_{ST}$  value (Table 1.5) as well as low  $G_{ST}$ ,  $G''_{ST}$ , and Jost's  $D$  values (Table 1.6) suggest relative weak differentiation between populations from the three sampling regions. For *P. syringae*, the relatively high overall  $F_{ST}$  (Table 1.5) indicates greater differentiation between populations.  $G_{ST}$ ,  $G''_{ST}$ , and Jost's  $D$  values (Table 1.6) were all higher than for *P. citrophthora*. Differentiation was lowest for CV and IE isolates, and this reflects the fact that fruit from the IE is sometimes shipped to the large CV packinghouses, whereas fruit shipping between VE and CV or between VE and IE is less common.

The validity of some of the statistics used in our study has been criticized as the field of population genetics/genomics is continuing to develop. Some authors (Gerlach et al. 2010; Hedrick 2005; Jost 2008; Miermans and Hedrick 2010) argue that the original  $F_{ST}/G_{ST}$  statistics do not take population size into account and are dependent on within-population diversity. Subsequently various alternative statistics such as  $G'_{ST}$ ,  $G''_{ST}$ , and Jost's  $D$  were proposed by these authors that were claimed to more accurately measure “true differentiation”. Others, however, have found flaws in these newly proposed methods claiming that on their own, they do not provide full insight into the factors affecting population differentiation and structure, and that they should be viewed in the context of  $G_{ST}$ , not as replacements for it (Verity and Nichols 2014; Whitlock 2011). Yet another study (Alcala and Rosenberg 2019) assessed the constraints imposed on these metrics by allele frequencies and found them to often produce similar results, and in cases where differences were observed, those differences could be explained by features of the dataset more greatly affecting one metric than the others. While it is difficult to assess which of the metrics ( $G_{ST}$ ,  $G''_{ST}$ , Jost's  $D$ ) provides the “most accurate” measurement of “true differentiation”, the results obtained using all metrics were consistent for the two species of *Phytophthora* studied and provide confidence to the accuracy of our results.

In summary, the distinct lifestyles of the two main species of *Phytophthora* currently causing brown rot of citrus in California are reflected by the population structures described in this study. Both lifestyles, i.e., heterothallic but likely only asexually reproducing (*P. citrophthora* with overall high  $I_A$  values and an MSN with limited genetic

distance among fewer MLGs that is indicative of clonality) or homothallic and sexually and asexually reproducing (*P. syringae* with overall high  $I_A$  values and MSN graphs with greater genetic distance and more unique single-isolate MLGs based on region and host that is indicative of some degree of clonality but with greater diversity), are successful strategies in the survival of each species in environmentally diverse citrus production areas of the state. The genetic diversity of both species that we identified indicates that species evolution and development of regional sub-populations are ongoing and that they will continue to adapt to changing environments. Thus, as a quarantine pathogen in some export countries, *P. syringae* potentially will cause more damage to California citrus production in the future.

## LITERATURE CITED

- Adaskaveg, J. E., and Förster, H. 2014. Integrated postharvest strategies for management of *Phytophthora* brown rot of citrus in the United States. Pages 123-131 in: Post-harvest Pathology, Plant Pathology in the 21st Century. D. Prusky and M. L. Gullino, eds. Springer International Publishing, Cham, Switzerland.
- Alcala, N., and Rosenberg, N. A. 2019.  $G'_{ST}$ , Jost's  $D$ , and  $F_{ST}$  are similarly constrained by allele frequencies: A mathematical, simulation, and empirical study. *Mol. Ecol.* 28:1624–1636.
- Anonymous. 2022. California Agricultural Statistics Review. [www.cdfa.ca.gov/Statistics/PDFs/2022\\_Ag\\_Stats\\_Review.pdf](http://www.cdfa.ca.gov/Statistics/PDFs/2022_Ag_Stats_Review.pdf).
- Aronesty, E. 2013. Comparison of sequencing utility programs. *Open Bioinform.* 7:1-8
- Bankevich, A., Nurk, S., Antipov, D., Gurevich, A. A., Dvorkin, M., Kulikov, A. S., Lesin, V. M., Nikolenko, S. I., Pham, S., Prjibelski, A. D., Pyshkin, A., V., Sirokin, A. V., Vyahhi, N., Tesler, G., Alekseyev, M. A., and Pevzner, P. A. 2012. SPAdes: A new genome assembly algorithm and its applications to single-cell sequencing. *J. Comput. Biol.* 19:455–477.
- Browne, G. T., and Viveros, M. A. 1999. Lethal cankers caused by *Phytophthora* spp. in almond scions: Specific etiology and potential inoculum sources. *Plant Dis.* 83:739-745.
- Danecek, P., Auton, A., Abecasis, G., Albers, C. A., Banks, E., DePristo, M. A., Handsaker, R. E., Lunter, G., Marth, G. T., Sherry, S. T., McVean, G., Durbin, R. 2011. The variant call format and VCFtools. *Bioinformatics* 27:2156–2158.
- Danecek, P., Bonfield, J. K., Liddle, J., Marshall, J., Ohan, V., Pollard, M. O., Whitwham, A., Keane, T., McCarthy, S. A., Davies, R. M., and Li, H. 2021. Twelve years of SAMtools and BCFtools. *Gigascience* 10:giab008.
- Erwin, D. C., and Ribeiro, O. K. 1996. *Phytophthora* Diseases Worldwide. APS Press. St. Paul, MN.
- FAO. 2021. Citrus fruit statistical compendium 2020. Rome. <https://www.fao.org/3/cb6492en/cb6492en.pdf>.
- Feld, S. J., Menge, J. A., and Pehrson, J. E. 1979. Brown rot of citrus: A review of the disease. *Citrograph.* 64:101–107.

- Flynn, J. M., Hubley, R., Goubert, C., Rosen, J., Clark, A. G., Feschotte, C., and Smit, A. F. 2020. RepeatModeler2 for automated genomic discovery of transposable element families. *Proc. Natl. Acad. Sci. U. S. A.* 117:9451–9457.
- Francis, R. M. 2017. pophelper: an R package and web app to analyse and visualize population structure. *Mol. Ecol. Resour.* 17:27–32.
- Geisseler, D., and Horwath, W. R. 2016. Citrus production in California. [https://apps1.cdfa.ca.gov/FertilizerResearch/docs/Citrus\\_Production\\_CA.pdf](https://apps1.cdfa.ca.gov/FertilizerResearch/docs/Citrus_Production_CA.pdf).
- Gerlach, G., Jueterbock, A., Kraemer, P., Deppermann, J., and Harmand, P. 2010. Calculations of population differentiation based on  $G_{ST}$  and  $D$ : forget  $G_{ST}$  but not all of statistics! *Mol. Ecol.* 19:3845–3852.
- Graham, J., and Feichtenberger, E. 2015. Citrus Phytophthora diseases: Management challenges and successes. *J. Citrus Pathol.* 2. <https://doi.org/10.5070/C421027203>
- Graham, J. H., and Menge, J. A. 2000. Phytophthora-induced diseases. Pages 12–15 in: *Compendium of Citrus Diseases*. L. W. Timmer, S. M. Garnsey, and J. H. Graham, eds. APS Press, The American Phytopathological Society, St. Paul, MN.
- Gruber, B., Unmack, P. J., Berry, O. F., and Georges, A. 2018. dartR: An R package to facilitate analysis of SNP data generated from reduced representation genome sequencing. *Mol. Ecol. Resour.* 18:691–699.
- Gurevich, A., Saveliev, V., Vyahhi, N., and Tesler, G. 2013. QUAST: quality assessment tool for genome assemblies. *Bioinformatics* 29:1072–1075.
- Hao, W., Miles, T. D., Martin, F. N., Browne, G. T., Förster, H., and Adaskaveg, J. E. 2018. Temporal occurrence and niche preferences of *Phytophthora* spp. causing brown rot of citrus in the Central Valley of California. *Phytopathology* 108:384–391.
- Hedrick, P. W. 2005. A standardized genetic differentiation measure. *Evolution.* 59:1633–1638.
- Jombart, T. 2008. adegenet: a R package for the multivariate analysis of genetic markers. *Bioinformatics* 24:1403–1405.
- Jost, L. 2008.  $G_{ST}$  and its relatives do not measure differentiation. *Mol. Ecol.* 17:4015–4026.
- Kamvar, Z. N., Tabima, J. F., and Grünwald, N. J. 2014. Poppr: an R package for genetic analysis of populations with clonal, partially clonal, and/or sexual reproduction. *PeerJ.* 2:e281.

- Klotz, L. J. 1978. Fungal, bacterial, and nonparasitic diseases and injuries originating in the seedbed, nursery, and orchard. Pages 1-66 in: *The Citrus Industry*. Vol. IV. W. Reuther, E. C. Calavan, and G. E., Carman, eds. University of -California, Division of Agricultural and Sciences, Oakland, CA.
- Li, H. 2013. Aligning sequence reads, clone sequences and assembly contigs with BWA-MEM. arXiv:1303.3997.
- Li, H., Handsaker, B., Wysoker, A., Fennell, T., Ruan, J., Homer, N., Marth, G., Abecasis, G., and Durbin, R. 2009. The sequence alignment/map format and SAMtools. *Bioinformatics* 25:2078-2079.
- Manni, M., Berkeley, M. R., Seppy, M., and Zdobnov, E. M. 2021. BUSCO: Assessing genomic data quality and beyond. *Curr. Protoc.* 1:e323.
- McKenna, A., Hanna, M., Banks, E., Sivachenko, A., Cibulskis, K., Kernytsky, A., Garimella, K., Altshuler, D., Gabriel, S., Daly, M., DePristo, M. A. 2010. The genome analysis toolkit: A MapReduce framework for analyzing next-generation DNA sequencing data. *Genome Res.* 20:1297–1303.
- Meirmans, P. G., and Hedrick, P. W. 2011. Assessing population structure:  $F_{ST}$  and related measures. *Mol. Ecol. Resour.* 11:5–18.
- Nei, M. 1973. Analysis of gene diversity in subdivided populations. *Proc. Natl. Acad. Sci. U. S. A.* 70:3321–3323.
- Nei, M., and Chesser, R. K. 1983. Estimation of fixation indices and gene diversities. *Ann. Hum. Genet.* 47:253–259.
- Raj, A., Stephens, M., and Pritchard, J. K. 2014. fastSTRUCTURE: Variational inference of population structure in large SNP data sets. *Genetics* 197:573–589.
- Shakya, S. K., Grünwald, N. J., Fieland, V. J., Knaus, B. J., Weiland, J. E., Maia, C., et al. 2021. Phylogeography of the wide-host range panglobal plant pathogen *Phytophthora cinnamomi*. *Mol. Ecol.* 30:5164–5178.
- Tabima, J. F., Gonen, L., Gómez-Gallego, M., Panda, P., Grünwald, N. J., Hansen, E. M., McDougal, R., LeBoldus, J. M., Williams, N. M. 2021. Molecular phylogenomics and population structure of *Phytophthora pluvialis*. *Phytopathology* 111:108–115.
- Tarailo-Graovac, M., and Chen, N. 2009. Using RepeatMasker to identify repetitive elements in genomic sequences. *Curr. Protoc. Bioinformatics* 25:4.10.1-4.10.14.

- Van Poucke, K., Haegeman, A., Goedefroit, T., Focquet, F., Leus, L., Jung, M. H., Nave, C., Redondo, M. A., Husson, C., Kostov, K., Lyubenova, A., Christova, P., Chandelier, A., Slavov, S. de Cock, A., Bonants, P., Werres, S., Palau, J. O., Marçais, B., Jung, T., Stenlid, J., Ruttink, T., and Heungens, K. 2021. Unravelling hybridization in *Phytophthora* using phylogenomics and genome size estimation. *IMA Fungus* 12:16.
- Verity, R., and Nichols, R. A. 2014. What is genetic differentiation, and how should we measure it-- $G_{ST}$ ,  $D$ , neither or both? *Mol. Ecol.* 23:4216–4225.
- Vogel, G., Gore, M. A., and Smart, C. D. 2021. Genome-wide association study in New York *Phytophthora capsici* isolates reveals loci involved in mating type and mefenoxam sensitivity. *Phytopathology* 111:204–216.
- Whitlock, M. C. 2011.  $G'_{ST}$  and  $D$  do not replace  $F_{ST}$ . *Mol. Ecol.* 20:1083–1091.
- Wickham, H. 2016. *ggplot2: Elegant graphics for data analysis (3e)*. Springer-Verlag New York.
- Winter, D. J. 2012. *mmod: an R library for the calculation of population differentiation statistics*. *Mol. Ecol. Resour.* 12:1158–1160.
- Xu, S., Chen, M., Feng, T., Zhan, L., Zhou, L., and Yu, G. 2021. Use *ggbreak* to effectively utilize plotting space to deal with large datasets and outliers. *Front. Genet.* 12:774846
- Xu, S., Li, L., Luo, X., Chen, M., Tang, W., Zhan, L., Dai, Z., Lam, T. T., Guan, Y, and Yu, G. 2022. *Ggtree: A serialized data object for visualization of a phylogenetic tree and annotation data*. *iMeta.* 1:e56.
- Zhang, F., Chen, H., Zhang, X., Gao, C., Huang, J., Lü, L., Shen, D., Wang, L., Huang, C., Ye, W., Zheng, X., Wang, Y., Vossen, J. H. and Dong, S. 2021. Genome analysis of two newly emerged potato late blight isolates sheds light on pathogen adaptation and provides tools for disease management. *Phytopathology* 111:96–107.

**Table 1.1** Isolates of *Phytophthora* spp. from California used in this study, their host, geographic origin, and year of isolation

<b>Species</b>	<b>Host</b>	<b>Geographic origin</b>	<b>Year</b>	<b>No. isolates</b>
<i>P. citrophthora</i>	<i>Citrus reticulata</i> , fruit	Central Valley	2014	1
	<i>C. sinensis</i> , fruit	Central Valley	2012	1
	<i>C. sinensis</i> , fruit	Central Valley	2013	4
	<i>C. sinensis</i> , fruit	Central Valley	2014	53
	<i>C. sinensis</i> , fruit	Central Valley	2016	4
	<i>C. sinensis</i> , fruit	Central Valley	2017	1
	<i>C. sinensis</i> , fruit	Inland Empire	2018	1
	<i>C. sinensis</i> , fruit	Inland Empire	2019	25
	<i>C. sinensis</i> , root	Ventura Co.	2000 <sup>a</sup>	1
	<i>C. sinensis</i> , fruit	Ventura Co.	2019	36
	<i>C. sinensis</i> , soil	Central Valley	2016	6
<i>P. syringae</i>	<i>C. limon</i> , fruit	Central Valley	2014	1
	<i>C. sinensis</i> , fruit	Central Valley	2012 <sup>a</sup>	11
	<i>C. sinensis</i> , fruit	Central Valley	2013	18
	<i>C. sinensis</i> , fruit	Central Valley	2014	41
	<i>C. sinensis</i> , fruit	Central Valley	2016	2
	<i>C. sinensis</i> , fruit	Central Valley	2017	1
	<i>C. sinensis</i> , fruit	Inland Empire	2019	36
	<i>C. sinensis</i> , fruit	Ventura Co.	2019	14
	<i>C. sinensis</i> , leaf litter	Central Valley	2016	6
	<i>C. sinensis</i> , leaf litter	Central Valley	2017	1
	<i>Juglans regia</i> , soil	Central Valley	2017	4
	<i>Prunus avium</i> , soil	Central Valley	2020	1
	<i>P. dulcis</i>	Central Valley	2007	2
	<i>P. dulcis</i>	Central Valley	2020	3
	<i>P. dulcis</i> , soil	Central Valley	2017	14

<sup>a</sup> Isolates *P. syringae* 2440 and *P. citrophthora* 4571 were used for construction of reference genomes.



**Table 1.2** QCAST output for reference genome assemblies of *Phytophthora citrophthora* and *P. syringae*

<b>Species</b>	<b>No. of contigs</b>	<b>Largest contig</b>	<b>Total length</b>	<b>N50</b>	<b>L50</b>	<b>GC%</b>	<b>#N/100 kbp</b>
<i>P. citrophthora</i>	4904	1537029	42171630	37026	274	51.8	274.58
<i>P. syringae</i>	6950	153696	52547088	22629	629	52.8	27.58

**Table 1.3** BUSCO output for reference genome assemblies of *Phytophthora citrophthora* and *P. syringae*

<b>BUSCO category</b>	<b>Species</b>			
	<b><i>P. citrophthora</i></b>		<b><i>P. syringae</i></b>	
	<b>% of total</b>	<b>N</b>	<b>% of total</b>	<b>N</b>
Complete	92.8%	281	92.4%	280
Complete, single copy	89.8%	272	89.1%	270
Complete, duplicated	3.0%	9	3.3%	10
Fragmented	1.7%	5	1.3%	4
Missing	5.5%	17	6.3%	19
Total	NA	303	NA	303

**Table 1.4** Average index of association ( $I_A$ ) for simulated and actual datasets for overall and regional populations of *Phytophthora citrophthora* and *P. syringae*

Data evaluation <sup>a</sup>	Dataset	$I_A$ values <sup>b</sup>	
		<i>P. citrophthora</i>	<i>P. syringae</i>
Simulated	Sexual	0.00329	0.00331
	Semi-clonal	0.0645	0.0645
	Clonal	0.168	0.167
Actual	Overall	0.842	0.231
	Central Valley	0.889	0.0557
	Inland Empire	0.0332	0.135
	Ventura Co.	0.0325	0.418
	Non-citrus <sup>c</sup>	-	0.149

<sup>a</sup> Simulated datasets were calculated from 10,000 randomly selected SNPs for 100 replicates.

<sup>b</sup> For each species, all actual datasets were significantly different from simulated datasets based on an analysis of variance and Tukey's HSD mean separation procedures ( $P < 0.05$ ).

<sup>c</sup> All isolates from this dataset originated from non-citrus hosts, whereas all other datasets had only isolates from citrus.

**Table 1.5** Summary statistics for the genetic diversity of the overall population and geographic sub-populations of *Phytophthora citrophthora* and *P. syringae*

Species	Population	Measures of diversity <sup>a</sup>				
		$H_O$	$H_S$	$H_T$	$D_{ST}$	$F_{ST}$
<i>P. citrophthora</i>	Overall	0.1103	0.0700	0.0709	0.0009	0.012
	Central Valley	0.1475	0.1127	0.1127	0	0
	Ventura Co.	0.0914	0.0484	0.0484	0	0
	Inland Empire	0.0920	0.0485	0.0485	0	0
<i>P. syringae</i> <sup>b</sup>	Overall	0.1125	0.1301	0.2374	0.1074	0.4522
	Central Valley	0.0841	0.0928	0.0928	0	0
	Ventura Co.	0.1066	0.1212	0.1212	0	0
	Inland Empire	0.0921	0.0856	0.0856	0	0
	Non-citrus	0.1670	0.2218	0.2218	0	0

<sup>a</sup> Measures of diversity are as follows:  $H_O$ : observed heterozygosity;  $H_S$ : within population gene diversity;  $H_T$ : total genetic diversity;  $D_{ST}$ : gene diversity among populations; and  $F_{ST}$ : fixation index,  $D_{ST}/H_T$ .

<sup>b</sup> Only isolates from citrus were included for the Overall, Central Valley, Ventura Co., and Inland Empire populations of *P. syringae*.

**Table 1.6** Genetic distance statistics of *Phytophthora citrophthora* and *P. syringae*

<b>Species</b>	<b>Comparison of populations</b>	<b><math>G_{ST}</math></b>	<b><math>G''_{ST}</math></b>	<b>Jost's <math>D</math></b>
<i>P. citrophthora</i>	Central Valley - Ventura Co.	0.0094	0.0202	0.0017
	Central Valley - Inland Empire	0.0072	0.0157	0.0013
	Ventura Co. - Inland Empire	-0.0045	-0.0094	-0.0005
<i>P. syringae</i>	Central Valley <sup>a</sup> - Ventura Co.	0.2397	0.4328	0.0752
	Central Valley <sup>a</sup> - Inland Empire	0.0732	0.1497	0.0155
	Ventura Co. - Inland Empire	0.2601	0.4602	0.0807
	Central Valley <sup>a</sup> - Non-citrus	0.4295	0.7121	0.2787
	Inland Empire - Non-citrus	0.4406	0.7221	0.2843
	Ventura Co. - Non-citrus	0.4032	0.6932	0.2787

<sup>a</sup> Only isolates from citrus were included for the Central Valley population of *P. syringae*.

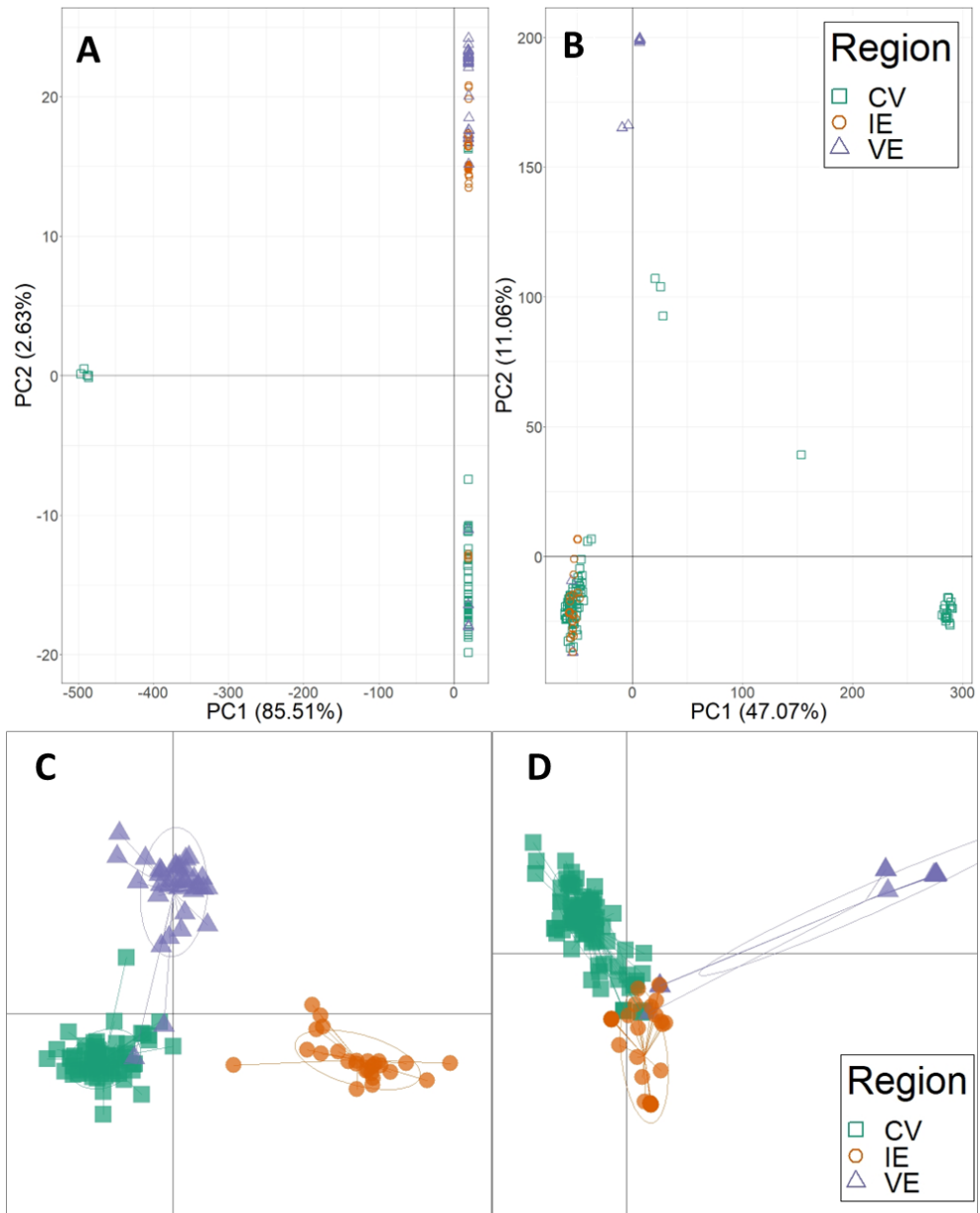


**Fig. 1.1.** A, B, Principal component analyses (PCA) and C, D, discriminant analyses of principal components (DAPC) visualizing the observed variance of A, C, *P. citrophthora* and B, D, *P. syringae* isolates grouped by geographic region. CV = Central Valley; IE = Inland Empire; VE = Ventura County.

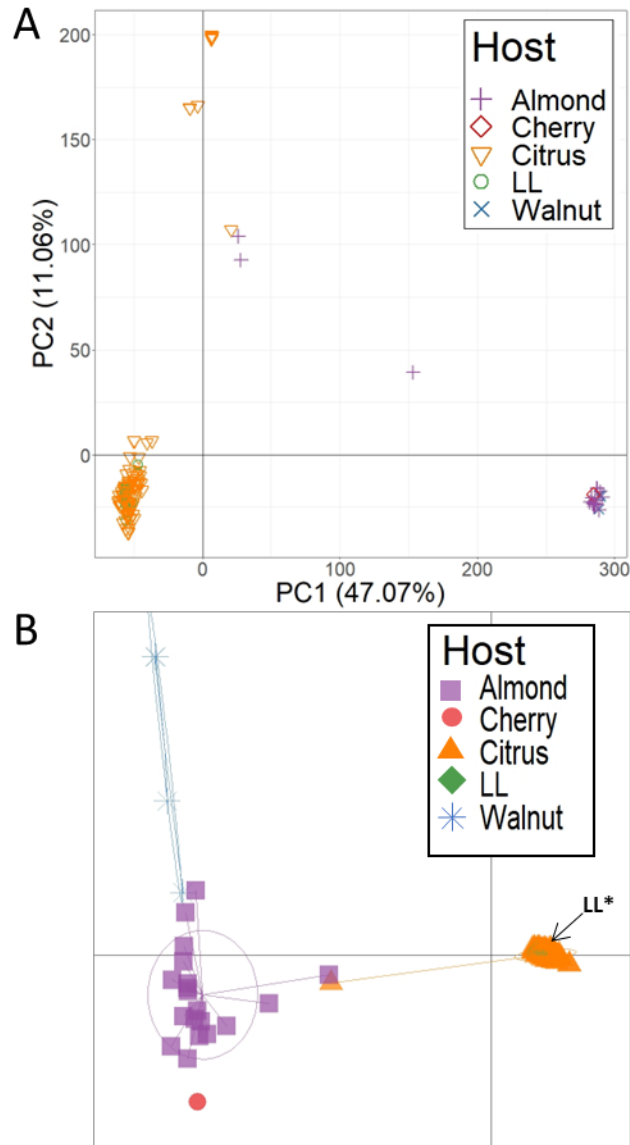


**Fig. 1.2. A**, Principal Component analysis (PCA) and **B**, discriminant analysis of principal components (DAPC) to visualize observed variance of *P. syringae* isolates grouped by host. LL = citrus leaf litter (LL\* = all LL isolates are within this cluster).

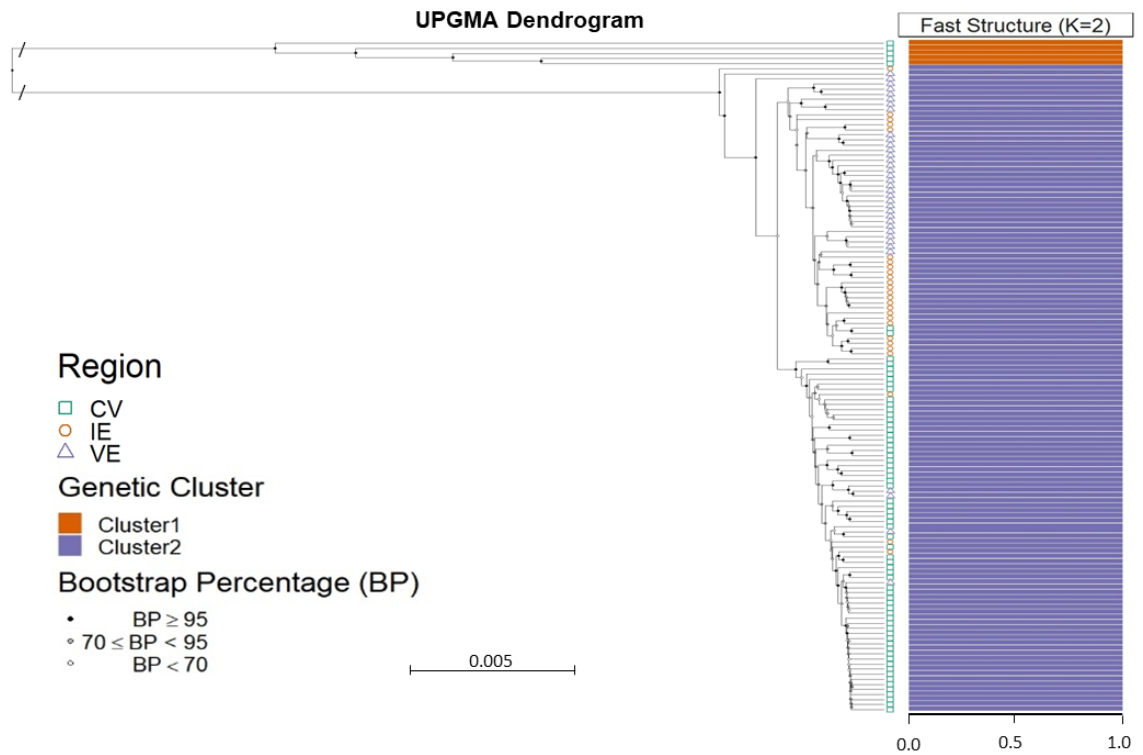


**Fig. 1.3.** Population structure of *P. citrophthora* visualized in UPGMA dendrograms that were constructed from observed variants and aligned to bar plots of the fastStructure output for each isolate. In the legend, color codes of the symbols refer to geographic origin of the isolates (CV = Central Valley; IE = Inland Empire; VE = Ventura Co.) In the fastStructure graphs, colors within a given bar represent the posterior membership probability of the isolate to be assigned to the predicted clusters that are color-coded in the squares of the legend.



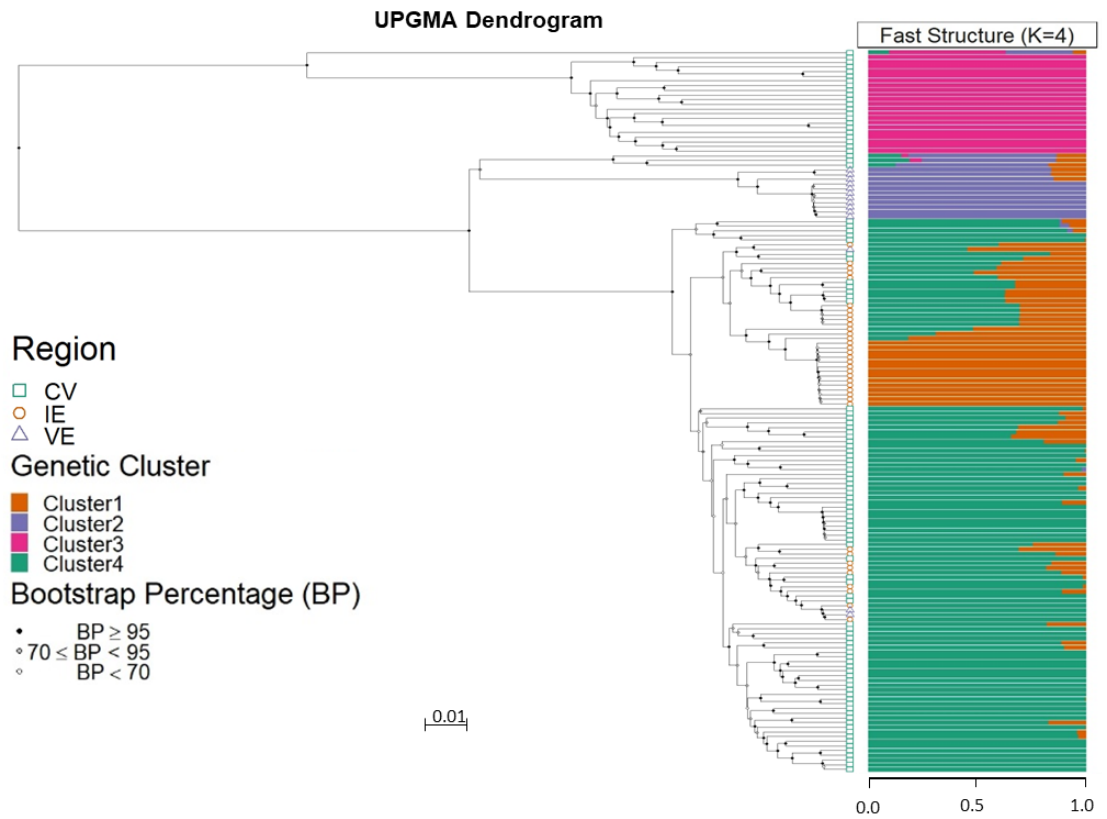


**Fig. 1.4.** Population structure of *P. syringae* visualized in UPGMA dendrograms that were constructed from observed variants and aligned to bar plots of the fastStructure output for each isolate. In the legend, color codes of the symbols refer to geographic origin of the isolates (CV = Central Valley; IE = Inland Empire; VE = Ventura Co.) In the fastStructure graphs, colors within a given bar represent the posterior membership probability of the isolate to be assigned to the predicted clusters that are color-coded in the squares of the legend.

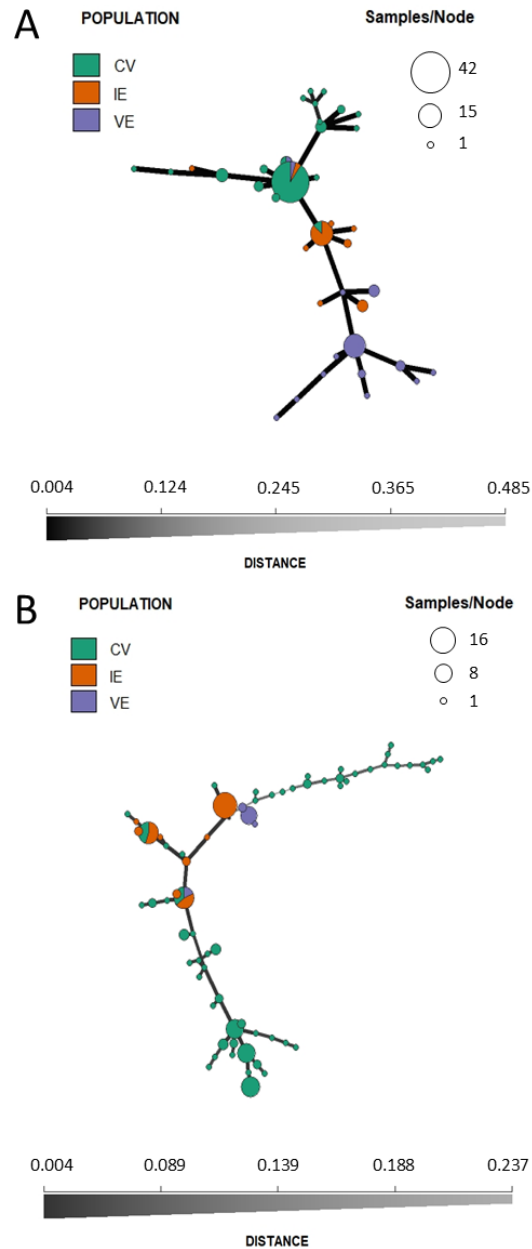


**Fig. 1.5.** Minimum spanning networks visualizing relationships of **A**, *P. citrophthora* and **B**, *P. syringae* isolates grouped by region (CV = Central Valley, IE = Inland Empire; VE = Ventura Co.). Nodes represent individual multilocus genotypes (MLGs). The distance scale represents bitwise distance (connecting lines) over all loci in a MLG. The size differences of the circles represent the number of individuals within that MLG.

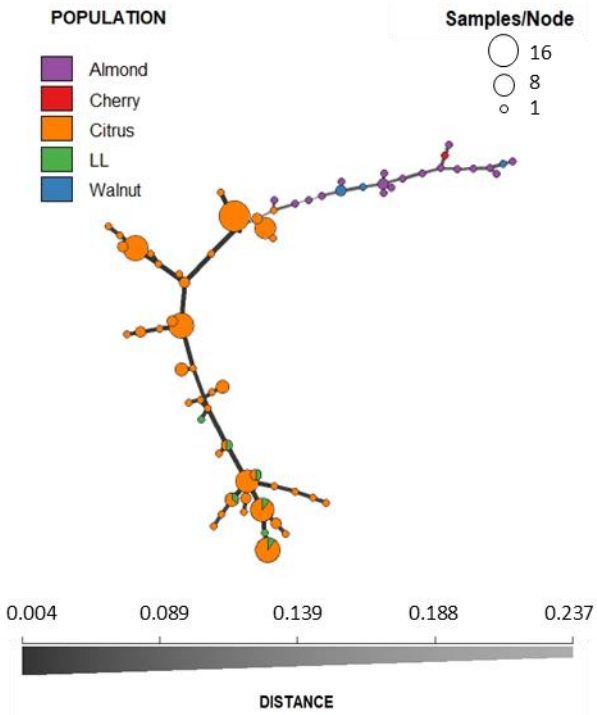


**Fig. 1.6.** Minimum spanning network visualizing relationships of *P. syringae* grouped by host type. Nodes represent individual multilocus genotypes (MLGs). The distance scale represents bitwise distance (connecting lines) over all loci in a MLG. The size differences in the circles represent the number of individuals within that MLG.

## **CHAPTER II. Regional Comparisons of Sensitivities of *P. citrophthora* and *P. syringae* Causing Citrus Brown Rot in California to Four New and Two Older Fungicides**

Reprinted with permission from: Riley, N.M., Förster, H., Adaskaveg, J.E. 2023. Regional comparisons of sensitivities of *P. citrophthora* and *P. syringae* causing citrus brown rot in California to four new and two older fungicides. Plant Disease. *Submitted*.

### **ABSTRACT**

Isolates of the citrus brown rot pathogens *P. citrophthora* and *P. syringae* from the Inland Empire (IE) and Ventura Co. (VE) regions of southern California were evaluated for their sensitivity to ethaboxam, fluopicolide, mandipropamid, and oxathiapiprolin, and the previously published baselines that were generated for Central Valley (CV) isolates of California were expanded. Fungicide toxicity was generally higher to CV isolates of both species for all four fungicides. Specific differences were found in the toxicity of ethaboxam to *P. syringae* where CV isolates on average were 6.8 or 8.2 times more sensitive than those from VE or IE regions, respectively. Based on grouping of isolates in an UPGMA dendrogram, as well as fastStructure analyses and plotting of PCAs, differences in ethaboxam sensitivity could be related to differences in genetic background of the isolates. Isolates of *P. citrophthora* from the IE and VE had slightly reduced (i.e., 1.5X) sensitivity to mandipropamid as compared with those from the CV and were found on distinct branches in the UPGMA dendrogram. Differences in genetic background of less sensitive isolates within each species indicate that these two phenotypes emerged multiple times independently. IE and VE isolates of both species were sensitive to mefenoxam. Moderate resistance to potassium phosphite (EC50 values of 25 to 75 µg/ml) was present in IE and VE isolates of *P. syringae*; whereas some IE isolates of *P.*

*citrophthora* were considered resistant with EC<sub>50</sub> values of up to 113.69 µg/ml.

Resistance to potassium phosphite did not relate to distinct genotypes.

## INTRODUCTION

Diseases caused by species of *Phytophthora* present a complex problem for citrus growers due to their ability to affect plants starting at their propagation in the nursery to tree maturity in the orchard. Newly germinated seedlings may be affected by damping-off, whereas *Phytophthora* root rot can cause reduced growth and even death of plants in the nursery and during orchard establishment, and cause tree decline and reduce production in mature orchards (Graham and Feichtenberger 2015). Additional *Phytophthora* diseases of citrus include foot rot and gummosis affecting tree crowns and trunks, as well as brown rot of fruit. Brown rot typically occurs on low hanging fruit on trees, and non-visible infections of harvested fruit may develop during transportation and storage and spread to adjacent non-infected fruit in shipping containers. In California, *P. citrophthora* and *P. syringae* are the primary species causing brown rot of citrus (Hao et al. 2018), while in other growing regions *P. palmivora*, *P. nicotianae*, and occasionally *P. citricola* are the major pathogens (Adaskaveg and Förster 2022; Erwin and Ribeiro 1996; Graham et al. 1998).

Management of these diseases can be achieved through the integration of cultural practices such as planting of tolerant cultivars, proper irrigation, and skirting of trees with the application of various Oomycota-targeted fungicide compounds (Adaskaveg and Förster 2022). Copper products (FRAC Code, FC M1) (FRAC 2022) that have been used in the past especially for management of brown rot have become less popular due to

phytotoxicity (Alva et al. 1993; Hippler et al. 2018) and potential environmental contamination of soil and watersheds. The overuse of phosphonates (FC P07/33; e.g., fosetyl-Al, potassium phosphite) to control infections of fruit, roots, and trunks and that of the phenylamides (FC 4; i.e., metalaxyl, mefenoxam) to control infections of roots and trunks have led to the development of resistance (Adaskaveg et al. 2017; Timmer et al. 1998). Efforts have therefore been made to increase the number of compounds with unique modes of action available for use on citrus in California against *Phytophthora* diseases. Recently registered compounds include the benzamide fluopicolide (FC 43) the carboxylic acid amide mandipropamid (FC 40), and the piperidinyl thiazole isoxazoline oxathiapiprolin (FC 49), whereas registration of the thiazole carboxamide ethaboxam (FC 22) is currently pending (Blum et al. 2010; Gray et al. 2018; Jiang et al. 2015; Pasteris et al. 2016; Uchida et al. 2005).

All four new compounds have single-site modes of action, and development of resistance in target populations is a concern. Therefore, vigilance in assessing potential resistance risk and monitoring target populations for resistance development is warranted. Baseline sensitivities of *Phytophthora* spp. affecting citrus in California to these new chemicals were previously established, and sensitivity to mefenoxam and potassium phosphite was characterized (Gray et al. 2018; Hao et al. 2021). These studies focused on isolates collected from the Central Valley (CV) of California. Most citrus production in the state is in this region, but a significant amount is also grown in southern counties including Riverside and San Bernardino Co. (i.e., the Inland Empire – IE), Ventura Co. (VE), as well as Imperial and San Diego Co. (Geisseler and Horwath 2016).

Investigations on the sensitivity of populations of *Phytophthora* spp. affecting citrus in some of these southern regions to the new compounds, as well as to mefenoxam and potassium phosphite will help to identify species and specific populations that may be subject to potential resistance development. In this study, our specific goals were to: 1) collect and evaluate *P. citrophthora* and *P. syringae* isolates in selected southern growing regions (i.e., the IE and VE) for their sensitivity to the new fungicides ethaboxam, fluopicolide, mandipropamid, and oxathiapiprolin as compared to the older compounds mefenoxam and potassium phosphite; 2) compare sensitivities to those of selected isolates from the CV previously determined (Gray et al. 2018; Hao et al. 2021) to establish expanded sensitivity ranges; and 3) utilize population genomic analyses to identify regional populations with increased potential for development of resistance and evaluate if sensitivity to specific fungicides can be related to specific genotypes.

## MATERIALS AND METHODS

**Isolate collection.** Selected isolates of *P. citrophthora* and *P. syringae* collected from brown-rotted citrus fruit (all from *Citrus sinensis* except one isolate from *C. reticulata*) in the CV of California between 2013 and 2015 were used from previous studies (Gray et al. 2018; Hao et al. 2021). Additional isolates were obtained from VE and the IE from symptomatic citrus fruit between 2018 and 2022. Isolations were done as described by Hao et al. (2018). Colonies resembling *Phytophthora* spp. were sub-cultured onto clarified 5% V8 agar (Ribeiro 1978). Species identification was based on morphology, TaqMan qPCR using species-specific probes (Hao et al. 2018) for a subset, and by genomic analyses of all isolates (Riley et al. 2023 *submitted for publication*). A

total of 84 isolates of *P. citrophthora* (35 from CV, 25 from IE, and 24 from VE) and 74 isolates of *P. syringae* (36 from CV, 24 from IE, and 14 from VE) were used in this study (Table 2.1).

**In vitro sensitivity of mycelial growth of isolates of *P. citrophthora* and *P. syringae* to Oomycota-specific fungicides.** For determining the sensitivity of mycelial growth to ethaboxam, fluopicolide, mandipropamid, oxathiapiprolin, and mefenoxam, the spiral gradient dilution (SGD) method was used (Förster et al. 2004). Each isolate was evaluated in two experiments for each fungicide. Isolates were grown on hydrophilic cellophane strips (5.5 by 0.5 cm; du Pont de Nemours, Wilmington, DE) on 10% V8C agar (Förster et al. 2004) by placing colonized agar strips between the cellophane strips. Plates were incubated for 1 to 2 weeks at 20°C until the mycelia had fully covered the strips. Aqueous stock solutions of ethaboxam (50 µg/ml), fluopicolide (117.6 µg/ml), mandipropamid (10 µg/ml), oxathiapiprolin (2.5 µg/ml), or mefenoxam (52.7 µg/ml for *P. citrophthora*, 15.8 µg/ml for *P. syringae*) were radially applied to 15-cm 10% V8C agar plates using a spiral plater (Autoplate 4000; Spiral Biotech, Norwood, MA) in the exponential deposition mode as previously described (Förster et al. 2004; Gray et al. 2018). Sterile water was applied to control plates. Plates were incubated at 20°C for 2 days (*P. citrophthora*) or 4 days (*P. syringae*). The location on each strip where mycelial growth was inhibited by 50% as compared with control plates was determined, and EC<sub>50</sub> (50% effective concentration) values were calculated using the SGE software (Spiral Biotech).



Sensitivity to potassium phosphite was evaluated using the agar dilution method (Hao et al. 2021). V8C agar (10%) was amended with final concentrations of 0 (control), 5, 25, or 100  $\mu\text{g/ml}$  potassium phosphite. Agar plugs 6 mm in diameter were transferred from the edge of actively growing cultures and placed into the center of two duplicated plates for each concentration. After incubation at 20°C for 4 days, colony diameters were measured, and percent inhibition was calculated based on growth of the control.  $\text{EC}_{50}$  values were calculated as described in Hao et al. (2021), and the experiment was performed twice for each isolate.

Average  $\text{EC}_{50}$  values for each fungicide were compared to sensitivity ranges previously reported (Gray et al. 2018; Hao et al. 2021). For ethaboxam, fluopicolide, mandipropamid, and oxathiapiprolin, isolates with average  $\text{EC}_{50}$  values higher, within, or lower than the reported ranges were categorized as “above baseline”, “within baseline”, or “below baseline”, respectively. For mefenoxam, isolates with  $\text{EC}_{50}$  values higher than the previously reported range (Gray et al. 2018) were categorized as “moderately resistant”, and those with values within or below the reported range were categorized as “sensitive”. For potassium phosphite, isolates with  $\text{EC}_{50}$  values  $<25 \mu\text{g/ml}$ , 25 to 75  $\mu\text{g/ml}$ , or  $>75 \mu\text{g/ml}$  were categorized as “sensitive”, “moderately resistant”, or “resistant”, respectively (Hao et al. 2021).

**Population genomic analyses.** DNA extraction, sequencing, and variant calling were performed as described by Riley et al. (2023 submitted). A subset of the data containing only isolates used in the current study was created using the BCFtools program from the Samtools Unix package (Danecek et al. 2021). Reference assemblies

for *P. citrophthora* and *P. syringae*, as well as the raw data for isolates used in this study have been deposited with links to BioProject accession number PRJNA1014129 in the NCBI BioProject database (<https://www.ncbi.nlm.nih.gov/bioproject/>). PCA analyses were conducted on non-clone corrected data for six fungicides evaluated using the adegenet R package (Jombart 2008), and the resulting PCA scores were plotted using the ggplot2 package (Wickham 2016) in R (version 4.1.3; R Core Team 2022). Unweighted pair-group method with arithmetic mean (UPGMA) dendrograms were generated for each species based on bitwise distance using the aboot function of the poppr R package (Kamvar et al. 2014). These were then plotted using the R package ggtree to extend the capabilities of ggplot2 (Xu et al. 2022). An associated matrix colored based on the sensitivity category assigned to each isolate for each fungicide was aligned to the UPGMA dendrogram for each species using the gheatmap function from the ggtree R package. The python program fastStructure (Raj et al. 2014) was used to analyze the population structure of each species, and the structure.py function was executed with a range of K probability clusters from 1 to 10, of which K=2 and K=4 were found to be the best fit for *P. citrophthora* and *P. syringae*, respectively. This population structure data was plotted using the pophelper package for R (Francis 2017), and the results were aligned to the UPGMA dendrograms and sensitivity heatmaps for each species.

**Statistical analysis.** EC<sub>50</sub> values for mycelial growth inhibition by each fungicide were analyzed using frequency histograms where EC<sub>50</sub> category bin widths were calculated from log<sub>10</sub>-transformed EC<sub>50</sub> values as described previously (Gray et al. 2018; Scott 1979). All statistical analyses were performed in R software (version 4.1.3; R Core

Team 2022). Results were considered significant at  $P \leq 0.05$ . Shapiro-Wilk tests of normality indicated that all sensitivity distributions for both species were non-normal, therefore,  $EC_{50}$  values for isolates from each region were compared using generalized linear models with the `glm` function of the R software. Various model distributions were evaluated, and a Gaussian distribution was determined to be the best fit for ethaboxam, fluopicolide, mandipropamid, oxathiapiprolin, and mefenoxam, while a log normal (*ln* transformed) distribution was found to be the best fit for potassium phosphite data. Pairwise least squares means (LSM) with the TUKEY adjustment were calculated for each chemical by region. Residuals for most models were not normally distributed; thus, the results of LSM analyses for each chemical were validated using a 1000x bootstrap.

## RESULTS

**In vitro sensitivity of mycelial growth of isolates of *P. citrophthora* and *P. syringae* from three regions to Oomycota-specific fungicides.** Scott's distribution histograms of  $EC_{50}$  values for *P. citrophthora* and *P. syringae* with frequency of isolates from each geographic region in each concentration range bin indicated by color code are shown in Figs. 2.1 and 2.2, respectively. For *P. citrophthora*, isolates from the three regions were mostly interspersed across the frequency distribution of each fungicide except for mandipropamid where IE and VE isolates generally had higher  $EC_{50}$  values than those from the CV (Fig. 2.1). Additionally, isolates from the IE and VE were mostly more sensitive than isolates from the CV. For *P. syringae*, isolates from the three regions were also interspersed among the fungicide frequency distributions except for ethaboxam

(Fig. 2.2). The distribution for ethaboxam appeared bimodal with IE and VE isolates being less sensitive.

The range, mean, and Tukey-adjusted LSM groupings of EC<sub>50</sub> values for isolates of *P. citrophthora* and *P. syringae* for each of the six fungicides evaluated are summarized in Tables 2.2 and 2.3, respectively. Results of the generalized linear models and LSM separations were validated with 1000x bootstrap analyses for each regional comparison and fungicide. Observed magnitude of bias in ethaboxam, fluopicolide, mandipropamid, oxathiapiprolin, and mefenoxam sensitivity data for both species was less than 3e-4 for all regional groups and less than 9e-5 for most groups, while the magnitude of bias observed in potassium phosphite sensitivity was less than 0.003 for all regional groups for both species. When compared with the results of the LSM originally calculated for each group, these magnitude of bias values were very small and indicated that the non-normal residuals and any other effects not accounted for in our models had no significant impact on the final results.

No resistance was detected to ethaboxam, fluopicolide, mandipropamid, and oxathiapiprolin in both species, but significant differences were present among isolates from the three growing regions. Thus, for *P. citrophthora*, significant ( $P < 0.05$ ) differences in sensitivity were revealed in regional isolates for all fungicides except for ethaboxam. These differences were in a very narrow range (differences in mean EC<sub>50</sub> values less than 2-fold) for the four new fungicides (Table 2.2). Mean EC<sub>50</sub> values for mefenoxam and potassium phosphite for CV isolates of this species were 2.2 or 3.9 times higher, respectively, than for VE isolates (Table 2.2). For *P. syringae*, mean EC<sub>50</sub> values

were in a narrow range for all fungicides except for ethaboxam, mefenoxam, and potassium phosphite. For this species, significant differences among growing regions were detected for ethaboxam where mean EC<sub>50</sub> values of IE and VE isolates were 8.2 or 6.8 times higher, respectively, than of CV isolates (Table 2.3). Overall, EC<sub>50</sub> values for both species were lowest for oxathiapiprolin (i.e., ranging from 0.0001 to 0.0009 µg/ml), followed by mandipropamid (i.e., ranging from 0.002 to 0.009 µg/ml). Among the new fungicides, values were highest for fluopicolide against *P. syringae* (ranging from 0.021 to 0.460 µg/ml), and for the fungicides overall, they were highest for potassium phosphite which ranged from 5.54 to 299.63 µg/ml for *P. citrophthora* and from 9.76 to 101.83 µg/ml for *P. syringae*.

**Population genomic analyses.** Combined UPGMA, sensitivity matrix, and fastStructure plots for both species exhibited patterns that suggest an association between sampling region and fungicide sensitivity (Fig. 2.3 & 2.4). For both species, UPGMA dendrograms and fastStructure membership probability primarily segregate isolates into groups by region, with mixing of populations occurring in some UPGMA branches and the selected fastStructure clusters (i.e., K=2 for *P. citrophthora*, and K=4 for *P. syringae*). This same pattern was not observed in the fungicide sensitivity matrices except for *P. citrophthora* sensitivity to mandipropamid and *P. syringae* sensitivity to ethaboxam. Thus, for *P. citrophthora*, most IE and VE isolates exhibited EC<sub>50</sub> values for mandipropamid above the previously established baseline, yet some closely related CV isolates in neighboring branches of the UPGMA dendrogram and in the same clusters of the fastStructure plot do not exhibit the same phenotype (Fig. 2.3). For *P. syringae*, most

VE and IE isolates that were associated with multiple UPGMA divisions and fastStructure clusters had EC<sub>50</sub> values for ethaboxam above the previously established baseline. Similar to *P. citrophthora*, CV isolates of *P. syringae* in neighboring branches of the UPGMA dendrogram and in the same clusters of the fastStructure plot were sensitive to ethaboxam (Fig 2.4).

For sensitivity to potassium phosphite, three isolates of *P. citrophthora* were classified as resistant, but no clear pattern was observed regarding their alignment to the UPGMA dendrogram. For *P. syringae*, a group of closely related IE isolates exhibited moderate resistance to potassium phosphite. Two CV isolates resistant to phosphite were identified but not associated with the group of IE isolates categorized as moderately resistant (Fig. 2.4). Additional isolates of both species were moderately resistant to phosphite were found in other UPGMA branches and not associated with any observed pattern described above.

PCA plots generated from genomic data of *P. citrophthora* isolates that were color-coded based on sensitivity to mandipropamid (Fig. 2.5A) or potassium phosphite (Fig. 2.5B), and of *P. syringae* isolates to ethaboxam (Fig. 2.5C) or potassium phosphite (Fig. 2.5D) support the results of Fig. 3 described above. Thus, the plots for *P. citrophthora* sensitivity to mandipropamid (Fig. 2.5A) and *P. syringae* sensitivity to ethaboxam (Fig. 2.5C) showed grouping of “above baseline” isolates and separation of those isolates from “within baseline” isolates. The plots for potassium phosphite (Fig. 2.5B and 2.5D respectively) are less conclusive, showing only loose groupings of

“moderately resistant” and “resistant” isolates with little separation from isolates categorized as “sensitive”.

## DISCUSSION

Evaluation of *P. citrophthora* and *P. syringae* isolates from the southern inland (i.e., IE) and coastal (i.e., VE) citrus growing regions of California for their sensitivity to ethaboxam, fluopicolide, mandipropamid, and oxathiapiprolin resulted in an expansion of the previously published baselines of these fungicides that were generated for isolates from the CV (Gray et al. 2018). Furthermore, our sensitivity testing of isolates of both species to mefenoxam and potassium phosphite that have been in use for over three decades on citrus provides valuable information to growers in the design of fungicide treatment programs based on the presence or absence of fungicide resistance in the different growing regions evaluated.

Among the new fungicides, significant differences among isolates from the three geographical regions were detected for fluopicolide, mandipropamid, and oxathiapiprolin for *P. citrophthora* and for ethaboxam and oxathiapiprolin for *P. syringae*. Fungicide toxicity was mostly higher (i.e., lower mean EC<sub>50</sub> values) for CV isolates of both species. The differences observed are unlikely to be accounted for by procedural changes in the evaluation method used for CV isolates in the previous (Gray et al. 2018) and for IE and VE isolates in the current study because the same equipment was used, and some of the same personnel were involved. Differences in toxicity were mostly in a very narrow

range with a less than 2-fold change in mean EC<sub>50</sub> values, and none of the isolates was determined to be resistant. Therefore, the efficacy of field applications with these new fungicides will unlikely be compromised by these slightly higher EC<sub>50</sub> values. The greatest difference was present for toxicity against ethaboxam in isolates of *P. syringae* where CV isolates were 6.8 or 8.2 times more sensitive than those from VE or the IE, respectively, and it remains to be determined if this difference will affect fungicide performance. In a similar study, others have characterized *P. capsici* populations by geography, host, and fluopicolide sensitivity, and two strongly supported genetic clusters corresponded with isolate sensitivity to the fungicide (Parada-Rojas and Quesada-Ocampo 2022). In the latter study, there was, however, only a weak correlation between fungicide sensitivity and geographical region, and this was explained by random mating of *P. capsici*.

The detected shifts in sensitivity to ethaboxam, fluopicolide, mandipropamid, and oxathiapiprolin are unlikely the result of exposure of collected isolates to these new fungicides that were only registered on citrus starting in 2019, with registration of ethaboxam still pending. Registration on other crops (e.g., annual vegetables) in California, some of which may be cultivated in proximity to citrus orchards in VE but not in areas of the IE where sampling of brown-rotted fruit was done, only occurred a few years before. Based on our grouping of isolates in the UPGMA dendrogram, as well as fastStructure analyses and plotting of PCAs, differences in sensitivity to fungicides could be related to differences in general genetic background of the isolates. Thus, IE and VE isolates of *P. syringae* with reduced sensitivity to ethaboxam were mostly found separate



from the more sensitive CV isolates in the UPGMA dendrogram and were generally assigned to different fastStructure clusters. Similarly, isolates of *P. citrophthora* from the IE and VE with a slightly reduced (i.e., 1.5-fold) sensitivity to mandipropamid as compared with those from the CV were mostly genetically distinct and were found on distinct branches in the UPGMA dendrogram. Based on studies with repeated applications of sub-lethal or excessive doses of mandipropamid on mixed isolates of *P. infestans* where no resistance selection occurred, the probability of resistance development in field populations was considered to be low (Cohen et al. 2007). In studies on flumorph that like mandipropamid is a member of the carboxylic acid amides and has high activity against Oomycota organisms, high resistance phenotypes in *P. sojae* developed gradually from isolates with low resistance in a stepwise process through accumulation of mutations in the Cesa3 target protein (Cai et al. 2021). Therefore, our observed slight decrease in sensitivity of *P. citrophthora* to mandipropamid may represent a first step in the selection process to resistance. Our population genomic analyses indicated that isolates less sensitive to ethaboxam or mandipropamid had slightly different genetic backgrounds, and therefore, reduced sensitivity to each of these fungicides likely emerged multiple times independently.

Although mefenoxam has been available to citrus growers for many years, and high resistance ( $EC_{50} > 100 \mu\text{g/ml}$ ) has been reported in *Phytophthora* spp. on other crops (Hu et al. 2008; Marin et al. 2021), all isolates included in our study were determined to be sensitive to this fungicide. One CV isolate each of *P. citrophthora* and *P. syringae* had  $EC_{50}$  values slightly higher (i.e.,  $0.160 \mu\text{g/ml}$  and  $0.090 \mu\text{g/ml}$ , respectively) than the

previously evaluated isolates from the CV (i.e., 0.150 µg/ml and 0.082 µg/ml, respectively; Gray et al. 2018).

In contrast, isolates conferring field resistance to potassium phosphite were previously reported from some CV locations, and EC<sub>50</sub> values were as high as 299.6 µg/ml for *P. citrophthora* and 162.4 µg/ml for *P. syringae* (Hao et al. 2021). Brown rot of citrus caused by these isolates was not managed using registered rates of potassium phosphite in preharvest treatments (Hao et al. 2021). Generally, potassium phosphite has been considered as low risk for resistance development (FRAC 2022). Among *Phytophthora* species, however, resistance has also been reported for *P. capsici* (Veena et al. 2010) and *P. cinnamomi* (Belisle et al. 2019; Wilkinson et al. 2001). In our study, only moderate resistance with EC<sub>50</sub> values of 25 to 75 µg/ml (based on Hao et al. 2021) but no resistance with EC<sub>50</sub> values >75 µg/ml was detected in *P. syringae* isolates from the IE and VE. *P. citrophthora* isolates from the IE were more variable in their sensitivity to potassium phosphite with a mean EC<sub>50</sub> value of 14.91, but some isolates were considered resistant to phosphite with EC<sub>50</sub> values of up to 113.69 µg/ml. While some small groupings of moderately resistant isolates of *P. syringae* were observed when aligned to the UPGMA dendrogram and fastStructure output, these groupings and other isolates with this phenotype did not separate into distinct genotype clusters as observed with mandipropamid and ethaboxam for *P. citrophthora* and *P. syringae*, respectively. The lack of any pattern was also visualized in the PCA plots generated from potassium phosphite sensitivity data for both species. This difference in resistance development between mefenoxam and potassium phosphite can be explained in part by their usage patterns:

mefenoxam is much more expensive and is therefore less commonly applied, whereas the cost-effective and highly efficacious potassium phosphite has sometimes been over-used in the absence of other treatment alternatives with different modes of action. These results indicate that mefenoxam can still be used effectively in all three growing regions for managing citrus diseases caused by *P. citrophthora* and *P. syringae*, whereas usage of potassium phosphite ideally should be based on assessment of pathogen sensitivity at a specific location to avoid further increases in frequency and magnitude of resistance and to maintain this compound as a valuable treatment option in a rotational or mixture program.

Our data provide evidence for regional differences in fungicide sensitivity and indicate that for establishing baseline sensitivities, isolates from multiple growing regions should be used. We present an expanded baseline for some of the new fungicides evaluated because isolates from growing regions not previously surveyed were collected before registration and/or commercial use. Fungicide sensitivity data were related to genomic characterization of isolates by geographical region.

The information obtained in our study could be used to predict resistance potential for these two *Phytophthora* species in the geographic regions where they were collected. For example, because of often higher EC<sub>50</sub> values found in IE and VE isolates of *P. citrophthora* for mandipropamid and of *P. syringae* for ethaboxam, these species are possibly at higher risk for resistance development to these respective fungicides. Population structure analyses indicated that these regional isolates were mostly genetically distinct from CV isolates, and usage of these fungicides will likely favor

selection of resistance if these fungicides are over-used. The sensitivity of California *P. citrophthora* isolates to mandipropamid and of *P. syringae* isolates to ethaboxam should be closely monitored once these fungicides are in commercial use especially in the IE and VE regions that are at higher risk.

### LITERATURE CITED

- Adaskaveg, J. E., and Förster, H. 2022. APS Book. Postharvest diseases of citrus. Pages 403-422 in: Postharvest Pathology of Fruit and Nut Crops – Principles, Concepts, and Management Practices. J. E. Adaskaveg, H. Förster, and D. B. Prusky, eds. American Phytopathological Society Press, St. Paul, MN.
- Adaskaveg, J. E., Förster, H., Hao, W., and Gray, M. 2017. Potassium phosphite resistance and new modes of action for managing *Phytophthora* diseases of citrus in the United States. Pages 205-210 in: Modern fungicides and antifungal compounds, Vol. VIII. H. B. Deising, B. Fraaije, A. Mehl, E. C. Oerke, H. Sierotzki, and G. Stammler, eds. Deutsche Phytomedizinische Gesellschaft, Braunschweig, Germany.
- Alva, A. K.; Graham, J. H.; Tucker, D. P. H. 1993. Role of calcium in amelioration of copper phytotoxicity for citrus. *Soil Sci.* 155:211-218.
- Belisle, R. J., Hao, W., McKee, B., Arpaia, M. L., Manosalva, P., and Adaskaveg, J. E. 2019. New Oomycota fungicides with activity against *Phytophthora cinnamomi* and their potential use for managing avocado root rot in California. *Plant Dis.* 103:2024-2032.
- Blum, M., Boehler, M., Randall, E., Young, V., Csukai, M., Kraus, S., Moulin, F., Scalliet, G., Avrova, A. O., and Whisson, S. C. 2010. Mandipropamid targets the cellulose synthase-like PiCesA3 to inhibit cell wall biosynthesis in the oomycete plant pathogen, *Phytophthora infestans*. *Mol. Plant Pathol.* 11: 227-243.
- Cai, M., Zhang, C., Wang, W., Peng, Q., Song, X., Tyler, B. M., and Liu, X. 2021. Stepwise accumulation of mutations in Cesa3 in *Phytophthora sojae* results in increasing resistance to CAA fungicides. *Evol. Appl.* 14:996–1008.
- Cohen, Y., Rubin, E., Hadad, T., Gotlieb, D., Sierotzki, H., and Gisi, U. 2007. Sensitivity of *Phytophthora infestans* to mandipropamid and the effect of enforced selection pressure in the field. *Plant Pathol.* 56:836–842.

- Danecek, P., Bonfield, J. K., Liddle, J., Marshall, J., Ohan, V., Pollard, M. O., Whitwham, A., Keane, T., McCarthy, S. A., Davies, R. M., and Li, H. 2021. Twelve years of SAMtools and BCFtools. *Gigascience* 10:giab008.
- Erwin, D. C., and Ribeiro, O. K. 1996. *Phytophthora Diseases Worldwide*. APS Press. St. Paul, MN.
- Förster, H., Kanetis, L., and Adaskaveg, J. E. 2004. Spiral gradient dilution, a rapid method for determining growth responses and 50% effective concentration values in fungus-fungicide interactions. *Phytopathology* 94:163-170.
- FRAC. 2022. FRAC Code List 2022: Fungicides sorted by mode of action (including FRAC Code numbering). Online publication. <http://www.frac.info>.
- Francis, R. M. 2017. pophelper: an R package and web app to analyse and visualize population structure. *Mol. Ecol. Resour.* 17:27–32.
- Geisseler, D., and Horwath, W. R. 2016. Citrus production in California. [https://apps1.cdfa.ca.gov/FertilizerResearch/docs/Citrus\\_Production\\_CA.pdf](https://apps1.cdfa.ca.gov/FertilizerResearch/docs/Citrus_Production_CA.pdf).
- Graham, J., and Feichtenberger, E. 2015. Citrus *Phytophthora* diseases: Management challenges and successes. *J. Citrus Pathol.* 2. <https://doi.org/10.5070/C421027203>.
- Graham, J. H., Timmer, L. W., Drouillard, D. L., and Peever, T. L. 1998. Characterization of *Phytophthora* spp. causing outbreaks of citrus brown rot in Florida. *Phytopathology* 88:724-729.
- Gray, M. A., Hao, W., Förster, H., and Adaskaveg, J.E. 2018. Baseline sensitivities of new fungicides and their toxicity to selected life stages of *Phytophthora* species from citrus in California. *Plant Dis.* 102:734-742.
- Hao, W., Förster, H., Adaskaveg, J. E. 2021. Resistance to potassium phosphite in *Phytophthora* species causing citrus brown rot and integrated practices for management of resistant isolates. *Plant Dis.* 105:972-977.
- Hao, W., Miles, T.D., Martin, F.N., Browne, G.T., Förster, H., and Adaskaveg, J.E. 2018. Temporal occurrence and niche preferences of *Phytophthora* species causing brown rot of citrus in the Central Valley of California. *Phytopathology* 108:384-391.
- Hippler, F. W. R., Peten, G., Boaretto, R. M., Quaggio, J. A., Azevedo, R. A., and Mattos, D. 2018. Mechanisms of copper stress alleviation in citrus trees after metal uptake by leaves or roots. *Environ. Sci. Pollut. Res.* 25:13134–13146.

- Hu, J. H., Hong, C. X., Stromberg, E. L., and Moorman, G. W. 2008. Mefenoxam sensitivity and fitness analysis of *Phytophthora nicotianae* isolates from nurseries in Virginia, USA. *Plant Pathol.* 57:728-736.
- Jiang, L., Wang, H., Xu, H., Qiao, K., Xia, X., and Wang, K. 2015. Transportation behaviour of fluopicolide and its control effect against *Phytophthora capsici* in greenhouse tomatoes after soil application. *Pest Manage. Sci.* 71: 1008-1014.
- Jombart, T. 2008. adegenet: a R package for the multivariate analysis of genetic markers. *Bioinformatics* 24:1403–1405.
- Kamvar, Z. N., Tabima, J. F., and Grünwald, N. J. 2014. Poppr: an R package for genetic analysis of populations with clonal, partially clonal, and/or sexual reproduction. *PeerJ.* 2:e281.
- Marin, M. V., Seijo, T. E., Zuchelli, E., and Peres, N. A. 2011. Resistance to mefenoxam of *Phytophthora cactorum* and *Phytophthora nicotianae* causing crown and leather rot in Florida strawberry. *Plant Dis.* 105:3490-3495.
- Parada-Rojas, C. H., and Quesada-Ocampo, L. M. 2022. *Phytophthora capsici* populations are structured by host, geography, and fluopicolide sensitivity. *Phytopathology* 112:1559-1567.
- Pasteris, R. J., Hanagan, M. A., Bisaha, J. J., Finkelstein, B. L., Hoffman, L. E., Gregory, V., Andreassi, J. L., Sweigard, J. A., Klyashchitsky, B. A., Henry, Y. T., and Berger, R. A. 2016. Discovery of oxathiapiprolin, a new oomycete fungicide that targets an oxysterol binding protein. *Bioorg. Med. Chem.* 24: 354-361.
- R Core Team. 2022. R: A language and environment for statistical computing. R Foundation for Statistical Computing, Vienna, Austria. <http://www.R-project.org/>.
- Raj, A., Stephens, M., and Pritchard, J. K. 2014. fastSTRUCTURE: Variational inference of population structure in large SNP data sets. *Genetics* 197:573–589.
- Ribeiro, O. K. 1978. A Source Book of the Genus *Phytophthora*. J. Cramer, Vaduz, Liechtenstein.
- Riley, N., Förster, H., and Adaskaveg, J. E. 2023. Diversity and clonality in populations of *Phytophthora citrophthora* and *P. syringae* causing brown rot of citrus in California. *Phytopathology* *Submitted*.
- Scott, D. W. 1979. On optimal and data-based histograms. *Biometrika* 66:605-610.

- Timmer, L. W., Graham, J. H., and Zitko, S. E. 1998. Metalaxyl-resistant isolates of *Phytophthora nicotianae*: Occurrence, sensitivity, and competitive ability on citrus. *Plant Dis.* 82:254-261.
- Uchida, M., Roberson, R. W., Chun, S. J., and Kim, D. S. 2005. In vivo effects of the fungicide ethaboxam on microtubule integrity in *Phytophthora infestans*. *Pest Manag. Sci.* 61:787-792.
- Veena, S. S., Anandaraj, M., and Sarma, Y. R. 2010. Variability in the sensitivity of *Phytophthora capsici* isolates to potassium phosphonate. *Indian Phytopathol.* 63:71-75.
- Wickham, H. 2016. *ggplot2: Elegant graphics for data analysis (3e)*. Springer-Verlag New York.
- Wilkinson, C. J., Shearer, B. L., Jackson, T. J., and Hardy, G. E. S. 2001. Variation in sensitivity of Western Australian isolates of *Phytophthora cinnamomi* to phosphite in vitro. *Plant Pathol.* 50:83-89.
- Xu, S., Li, L., Luo, X., Chen, M., Tang, W., Zhan, L., Dai, Z., Lam, T. T., Guan, Y., and Yu, G. 2022. Ggtree: A serialized data object for visualization of a phylogenetic tree and annotation data. *iMeta.* 1:e56.

**Table 2.1** Isolates of *Phytophthora* spp. from citrus fruit with brown rot in California used in this study, their geographic origin, and year of isolation

<b>Species</b>	<b>Host</b>	<b>Geographic origin<sup>a</sup></b>	<b>Year</b>	<b>No. isolates</b>
<i>P. citrophthora</i>	<i>Citrus reticulata</i>	Central Valley	2014	1
	<i>C. sinensis</i>	Central Valley	2013	3
	<i>C. sinensis</i>	Central Valley	2014	31
	<i>C. sinensis</i>	Inland Empire	2018	1
	<i>C. sinensis</i>	Inland Empire	2019	24
	<i>C. sinensis</i>	Ventura Co.	2019	24
<i>P. syringae</i>	<i>C. sinensis</i>	Central Valley	2012	5
	<i>C. sinensis</i>	Central Valley	2013	9
	<i>C. sinensis</i>	Central Valley	2014	22
	<i>C. sinensis</i>	Inland Empire	2019	24
	<i>C. sinensis</i>	Ventura Co.	2019	14

<sup>a</sup> All isolates from the Central Valley were obtained from a previous study (Gray et al. 2018).



**Table 2.2** In vitro sensitivities of mycelial growth of isolates of *Phytophthora citrophthora* from three major citrus growing regions in California to six Oomycota fungicides<sup>a</sup>

<b>Fungicide</b>	<b>Region</b>	<b>Range</b>	<b>Mean</b>	<b>Tukey LSM groups<sup>b</sup></b>
Ethaboxam	Overall	0.017 - 0.146	0.064	-
	Central Valley	0.020 - 0.107	0.068	a
	Inland Empire	0.020 - 0.136	0.063	a
	Ventura Co.	0.017 - 0.146	0.061	a
Fluopicolide	Overall	0.037 - 0.092	0.060	-
	Central Valley	0.037 - 0.085	0.049	a
	Inland Empire	0.060 - 0.092	0.074	c
	Ventura Co.	0.043 - 0.091	0.061	b
Mandipropamid	Overall	0.003 - 0.009	0.005	-
	Central Valley	0.003 - 0.005	0.004	a
	Inland Empire	0.005 - 0.009	0.006	b
	Ventura Co.	0.004 - 0.008	0.006	b
Oxathiapiprolin	Overall	0.0002 - 0.0009	0.00038	-
	Central Valley	0.0002 - 0.0009	0.00029	a
	Inland Empire	0.0003 - 0.0008	0.00051	c
	Ventura Co.	0.0002 - 0.0005	0.00037	b
Mefenoxam	Overall	0.015 - 0.160	0.038	-
	Central Valley	0.026 - 0.160	0.052	b
	Inland Empire	0.018 - 0.059	0.031	a
	Ventura Co.	0.015 - 0.033	0.024	a
Potassium phosphite	Overall	5.54 - 299.63	18.67	-
	Central Valley	5.54 - 299.63	29.10	b
	Inland Empire	9.07 - 113.69	14.91	ab
	Ventura Co.	5.62 - 11.44	7.39	a

<sup>a</sup> Isolates (35 from the Central Valley, 25 from the Inland Empire, and 24 from Ventura Co.) were collected from citrus fruit with brown rot symptoms between 2013 and 2022.

<sup>b</sup> Statistical comparisons were done separately for each fungicide.

**Table 2.3** In vitro sensitivities of mycelial growth of isolates of *Phytophthora syringae* from three major citrus growing regions in California to six Oomycota fungicides<sup>a</sup>

<b>Fungicide</b>	<b>Region</b>	<b>Range</b>	<b>Mean</b>	<b>Tukey LSM groups<sup>b</sup></b>
Ethaboxam	Overall	0.001 - 0.076	0.026	-
	Central Valley	0.001 - 0.029	0.006	a
	Inland Empire	0.035 - 0.076	0.049	c
	Ventura Co.	0.028 - 0.054	0.041	b
Fluopicolide	Overall	0.021 - 0.460	0.072	-
	Central Valley	0.021 - 0.460	0.068	a
	Inland Empire	0.049 - 0.133	0.079	a
	Ventura Co.	0.055 - 0.102	0.071	a
Mandipropamid	Overall	0.002 - 0.006	0.003	-
	Central Valley	0.002 - 0.006	0.003	a
	Inland Empire	0.003 - 0.004	0.003	a
	Ventura Co.	0.002 - 0.004	0.003	a
Oxathiapiprolin	Overall	0.0001 - 0.0005	0.0003	-
	Central Valley	0.0001 - 0.0005	0.0003	ab
	Inland Empire	0.0002 - 0.0003	0.0003	b
	Ventura Co.	0.0001 - 0.0002	0.0002	a
Mefenoxam	Overall	0.003 - 0.090	0.011	-
	Central Valley	0.003 - 0.090	0.011	a
	Inland Empire	0.007 - 0.029	0.012	a
	Ventura Co.	0.005 - 0.026	0.011	a
Potassium phosphite	Overall	9.76 - 101.83	23.61	-
	Central Valley	9.76 - 101.83	23.79	a
	Inland Empire	17.63 - 37.14	25.54	a
	Ventura Co.	14.68 - 27.45	19.85	a

<sup>a</sup> Isolates (36 from the Central Valley, 24 from the Inland Empire, and 14 from Ventura Co.) were collected from orange fruit with brown rot symptoms between 2013 and 2022.

<sup>b</sup> Statistical comparisons were done separately for each fungicide.

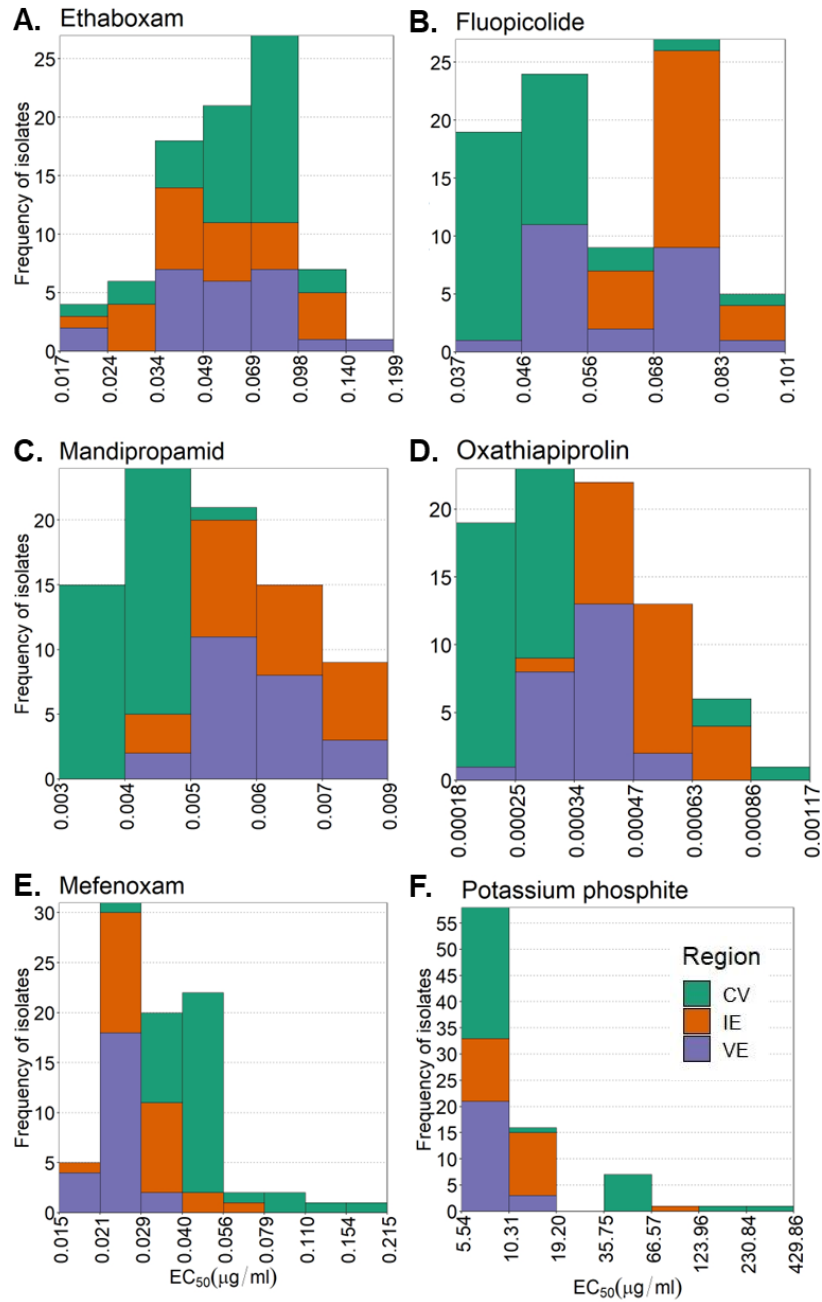


**Fig. 2.1.** Frequency histograms of EC<sub>50</sub> values of *P. citrophthora* to **A**, ethaboxam, **B**, fluopicolide, **C**, mandipropamid, **D**, oxathiapiprolin, **E**, mefenoxam, and **F**, potassium phosphite. Bar height indicates the number of isolates within each bin, and bin width was calculated based on Scott (1979). Bars are color-coded based on the geographic origin of isolates (CV = Central Valley; IE = Inland Empire; VE = Ventura Co.).

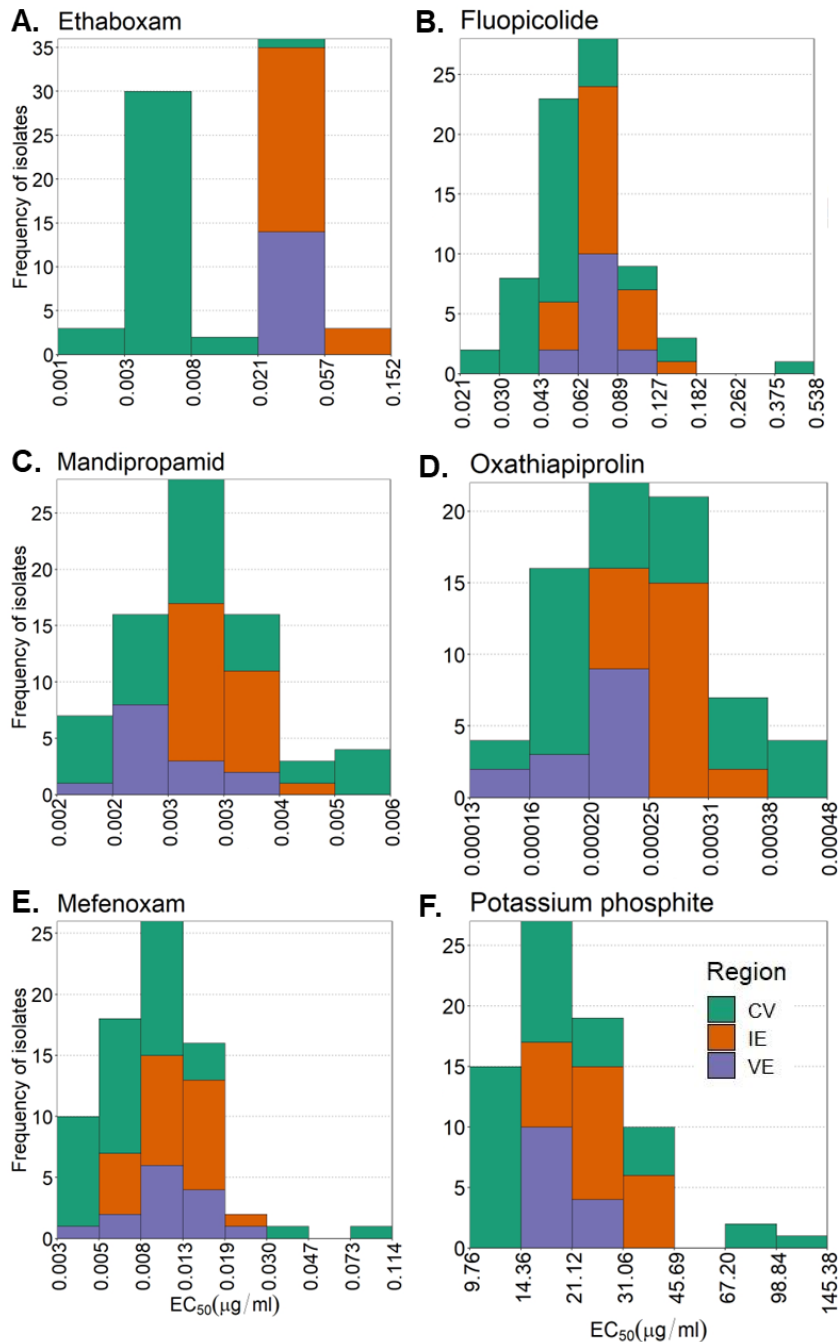


**Fig. 2.2.** Frequency histograms of EC<sub>50</sub> values of *P. syringae* to **A**, ethaboxam, **B**, fluopicolide, **C**, mandipropamid, **D**, oxathiapiprolin, **E**, mefenoxam, and **F**, potassium phosphite. Bar height indicates the number of isolates within each bin, and bin width was calculated based on Scott (1979). Bars are color-coded based on their geographic origin of isolates (CV = Central Valley; IE = Inland Empire; VE = Ventura Co.).

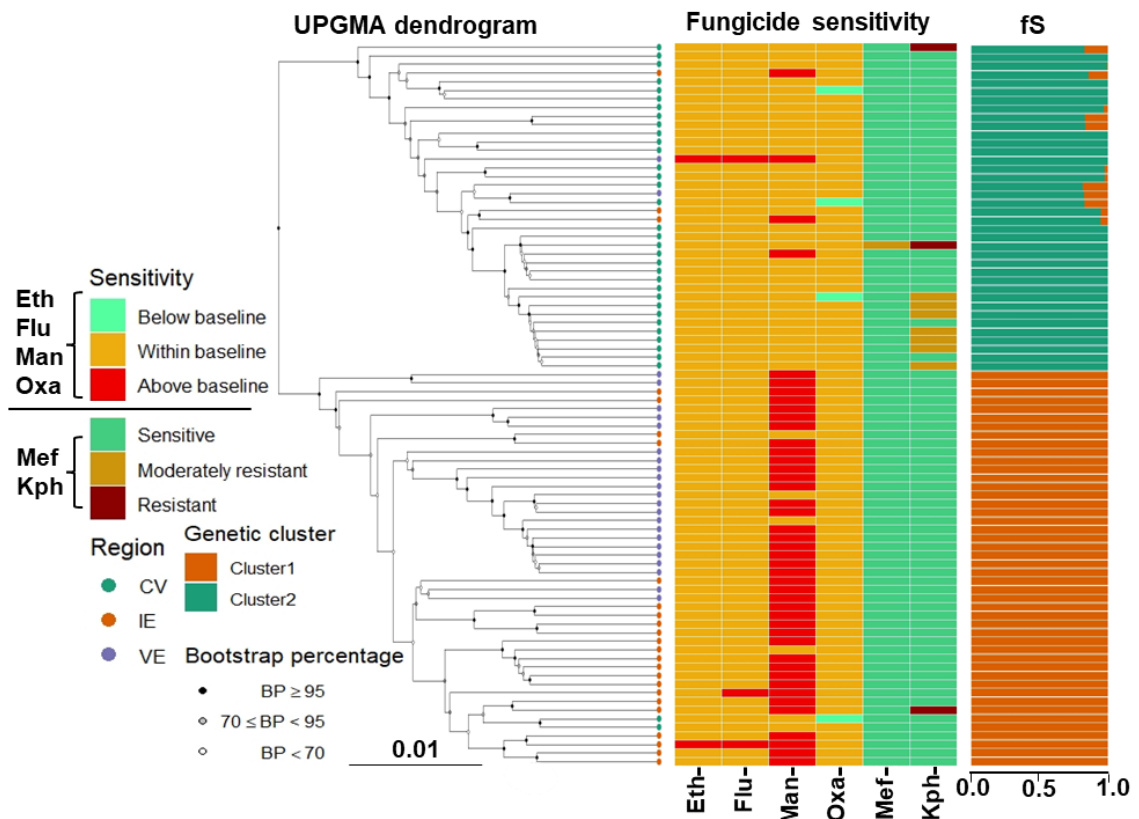


**Fig. 2.3.** Population structure of *P. citrophthora* visualized in UPGMA dendrograms that were constructed from observed variants and aligned to sensitivity to ethaboxam (Eth), fluopicolide (Flu), mandipropamid (Man), oxathiapiprolin (Oxa), mefenoxam (Mef), and potassium phosphite (Kph). Bootstrap percentages (BP) are shown at the nodes of the dendrogram as  $BP \geq 95$ ,  $70 \leq BP < 95$ , and  $BP < 70$ . fastStructure (fS) cluster membership probability is shown for each isolate with  $K=2$  for *P. citrophthora* and  $K=4$  for *P. syringae*. In the legend, color codes of the circles refer to geographic origin of the isolates (CV = Central Valley; IE = Inland Empire; VE = Ventura Co.). Fungicide sensitivity is color-coded for the new fungicides as below, within, and above baselines and for the older fungicides as sensitive, moderately resistant, and resistant as compared to previously determined values for CV isolates (Gray et al. 2018). In the fastStructure graphs, colors within a given bar represent the posterior membership probability of the isolate to be assigned to the predicted genetic clusters that are color-coded in the squares of the legend.

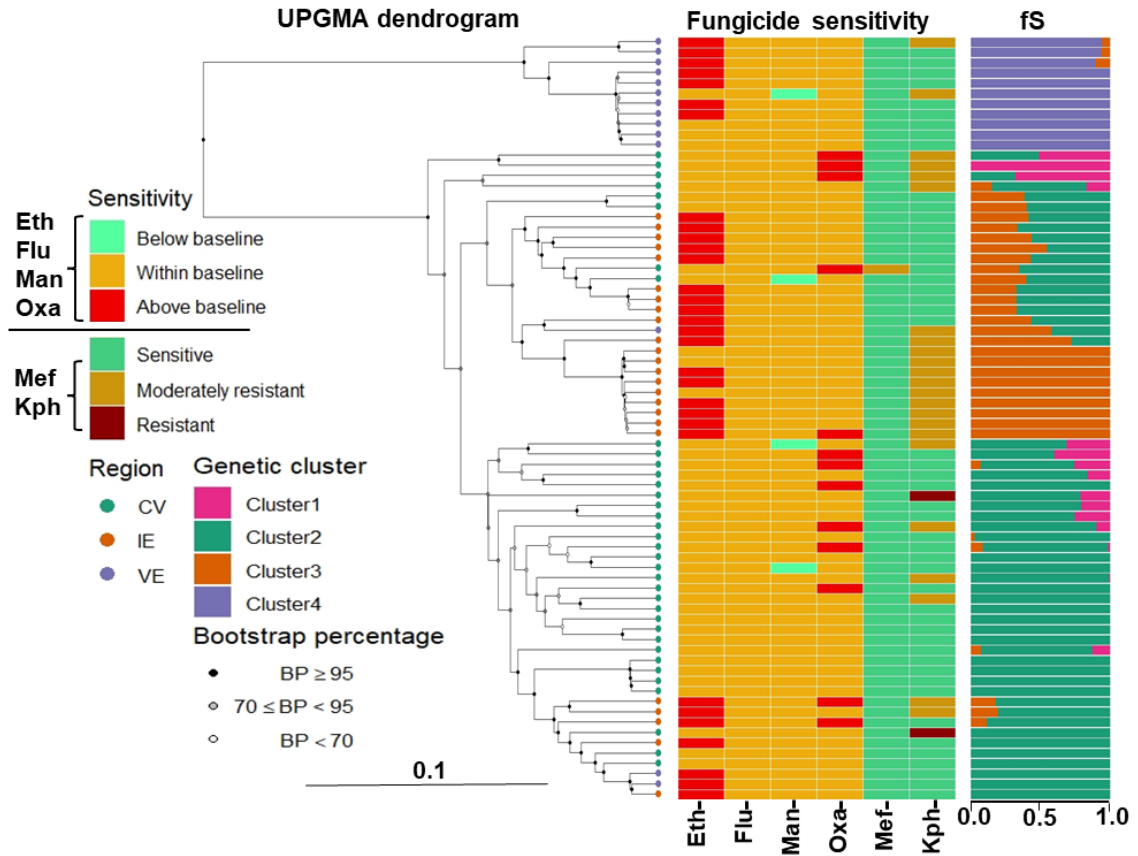


**Fig. 2.4.** Population structure of *P. syringae* visualized in UPGMA dendrograms that were constructed from observed variants and aligned to sensitivity to ethaboxam (Eth), fluopicolide (Flu), mandipropamid (Man), oxathiapiprolin (Oxa), mefenoxam (Mef), and potassium phosphite (Kph). Bootstrap percentages (BP) are shown at the nodes of the dendrogram as  $BP \geq 95$ ,  $70 \leq BP < 95$ , and  $BP < 70$ . fastStructure (fS) cluster membership probability is shown for each isolate with  $K=2$  for *P. citrophthora* and  $K=4$  for *P. syringae*. In the legend, color codes of the circles refer to geographic origin of the isolates (CV = Central Valley; IE = Inland Empire; VE = Ventura Co.). Fungicide sensitivity is color-coded for the new fungicides as below, within, and above baselines and for the older fungicides as sensitive, moderately resistant, and resistant as compared to previously determined values for CV isolates (Gray et al. 2018). In the fastStructure graphs, colors within a given bar represent the posterior membership probability of the isolate to be assigned to the predicted genetic clusters that are color-coded in the squares of the legend.

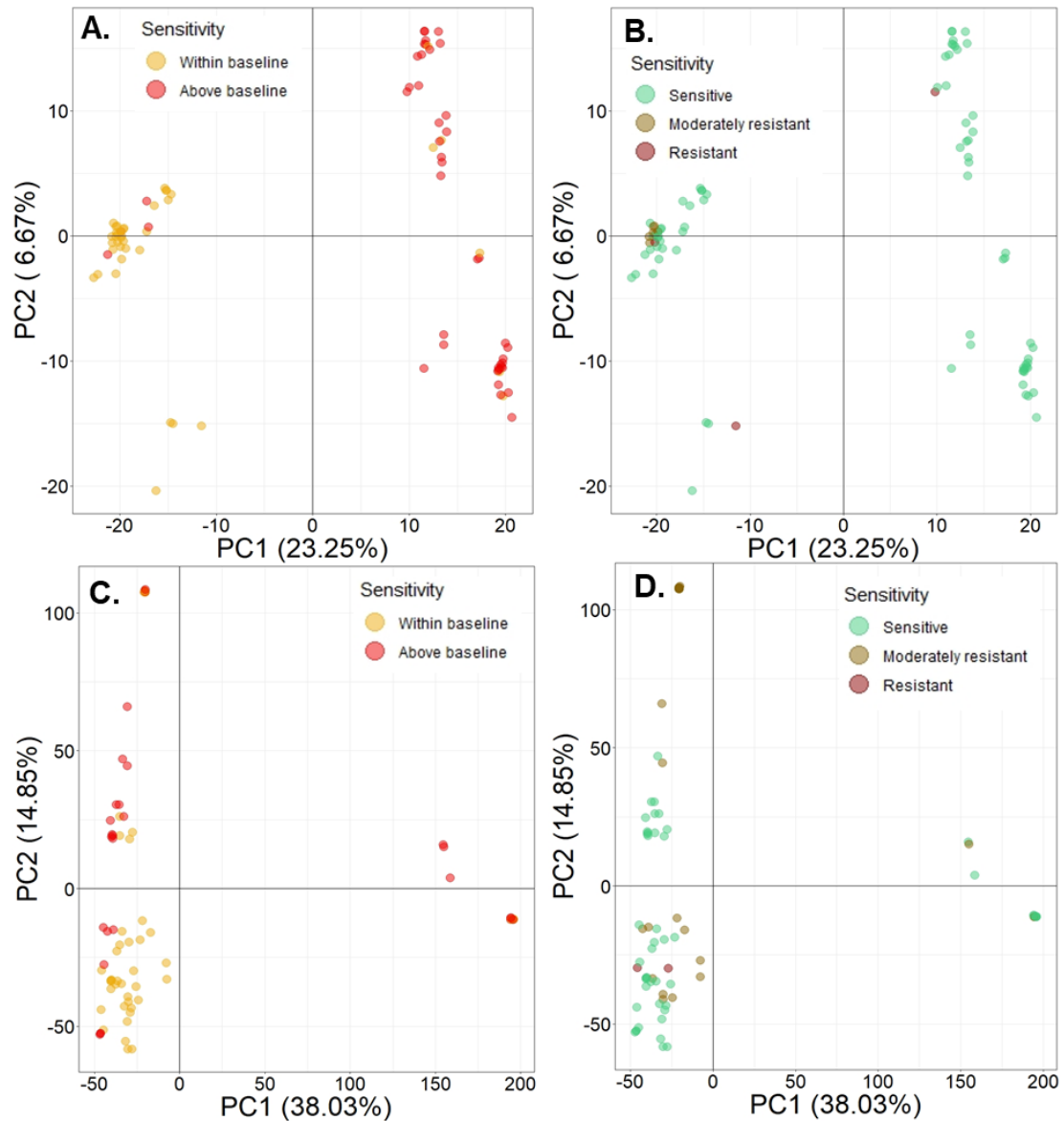


**Fig. 2.5.** Principal component analyses (PCA) of fungicide sensitivity of **A, B, *P. citrophthora*** to **A, mandipropamid** and **B, potassium phosphite** and **C, D, *P. syringae*** isolates to **C, ethaboxam**, and **D, potassium phosphite** grouped by fungicide sensitivity (i.e., within or above baseline for mandipropamid and ethaboxam or sensitive, moderately resistant, or resistant for potassium phosphite) as compared to previously determined values for CV isolates (Gray et al. 2018).

### **CHAPTER III. Root Absorption and Limited Mobility of Mandipropamid as Compared to Oxathiapiprolin and Mefenoxam After Soil Treatment of Citrus Plants for Managing Phytophthora Root Rot**

Reprinted with permission from: Belisle, R.J., Hao, W., Riley, N., Förster, H., Adaskaveg, J.E. 2023. Root Absorption and Limited Mobility of Mandipropamid as Compared to Oxathiapiprolin and Mefenoxam After Soil Treatment of Citrus Plants for Managing Phytophthora Root Rot. *Plant Disease*. 107:1107-1114

#### **ABSTRACT**

Phytophthora root rot can greatly impact citrus production worldwide, especially in newly established orchards by reducing crop yield and increasing the cost of disease management. Mandipropamid is an Oomycota fungicide that is currently registered as a soil treatment for citrus nursery container plants to manage Phytophthora root rot. In this study, we investigated the uptake of mandipropamid into citrus roots and its translocation to stems and leaves after soil application and evaluated its mobility in roots as compared to oxathiapiprolin and mefenoxam using split-root potted plants and trees in the field. A bioassay and liquid chromatography-tandem mass spectrometry were used to detect and quantify fungicides in citrus tissues, and overall, similar results were obtained using the two methods. When applied to the soil of potted, 6- to 7-month-old citrus plants using labeled rates, the majority of mandipropamid was found in root tissues (4.9 to 18.1  $\mu\text{g/g}$ ), but small amounts were also present in stems (0.18 to 0.32  $\mu\text{g/g}$ ) and leaves (0.03 to 0.22  $\mu\text{g/g}$ ). There was no significant increase in concentrations in all three tissues between 1 and 4 weeks after application. Concentrations in all tissues exceeded established  $\text{EC}_{50}$  values for mycelial growth inhibition of *P. citrophthora* and *P. nicotianae*, the main citrus root rot pathogens in California. In a split-root study where the root systems of single plants were separated, no basipetal phloem-based mobility of mandipropamid or



oxathiapiprolin was observed, but relative uptake into roots was higher for mandipropamid. In contrast, low amounts of mefenoxam were also present in roots in the untreated soil. Similar results were obtained in a field study where part of the root system was treated, and fungicides were extracted from nontreated roots. All three fungicides persisted inside roots over the 8-week period of this study. Uptake and persistence inside roots, as well as the previously reported high efficacy against citrus root rot in greenhouse and field studies support the use of mandipropamid in citrus nurseries and potentially in the orchard.

## INTRODUCTION

Citrus production worldwide was valued at over \$75 billion in 2020 with an approximate value of \$3.4 billion for the United States (FAOSTAT 2020), including \$2.3 billion for California (U.S. Department of Agriculture 2020). Phytophthora root rot can greatly impact citrus production, especially in new orchards where trees may need to be replaced. Crop yield in established orchards is reduced, and overall, there is an increase in costs associated with disease management. Symptoms of the disease include destruction of feeder roots with subsequent yellowing of leaves and branch dieback. Serious soil infestations with subsequent infections can lead to the eventual death of the tree. Symptoms are more severe on young trees because their limited root systems are unable to compensate for the damage to the feeder roots. The two main causal agents of Phytophthora root rot of citrus in California are *Phytophthora nicotianae* Breda de Haan (syn. *P. parasitica* Dastur) that is mostly active during the warmer months of the year and *P. citrophthora* (R. E. Sm. & E. H. Sm.) Leonian (Erwin and Ribeiro 1996) that is active

year-round (Hao et al. 2018). In Florida, *P. nicotianae* and *P. palmivora* (E. J. Butler) E. J. Butler are the major citrus root rot pathogens (Graham and Menge 1999).

Management strategies to maintain the productivity of citrus orchards in the presence of *Phytophthora* root rot pathogens include cultural practices and chemical treatments. Tolerant rootstocks available include trifoliate orange and Swingle citrumelo (Graham 1995), and other cultural practices focus on planting trees on berms and preventing over-watering. Chemical treatments used extensively in the citrus industry for the past 40 years are phosphonate (e.g., potassium phosphite) and phenylamide (e.g., metalaxyl, mefenoxam) fungicides. Due to the limited number of alternative treatments available and their extensive usage, resistance in pathogen populations to both chemistries has developed, resulting in reduced treatment efficacy. Phenylamide resistance has been found in many *Phytophthora* species including *P. nicotianae*, *P. cinnamomi*, *P. infestans*, *P. citricola*, and *P. megasperma* (Coffey et al. 1984; Ferrin and Kabashima 1991; Gisi and Sierotzki 2015; Hwang and Benson 2005; Stack and Millar 1985). Reduced sensitivity to potassium phosphite in several *Phytophthora* spp., including *P. citrophthora* and *P. nicotianae* from citrus, has been reported in California (Adaskaveg et al. 2017; Hao et al. 2021). The mode of action of phosphites is still unknown, but direct inhibition has been demonstrated for *P. cinnamomi* (Belisle et al. 2019) as well as species of *Phytophthora* infecting citrus (Hao et al. 2021). An induced plant-defense response has been demonstrated in the control of *P. cinnamomi* (Eshraghi et al. 2013).

Alternative chemical treatments to manage Phytophthora diseases of citrus include mandipropamid (Fungicide Resistance Action Committee - FRAC Code 40) and oxathiapiprolin (FRAC Code 49) (FRAC 2021). The carboxylic acid amide mandipropamid targets cellulose synthase in the pathogen and thereby inhibits cell wall synthesis (Blum et al. 2010a). It is registered as a foliar field application for Phytophthora brown rot of citrus fruit and as a soil treatment for *Phytophthora* diseases of container nursery plants. Mandipropamid has effectively reduced late blight of tomatoes caused by *P. infestans*, downy mildew of grape caused by *Plasmopara viticola*, Phytophthora root rot of avocado caused by *P. cinnamomi*, and Phytophthora root rot (Belisle et al. 2019; Hao et al. 2019; Lamberth et al. 2008) and brown rot of citrus (Adaskaveg, unpublished). Mandipropamid is a chiral fungicide; the S-enantiomer is resistant to soil degradation, while the R-enantiomer is preferentially degraded (Zhang et al. 2021).

The molecular target of oxathiapiprolin is the oxysterol binding protein (Pasteris et al. 2016). Oxathiapiprolin is registered on citrus for foliar and soil applications against Phytophthora diseases. It was also found to be highly effective against other diseases caused by various *Phytophthora* pathogens including *P. capsici*, *P. cinnamomi*, *P. citrophthora*, *P. infestans*, and *P. nicotianae* (Bittner and Mila 2016; Hao et al. 2019; Miao et al. 2016; Qu et al. 2016).

The systemic movement of mefenoxam and oxathiapiprolin has been previously investigated. Metalaxyl as well as its R-enantiomer mefenoxam are highly systemic in plants and are transported predominantly acropetally in roots, stems, and leaves in the transpiration stream (Cohen and Coffey 1986; Kennelly et al. 2007; Zaki et al. 1981) with

only small amounts translocated from upper plant parts into the roots (Zaki et al. 1981). On grapevine, however, an apparent ambimobile movement of mefenoxam and protection of fruit from downy mildew after leaf treatment was demonstrated to be due to the fungicide's vapor activity (Kennelly et al. 2007).

Acropetal systemic movement of oxathiapiprolin in annual crops (Cohen 2015) and citrus plants (Gray et al. 2020) has been demonstrated previously. For citrus, uptake of the fungicide at low but sufficient concentrations into plant roots provided an explanation for its long-lasting high activity in the management of *Phytophthora* root rot. The mobility of mandipropamid in plants has not been studied previously, and this information is important to understand its protective and eradivative activities against *Phytophthora* diseases and to provide information on the best strategies for field usage of this compound. Therefore, the objectives of this study were to determine: (i) whether mandipropamid is taken up by roots and translocated to stems and leaves of citrus plants after soil application; (ii) if concentrations of the fungicide inside the plant are high enough to be effective against *Phytophthora* species causing root rot; and (iii) if mandipropamid in comparison with oxathiapiprolin and mefenoxam is ambimobile and is translocated from treated roots to nontreated parts of the root system.

## MATERIALS AND METHODS

***P. citrophthora* used for bioassays.** *P. citrophthora* (isolate 2440) obtained from citrus in California was cultured on clarified 10% V8 (V8C) agar (Ribeiro 1978) in the dark at 25°C and was stored long-term in liquid nitrogen. Sporangia and zoospores of *P. citrophthora* were produced using the protocol described in Adaskaveg et al. (2015).

Zoospores were encysted by shaking at maximum speed for 1.5 min using a Vortex-Genie 2 (Scientific Industries, Bohemia, NY). Cyst suspensions of *P. citrophthora* were prepared freshly for each bioassay and adjusted to  $2.5 \times 10^4$  cysts/ml.

**Fungicides used in the study.** Mandipropamid, oxathiapiprolin, and mefenoxam were used as formulated products (Revus, Orondis, and Ridomil Gold SL, respectively; Syngenta Crop Protection; Greensboro, NC) for soil treatments of citrus plants in growth chamber and field studies as well as for standard concentrations for bioassays. Analytical grade mandipropamid ( $\geq 98.5\%$  purity; Syngenta Crop Protection) was used as a standard in high performance liquid chromatography-tandem mass spectrometry (HPLC-MS/MS) analytical residue analyses.

**Soil treatments with mandipropamid to evaluate uptake and acropetal movement in sweet orange plants in growth chamber studies.** Sweet orange (*Citrus sinensis* [L.] Osbeck) 'Madam Vinous' plants in 10.2- × 10.2- × 10.2-cm pots were grown from seeds in the greenhouse at 24 to 30°C for 6 to 7 months in UC soil mix I (plaster sand:bark:peat moss = 2:1:1, vol/vol/vol). This soil mix was used to simulate the potting substrate nurseries are using for citrus plants. Prior to treatment, 40- to 50-cm-tall plants were moved to a growth chamber (Model 1-36LLVL; Percival Scientific Inc., Perry, IA) set for a 12-h photoperiod with 34°C during the light cycle (10,000 to 12,000 Lux) and 26.7°C during the dark cycle. Three single-plant replicates were used for each fungicide treatment and the untreated control for each of the four evaluation times (1, 2, 3, and 4 weeks). Plants were arranged in a randomized complete block design (RCBD) with all four evaluation times in each block. A solution of mandipropamid (50 ml of 675 µg/ml)

in deionized water was added to each pot without wetting the stem of the plant, resulting in final application amounts of 34 mg active ingredient (a.i.) per pot. These amounts are comparable to labeled chemigation rates (e.g., 291 g a.i./ ha) based on the total basin area for 296 trees/ha and considering that the treatment area of a potted plant is approximately 1/25 of the basin of a newly planted citrus tree. Deionized water was used for the controls. Each pot was then placed in a plastic bag that was tied around the base of the stem to reduce evaporation. Plants were watered equally once every week. Fungicide extractions were conducted from root, stem, and leaf tissues of each plant as described below. The experiment was done twice.

**Evaluation of the mobility of three Oomycota fungicides within the root system of split-root sweet orange plants in growth chamber studies.** For growth chamber studies, 2-month-old sweet orange (*C. sinensis*) 'Madam Vinous' plants in 10.2- × 10.2- × 10.2-cm pots were transplanted by equally dividing the root system into two pots of the same size containing UC soil mix I and grown in the greenhouse at 24 to 30°C. Plants were used for experiments after 8 months at a height of 45 to 70 cm. Prior to treatment, plants were moved to a growth chamber (Precision Plant Growth Chamber; Thermo Fisher Scientific, Waltham, MA) set for a 12-h photoperiod with 34°C during the light cycle (6,000 Lux) and 26.7°C during the dark cycle. Four split-root plants were used for each fungicide and the untreated control and were arranged in an RCBD with one plant for each fungicide in each block. Solutions of mandipropamid (675 µg/ml), oxathiapiprolin (1,000 µg/ml), and mefenoxam (5,200 µg/ml) were prepared in deionized water, and 50 ml were added to one pot of each split-root plant without wetting the stem.

The final application amounts of mandipropamid, oxathiapiprolin, and mefenoxam were 34, 50, and 259 mg/pot, respectively, which were comparable to labeled chemigation rates of the two fungicides registered as field treatments (e.g., 140 g a.i./ha for oxathiapiprolin and 2,242 g a.i./ha for mefenoxam). Deionized water was used for the controls. Each pot of the split-root plants was placed in a plastic bag that was tied around the base of the stem to reduce evaporation. Plants were watered equally once every week. Fungicides were extracted from roots in treated and nontreated pots of each split-root plant 4 weeks after treatment as described below. This experiment was conducted twice.

**Evaluation of the mobility of three Oomycota fungicides within the root system of orange trees in field studies.** Eight-year-old crop-producing 'Fukumoto' navel orange trees grafted on 'Carrizo citrange' rootstock in an orchard with a Hanford fine sandy loam at the University of California, Riverside were used. These trees were healthy, and no *Phytophthora* spp. were recovered from feeder roots or rhizosphere soil. They were planted at 2.9-m between-tree and 6.4-m between-row spacings and were approximately 2.5 m tall with an average canopy diameter of 1.1 m. An RCBD with three single tree replications was used for each treatment. Aqueous suspensions of mandipropamid, oxathiapiprolin, and mefenoxam were applied at 291, 140, and 2,242 g a.i./ha, respectively, using a backpack air-blast sprayer (SR 430; Stihl Inc., Virginia Beach, VA) calibrated to deliver 3.16 liter/tree (935 liter/ha per 296 trees). The solution was applied evenly to the soil surface under half of the tree canopy area approximately 30 cm from the trunk at the lowest engine speed where the output was a light drizzle that minimized any spray drift. Trees treated with water were used as controls. Trees were

then irrigated for 2 h to move solutions to the root zone. There was one micro-sprinkler per tree that delivered 25 liter/h. This amount of water rapidly penetrated the soil and did not flood the basin around the trunk. After 2, 4, and 8 weeks, feeder roots were collected from a depth of  $\leq 20$  cm for fungicide extraction as described below. Sampling was done 46 to 61 cm from the tree trunk in the midsections of treated and nontreated areas. The field trials were conducted twice, one from July to September and another one from September to November 2019.

**Extraction of fungicides from citrus tissues.** Immediately after sampling, roots were rinsed with tap water, whereas stems and leaves were processed unwashed. One gram of each tissue sample was then lyophilized, and fungicides were extracted as described by Gray et al. (2020). Lyophilized tissue was homogenized and soaked in 4.22 ml extraction buffer containing 1.8 ml sterile ultrapure water (ddiH<sub>2</sub>O), 2.4 ml acetonitrile, and 20  $\mu$ l formic acid (both chemicals: Optima LC/MS grade; Thermo Fisher Scientific, Waltham, MA). The suspension was mixed on an orbital shaker at 300 rpm for 5 min and then centrifuged at  $1,380 \times g$  for 10 min. The supernatant comprised the fungicide extract and was stored at  $-20^{\circ}\text{C}$  until fungicide quantification. For analytical residue analyses using HPLC-MS/MS, four parts methanol (Optima LC/MS grade; Thermo Fisher Scientific) and nine parts 1% formic acid were added. HPLC-MS/MS analyses were performed by Environmental Micro Analysis Inc. (Woodland, CA) as described in detail previously (Gray et al. 2020). Standards consisted of analytical grade mandipropamid that was dissolved in acetonitrile and serially diluted in 1% formic acid/methanol (70:30, vol/vol) to 100, 10, 1, 0.1, 0.05, and 0.01  $\mu\text{g/ml}$ . For each tissue



type and sampling time, as well as for the positive and negative controls, a composite extract from three replicated plants was submitted for each of two repeated experiments. The amount of mandipropamid ( $\mu\text{g}$ ) per gram of roots was calculated from the concentration ( $\text{ng/ml}$ ) obtained in the HPLC-MS/MS output using a dilution factor of 59 (4.22 ml of extract/g tissue was diluted with 13 parts methanol/formic acid). The limit of detection of mandipropamid was determined from dilutions of decreasing concentrations as 0.1  $\text{ng/kg}$ .

To evaluate the efficiency of mandipropamid recovery based on HPLC-MS/MS, 0.2 ml of a 1,700- $\mu\text{g/ml}$  solution of mandipropamid in  $\text{ddiH}_2\text{O}$  was added to 1 g of finely cut up root, stem, or leaf tissue from untreated citrus plants, resulting in a concentration of 340  $\mu\text{g/g}$ . This is equivalent to 34 mg mandipropamid per pot assuming the fresh weight of a citrus seedling is approximately 100 g. Extractions were done as described above.

To test if mandipropamid detected in root tissues was from root uptake or from fungicide adhering to the root surface, roots from untreated greenhouse-grown plants or trees in the field were first rinsed with water to remove soil and tapped dry. Roots were then submerged for 30 s in either water or a mandipropamid solution at 311  $\text{mg/liter}$ , which is equivalent to the field rate of 291  $\text{g/935 liter/ ha}$ . Roots were then rinsed with tap water, which is similar as described above for roots from plants that received soil applications with mandipropamid and were processed for fungicide extraction and detection using the bioassay.

**Bioassays using *P. citrophthora* to quantify fungicide concentrations in citrus tissue extracts.** Aliquots of 800  $\mu\text{l}$  of a freshly prepared cyst suspension of *P. citrophthora* ( $2.5 \times 10^4$  /ml) were uniformly spread onto 10-cm 10% V8C agar plates, and plates were allowed to air-dry in a laminar flow hood for 1 to 2 h. Four 6.35-mm-diameter filter paper discs (No. 740-E; Carl Schleicher & Schuell Co., Keene, NH) were placed equidistantly from each other on the agar surface, and 20- $\mu\text{l}$  aliquots of plant extracts were deposited onto each disk. Extracts were used either unmodified or were concentrated 25 $\times$  using a SpeedVac concentrator (Savant DNA120; Thermo Scientific, Waltham, MA) for any tissues where mandipropamid was detected by HPLC-MS/MS but not by the standard bioassay. The latter samples included stem and leaf tissues of mandipropamid-treated and control plants in growth chamber studies as well as root tissues from control trees and from the untreated side of mandipropamid half-treated trees in the field studies. For the solvent control plates, 20- $\mu\text{l}$  aliquots of 57% acetonitrile (final concentration in plant extracts), 0.5% formic acid (final concentration in plant extracts), a mixture of 57% acetonitrile and 0.5% formic acid, or ddiH<sub>2</sub>O, were deposited onto each of four disks, respectively. Calculated fungicide concentrations were adjusted for any inhibition zones developing using tissues from control plants. Three replicated plates were used for every plant extract, including the negative control extract, as well as the solvent controls. Diameters of zones where mycelial growth of *P. citrophthora* was inhibited by  $\geq 95\%$  were measured after 48 h of incubation at 25°C.

A standard curve for mandipropamid was developed using inhibition zones from known amounts (0.01, 0.05, 0.1, 0.25, or 0.4  $\mu\text{g}$ ) applied to filter paper disks. Bioassays

and measurements of inhibition zones were done as described above. This experiment was done three times. Curve equations for oxathiapiprolin and mefenoxam were determined previously (Gray et al. 2020).

**Statistical analysis of data.** All statistical analyses were performed in SAS (version 9.4; SAS Institute, Inc., Cary, NC). Results were considered significant at  $P < 0.05$ . For the standard curve for the mandipropamid bioassay, linear regression analyses of  $\log_{10}$ -transformed inhibition zones of mycelial growth of *P. citrophthora* (mm) on known amounts of mandipropamid deposited onto filter disks ( $\mu\text{g}$ ) were performed using the PROC REG procedure. The curve equation was used for calculating unknown mandipropamid amounts applied to the filter disks from bioassay inhibition zones. To determine the amount of fungicide per gram of root tissue, values were then adjusted by a factor of 211 (based on using 20  $\mu\text{l}$  in the bioassay of a total of 4.22 ml of extract/g tissue).

For the experiments on mandipropamid uptake at selected times after treatment, the effects of tissue type (i.e., roots, stems, or leaves) or sampling time (i.e., 1, 2, 3, or 4 weeks) on calculated amount of mandipropamid per gram of tissue were analyzed. For this, fungicide amounts in the extracts and weeks after treatment were treated as fixed effects, and experiment and block (not included for HPLC-MS/MS data) were treated as random effects. For the fungicide mobility experiments with split-root plants, effect of treatments (treated versus untreated) on the calculated amount of fungicide was analyzed separately for each fungicide. Treatment was the fixed effect, and experiment and block were the random effects. For fungicide mobility trials in the field, effects of fungicides

(i.e., mandipropamid, oxathiapiprolin, and mefenoxam) or sampling times (i.e., 2, 4, and 8 weeks), treatments (roots from treated versus untreated parts of the tree basin), and their interactions on calculated amounts of fungicides were analyzed.

For each analysis, the generalized linear mixed model was used following the PROC GLIMMIX procedure and Gaussian response distribution with the link function identity. Least square means of each citrus tissue and each time point were calculated using the LSMEANS statement with the TUKEY adjustment. Contrast estimates for pairs of treatments were used to determine multiple comparison differences among treatment means. For comparisons of mandipropamid concentrations in tissue extracts based on HPLCMS/MS or bioassays, regression analyses were performed using PROC REG.

## RESULTS

### **Bioassays using *P. citrophthora* to quantify mandipropamid concentrations.**

Mycelial growth inhibition of *P. citrophthora* was observed on bioassay plates around filter paper disks containing standard amounts of mandipropamid, and the width of the inhibition zone after 2 days of incubation depended on the amount of fungicide applied (Fig. 3.1A). In regression analyses, there was a significant ( $P < 0.0001$ ) linear relationship between log<sub>10</sub>-transformed mean inhibition zones and fungicide amounts applied to the disks (between 0.01 and 0.4 mg) with an  $R^2$  value of 0.9525, and the equation of the standard curve was calculated as  $y = 0.7522x + 1.8249$  (Fig. 3.1B). No inhibition zones were observed for the solvent controls or the lowest amount of mandipropamid used in the dilution series (i.e., 0.01 µg/disk).

**Soil treatments with mandipropamid to evaluate uptake and acropetal movement in sweet orange plants in growth chamber studies.** Distinct inhibition zones of *P. citrophthora* growth were observed in the bioassays when root extracts of citrus plants treated with soil applications of mandipropamid were added to the filter paper disks. Mean inhibition zones for samples collected 1, 2, 3, and 4 weeks after treatment were 2.9, 4.9, 4.9, and 5.0 mm, respectively. Using the standard equation  $y = 0.7522x + 1.8249$ , these were calculated to correspond to 4.9, 8.4, 8.5, and 8.6  $\mu\text{g/g}$  tissue, respectively (Fig. 3.2A). For stem and leaf extracts, inhibition zones were only observed when extracts were concentrated 25 $\times$  before use. Concentrations for stems ranged from 0.18 to 0.24  $\mu\text{g/g}$ , and those for leaves from 0.05 to 0.22  $\mu\text{g/g}$  tissue. For all three tissue types, there was no significant ( $P > 0.05$ ) difference among sampling times. Concentrations in roots were significantly ( $P \leq 0.0006$ ) higher as compared to stems and leaves in the 2-, 3-, and 4-week samplings, whereas in the 1-week sampling, root concentrations were significantly ( $P = 0.0360$ ) higher as compared to leaves (Fig. 3.2A). No inhibition of *P. citrophthora* growth was observed using nonmodified extracts from water-treated control plants; however, concentrated stem and leaf extracts resulted in inhibition zones that were used to adjust the detected mandipropamid concentrations in these tissues. There was no growth inhibition using extracts of roots of greenhouse plants or field trees that were submerged for 30 s in mandipropamid solutions and then rinsed with water.

In comparison, HPLC-MS/MS analyses detected mandipropamid concentrations of 5.2, 10.0, 10.6, and 18.1  $\mu\text{g/g}$  root tissue, respectively, for the four sampling times, and

there was no significant ( $P = 0.1140$ ) difference among samplings (Fig. 3.2B). Similar to the bioassay, low amounts of mandipropamid were also detected in stem (i.e., 0.18 to 0.32  $\mu\text{g/g}$ ) and leaf (i.e., 0.03 to 0.15  $\mu\text{g/g}$ ) tissues (Fig. 3.2B), with no significant ( $P = 0.8813$  for stems,  $P = 0.4364$  for leaves) differences among sampling times. Except for samples taken 1 week after treatment ( $P = 0.2667$ ), mandipropamid concentrations in root extracts were significantly ( $P \leq 0.0120$ ,  $P \leq 0.0045$ , and  $P \leq 0.0467$  for 2-, 3-, and 4-week samplings, respectively) higher as compared with stem or leaf extracts. When  $\log_{10}$ -transformed concentrations in root (Fig. 3.3A) or stem (Fig. 3.3B) extracts based on HPLC-MS/MS analyses were regressed on those calculated from the bioassays for the same extracts, linear relationships were obtained with  $R^2$  values of 0.7923 ( $P = 0.0018$ ; equation of the regression line:  $y = 1.8994x - 0.6674$ ) or 0.7522 ( $P = 0.1327$ ; equation of the regression line:  $y = 1.9147x + 0.7104$ ), respectively. The regression for mandipropamid concentrations in leaf tissues had an  $R^2$  value of 0.1107 and a probability value of 0.6673 (regression not shown).

Root, stem, and leaf tissue samples spiked with 340  $\mu\text{g}$  mandipropamid/g before extraction resulted in detection of 281.7, 285.8, and 337.5  $\mu\text{g/g}$  of mandipropamid, respectively, using HPLCMS/MS; this represents recovery rates of 82.8, 84.0, and 99.3%, respectively.

**Evaluation of the mobility of three Oomycota fungicides within the root system of split-root sweet orange plants in growth chamber studies.** In the statistical analysis, there was a significant ( $P < 0.0001$ ) interaction between fungicides used and fungicide amount detected in roots of treated or untreated soils in split-root plant studies.

Therefore, results are presented separately for each fungicide. For mandipropamid and oxathiapiprolin, only root extracts from fungicide-treated soils, but not from untreated soils, resulted in inhibition zones in bioassays with *P. citrophthora* when sampled 4 weeks after fungicide application. Using standard equations, concentrations were calculated as 12.62 and 0.82  $\mu\text{g/g}$  root tissue for the two fungicides, respectively (Fig. 3.4A and B). Both fungicides were also not detected in the untreated soils using HPLC-MS/MS analyses. For mefenoxam, however, root extracts from treated and untreated pots resulted in bioassay inhibition zones. The calculated concentration of 1,086.26  $\mu\text{g}$  mefenoxam/g root tissue for treated soils was significantly ( $P < 0.0001$ ) higher than for the roots in untreated soils with 71.13  $\mu\text{g/g}$  root tissue (Fig. 3.4C).

**Evaluation of the mobility of three Oomycota fungicides within the root system of orange trees in field studies.** In the statistical analysis, a significant ( $P = 0.0216$ ) interaction occurred between fungicides, sample time (2, 4, and 8 weeks), and roots from treated and untreated soils of the tree basin. Additionally, for each fungicide, there was a significant interaction ( $P < 0.0001$  for mandipropamid,  $P = 0.0016$  for oxathiapiprolin, and  $P = 0.0445$  for mefenoxam) between sampling time and amount of fungicide detected in roots. Therefore, data are presented separately for each fungicide.

Based on bioassay inhibition zones, concentrations of mandipropamid in roots from treated soil were significantly ( $P \leq 0.0033$ ) higher than in roots from untreated soil and were calculated as 0, 8.16, and 8.10  $\mu\text{g/g}$  tissue for the 2-, 4-, and 8-week samplings, respectively (Fig. 3.5A). There was a significant ( $P \leq 0.0001$ ) increase in fungicide concentration between the 2- and 4-week samplings but not between the 4- and 8-week

samplings ( $P = 0.9966$ ). Roots from nontreated soil were calculated to contain 0.16  $\mu\text{g/g}$  8 weeks after application, but mandipropamid was not detected in the earlier samplings. For comparison, HPLC-MS/MS analyses detected 0, 0.01, and 0.02  $\mu\text{g/g}$  in the 2-, 4-, and 8-week samplings, respectively.

Based on the bioassay, oxathiapiprolin was present at 0.22, 0.55, and 0.84  $\mu\text{g/g}$  in root samples from treated soil obtained 2, 4, and 8 weeks after application, respectively, with a significant ( $P = 0.0034$ ) increase between the 2- and 8-week samplings (Fig. 3.5B). Using both detection methods, no fungicide was found in roots from untreated soil at the three sampling times.

For mefenoxam, bioassay inhibition zones were observed in root extracts from treated and untreated soil at each sampling time. Calculated concentrations in root extracts were significantly higher for the treated than the untreated soil for both the 2-week ( $P = 0.0002$ ) and 4-week ( $P = 0.0385$ ) samplings but not for the 8-week ( $P = 0.1655$ ) sampling (Fig. 3.5C). Mefenoxam concentrations in roots from treated soil were not significantly ( $P \geq 0.1060$ ) different among sampling times (Fig. 3.5C). Extracts from roots in the untreated soil showed a significant increase ( $P = 0.0454$ ) at 8 weeks as compared to 2 weeks after application, but there were no statistical differences between the 2- and 4-week samplings ( $P = 0.6929$ ) or the 4- and 8week samplings ( $P = 0.1828$ ).

## DISCUSSION

New Oomycota fungicides have become available in recent years for the management of Phytophthora diseases of many crops, including citrus, where no new modes of action were introduced since the 1980s. Mandipropamid was previously shown



to effectively reduce soil populations of *P. citrophthora* and *P. nicotianae* and manage Phytophthora root rot of potted citrus plants and of orchard trees (Hao et al. 2019). Currently, it is registered on citrus as a soil treatment of container plants in nurseries and as a foliar application for management of Phytophthora brown rot.

In this study, we demonstrate root uptake and limited acropetal mobility of mandipropamid in citrus plants. The fungicide was taken up by roots when applied to soil of 6- to 7-month-old plants, but small amounts were also detected in stem and leaf tissues. Concentrations in all tissues analyzed were high enough to inhibit growth of *Phytophthora* species causing root rot of citrus in California based on reported mean EC<sub>50</sub> values for mycelial growth inhibition of *P. citrophthora* and *P. nicotianae* of 0.004 and 0.005 µg/ml, respectively (Gray et al. 2018). Concentrations in roots also exceeded reported mean EC<sub>50</sub> values for sporangium formation and cyst germination of *P. citrophthora* or of chlamydospore and oospore formation of *P. nicotianae* (Gray et al. 2018). Additionally, concentrations in roots of orchard trees were found to be persistent for at least 8 weeks. The presence of mandipropamid in root tissues was determined to be due to actual uptake because it was not detected when roots were submerged for 30 s in fungicide solution and then rinsed with water. There was no basipetal phloem-based mobility of mandipropamid from roots in treated to those in untreated soil in the split-root study where the root systems of single plants were clearly separated. Low detections in untreated parts of the root system in the field at the 8-week sampling time could be due to root system architecture (e.g., roots originating from the treated side of the root basin

growing into the untreated side) or diffusion of fungicide in the soil with irrigations over the 8-week period.

These results indicate that mobility of mandipropamid in plants is qualitatively similar to that of oxathiapiprolin (Gray et al. 2020). Quantitatively, however, a much higher portion of mandipropamid was absorbed by roots considering that 34 mg/pot of mandipropamid or 50 mg/pot of oxathiapiprolin were applied in the split-root study and 12.6 or 0.82  $\mu\text{g/g}$  tissue were detected in roots after 4 weeks, respectively. Similarly, in the field study, 291 g/ha of mandipropamid or 140 g/ha of oxathiapiprolin was applied, and residues in roots after 8 weeks were 8.1 or 0.84  $\mu\text{g/g}$  tissue, respectively. Fungicide mobility in plants can be predicted using an adapted Bromilow model (Teicher 2017) based on the partition coefficient  $\log P$  that indicates the lipophilicity or hydrophilicity and the acid dissociation constant  $\text{pK}_a$  of a compound. Using the  $\log P$  and  $\text{pK}_a$  values for mandipropamid (3.3 and 0, respectively) and oxathiapiprolin (3.6 and 0.78, respectively) (Pesticide Properties Database, <http://sitem.herts.ac.uk/aeru/ppdb/en/>), both fungicides are predicted to have mobility limited to the xylem, and our results support this model's prediction. Still, higher uptake was observed for mefenoxam where applications of 259 mg/pot in the split-root study or of 2,242 g/ha in the field study resulted in fungicide concentrations in roots of 1,086 or  $>100$   $\mu\text{g/g}$ , respectively. Uptake of oxathiapiprolin and mefenoxam, however, may be more rapid because they were found to be present in roots of orchard trees 2 weeks after application, whereas mandipropamid was only detected starting 4 weeks after application. Additionally, we confirmed results of other studies (Zaki et al. 1981) where mefenoxam had limited ambimobile properties. In our study, this

fungicide was detected at low concentrations in roots of the untreated pot in the split-root studies and in roots of the untreated side of orange trees in the field. The logP and pKa values for mefenoxam are 1.71 and 1.41, respectively, and the adapted Bromilow model predicts phloem and xylem mobility. Thus, our results support the model's predicted mobility of mefenoxam.

Bioassays and analytical HPLC-MS/MS analyses were used to detect and quantify the fungicides in tissue extracts, and most mandipropamid was found in root tissues. Overall, similar results were obtained using the two methods. For detecting mandipropamid in stem and leaf tissues, however, extracts needed to be concentrated in contrast to a previous study done with citrus plants using oxathiapiprolin (Gray et al. 2020). This can be explained by the approximately 10-fold higher toxicity of oxathiapiprolin to *P. citrophthora* that was used in the assay (mean EC<sub>50</sub> value for mycelial growth inhibition 0.0003 µg/ml) as compared to mandipropamid (mean EC<sub>50</sub> value 0.004 µg/ml) (Gray et al. 2018). There was a highly significant relationship between mandipropamid concentrations in root tissues obtained by bioassays and HPLC-MS/MS. This relationship had a low significance level for stem tissues, and there was no correlation between the two methods for leaf tissues. This lack of correlation in fungicide quantification between the methods for stem and leaf tissues can have two reasons. Few data points were used in the regressions due to the high cost associated with analytical analyses by an outside lab. Additionally, fungicide concentrations detected were near the limits of detection for both methods, and higher errors can be expected. Overall, the

bioassay can be considered a reasonably accurate and cost-effective method to determine fungicide residues in plants.

Soil applications of mandipropamid have been registered on citrus for management of *Phytophthora* root rot of nursery container plants, and our findings of uptake and persistence in roots, as well as the previously reported high efficacy against citrus root rot in greenhouse and field studies (Hao et al. 2019), support this usage. Isolates of *Plasmopora viticola* resistant to mandipropamid have been discovered (Gisi et al. 2007), and the mutation that confers resistance was identified (Blum et al. 2010b); to date, no resistance has been detected in *Phytophthora* species, including those from citrus (Gray et al. 2018; Siegenthaler and Hansen 2021). The mode of action of mandipropamid is different from previously (i.e., potassium phosphite, mefenoxam, etc.) and other recently registered (i.e., oxathiapiprolin, fluopicolide) fungicides, and therefore, it fits well into a resistance management program with a mode of action applied in nurseries that is different from field applications. Still, a potential registration of mandipropamid for soil application in the field of the stable S-enantiomer (Zhang et al. 2021) with label requirements for rotation to other modes of action at tree planting is also supported by this study.

## LITERATURE CITED

- Adaskaveg, J. E., Förster, H., Hao, W., and Gray, M. 2017. Potassium phosphite resistance and new modes of action for managing *Phytophthora* diseases of citrus in the United States. Pages 205-210 in: *Modern Fungicides and Antifungal Compounds*, Vol. VIII. H. B. Deising, B. Fraaije, A. Mehl, E. C. Oerke, H. Sierotzki, and G. Stammler, eds. Deutsche Phytomedizinische Gesellschaft, Braunschweig, Germany.
- Adaskaveg, J. E., Hao, W., and Förster, H. 2015. Postharvest strategies for managing *Phytophthora* brown rot of citrus using potassium phosphite in combination with heat treatments. *Plant Dis.* 99:1477-1482.
- Belisle, R. J., Hao, W., McKee, B., Arpaia, M. L., Manosalva, P., and Adaskaveg, J. E. 2019. New Oomycota fungicides with activity against *Phytophthora cinnamomi* and their potential use for managing avocado root rot in California. *Plant Dis.* 103:2024-2032.
- Bittner, R. J., and Mila, A. L. 2016. Effects of oxathiapiprolin on *Phytophthora nicotianae*, the causal agent of black shank of tobacco. *Crop Prot.* 81:57-64.
- Blum, M., Boehler, M., Randall, E., Young, V., Csukai, M., Kraus, S., Moulin, F., Scalliet, G., Avrova, A. O., Whisson, S. C., and Fonne-Pfister, R. 2010a. Mandipropamid targets the cellulose synthase-like PiCesA3 to inhibit cell wall biosynthesis in the oomycete plant pathogen, *Phytophthora infestans*. *Mol. Plant Pathol.* 11:227-243.
- Blum, M., Waldner, M., and Gisi, U. 2010b. A single point mutation in the novel PvCesA3 gene confers resistance to the carboxylic acid amide fungicide mandipropamid in *Plasmopara viticola*. *Fungal Genet. Biol.* 47:499-510.
- Coffey, M. D., Klure, L. J., and Bower, L. A. 1984. Variability in sensitivity to metalaxyl of isolates of *Phytophthora cinnamomi* and *Phytophthora citricola*. *Phytopathology* 74:417-422.
- Cohen, Y. 2015. The novel oomycide oxathiapiprolin inhibits all stages in the asexual life cycle of *Pseudoperonospora cubensis* - causal agent of cucurbit downy mildew. *PLoS One* 10:e0140015.
- Cohen, Y., and Coffey, M. D. 1986. Systemic fungicides and the control of oomycetes. *Ann. Rev. Phytopathol.* 24:311-338.
- Erwin, D. C., and Ribeiro, O. K. 1996. *Phytophthora Diseases Worldwide*. American Phytopathological Society, St. Paul, MN.

- Eshraghi, L., Anderson, J. P., Aryamanesh, N., McComb, J. A., Shearer, B., and Hardy, G. E. S. J. 2013. Defence signalling pathways involved in plant resistance and phosphite-mediated control of *Phytophthora cinnamomi*. *Plant Mol. Biol. Rep.* 32:342.
- FAOSTAT. 2020. FAOSTAT Statistics Division, Food and Agriculture Organization of the United Nations. <https://www.fao.org/faostat/en/#home>
- Ferrin, D. M., and Kabashima, J. N. 1991. In vitro insensitivity to metalaxyl of isolates of *Phytophthora citricola* and *P. parasitica* from ornamental hosts in southern California. *Plant Dis.* 75:1041-1044.
- FRAC. 2021. FRAC Code List: Fungicides Sorted by Mode of Action. Fungicide Resistance Action Committee (FRAC). <http://www.frac.info>
- Gisi, U., and Sierotzki, H. 2015. Oomycete fungicides: Phenylamides, quinone outside inhibitors, and carboxylic acid amides. Pages 145-174 in: *Fungicide Resistance in Plant Pathogens*. H. Ishii, and D. W. Hollomon, eds. Springer, Tokyo, Japan.
- Gisi, U., Waldner, M., Kraus, N., Dubuis, P. H., and Sierotzki, H. 2007. Inheritance of resistance to carboxylic acid amide (CAA) fungicides in *Plasmopara viticola*. *Plant Pathol.* 56:199-208.
- Graham, J. H. 1995. Root regeneration and tolerance of citrus rootstocks to root rot caused by *Phytophthora nicotianae*. *Phytopathology* 85:111-117.
- Graham, J. H., and Menge, J. A. 1999. Root diseases. Pages 126-135 in: *Citrus Health Management*. L. W. Timmer, and L. W. Duncan, eds. American Phytopathological Society, St. Paul, MN.
- Gray, M. A., Hao, W., Förster, H., and Adaskaveg, J. E. 2018. Baseline sensitivities of new fungicides and their toxicity to selected life stages of *Phytophthora* species from citrus in California. *Plant Dis.* 102:734-742.
- Gray, M. A., Nguyen, K. A., Hao, W., Belisle, R. J., Förster, H., and Adaskaveg, J. E. 2020. Mobility of oxathiapiprolin and mefenoxam in citrus seedlings after root application and implications for managing *Phytophthora* root rot. *Plant Dis.* 104:3159-3165.
- Hao, W., Miles, T. D., Martin, F. N., Browne, G. T., Förster, H., and Adaskaveg, J. E. 2018. Temporal occurrence and niche preferences of *Phytophthora* spp. causing brown rot of citrus in the Central Valley of California. *Phytopathology* 108:384-391.

- Hao, W., Gray, M. A., Förster, H., and Adaskaveg, J. E. 2019. Evaluation of new Oomycota fungicides for management of *Phytophthora* root rot of citrus in California. *Plant Dis.* 103:619-628.
- Hao, W., Förster, H., and Adaskaveg, J. E. 2021. Resistance to potassium phosphite in *Phytophthora* species causing citrus brown rot and integrated practices for management of resistant isolates. *Plant Dis.* 105:972-977.
- Hwang, J., and Benson, D. M. 2005. Identification, mefenoxam sensitivity, and compatibility type of *Phytophthora* spp. attacking floriculture crops in North Carolina. *Plant Dis.* 89:185-190.
- Kennelly, M. M., Gadoury, D. M., Wilcox, W. F., and Seem, R. C. 2007. Vapor activity and systemic movement of mefenoxam control grapevine downy mildew. *Plant Dis.* 91:1260-1264.
- Lamberth, C., Jeanguenat, A., Cederbaum, F., De Mesmaeker, A., Zeller, M., Kempf, H. J., and Zeun, R. 2008. Multicomponent reactions in fungicide research: The discovery of mandipropamid. *Bioorg. Med. Chem.* 16:1531-1545.
- Miao, J., Dong, X., Lin, D., Wang, Q., Liu, P., Chen, F., Du, Y., and Liu, X. 2016. Activity of the novel fungicide oxathiapiprolin against plant-pathogenic oomycetes. *Pest. Manag. Sci.* 72:1572-1577.
- Pasteris, R.J., Hanagan, M.A., Bisaha, J.J., Finkelstein, B.L., Hoffman, L. E., Gregory, V., Andreassi, J. L., Sweigard, J. A., Klyashchitsky, B. A., Henry, Y. T., and Berger, R. A. 2016. Discovery of oxathiapiprolin, a new oomycete fungicide that targets an oxysterol binding protein. *Bioorg. Med. Chem.* 24:354-361.
- Qu, T., Shao, Y., Csinos, A. S., and Ji, P. 2016. Sensitivity of *Phytophthora nicotianae* from tobacco to fluopicolide, mandipropamid, and oxathiapiprolin. *Plant Dis.* 100:2119-2125.
- Ribeiro, O. K. 1978. A Source Book of the Genus *Phytophthora*. J. Cramer, Vaduz, Liechtenstein.
- Siegenthaler, T. B., and Hansen, Z. R. 2021. Sensitivity of *Phytophthora capsici* from Tennessee to mefenoxam, fluopicolide, oxathiapiprolin, dimethomorph, mandipropamid, and cyazofamid. *Plant Dis.* 105:3000-3007.
- Stack, J., and Millar, R. 1985. Isolation and characterization of a metalaxyl-insensitive isolate of *Phytophthora megasperma* f. sp. *medicaginis*. *Phytopathology* 75: 1387-1392.

- Teicher, H. 2017. The Labcoat Guide to Pesticide Mode of Action: Pesticide Solubility and Biological Parameters. BioScience Solutions. Retrieved from <https://biocomm.eu/2017/10/03/labcoat-guide-pesticide-mode-actionpesticide-solubility-biological-parameters/>
- U.S. Department of Agriculture. 2020. Citrus Fruits – 2020 Summary. U.S. Department Of Agriculture National Agricultural Statistics Service. [https://www.nass.usda.gov/Publications/Todays\\_Reports/reports/cfrt0820.pdf](https://www.nass.usda.gov/Publications/Todays_Reports/reports/cfrt0820.pdf)
- Zaki, A. I., Zentmyer, G. A., and LeBaron, H. M. 1981. Systemic translocation of <sup>14</sup>C-labeled metalaxyl in tomato, avocado, and *Persea indica*. *Phytopathology* 71:509-514.
- Zhang, J., Wu, Q., Zhong, Y., Wang, Z., He, Z., Zhang, Y., and Wang, M. 2021. Enantioselective bioactivity, toxicity, and degradation in vegetables and soil of chiral fungicide mandipropamid. *J. Agric. Food Chem.* 69:13416-13424.



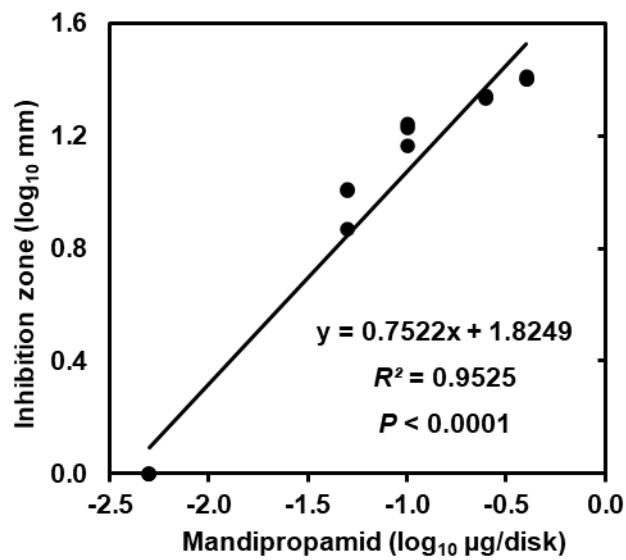
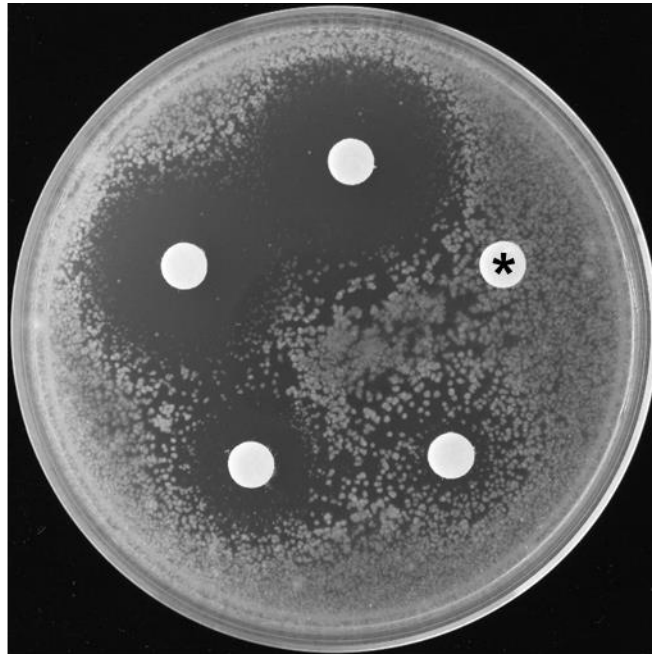


**Fig. 3.1. A**, Inhibition zones of mycelial growth of *Phytophthora citrophthora* in a bioassay with standard amounts of (starting clockwise from the asterisk) 0.01, 0.05, 0.1, 0.25, or 0.4 µg mandipropamid/disk after two days of incubation at 25°C, and **B**, regressions of mean inhibition zones of mycelial growth on amounts of mandipropamid.

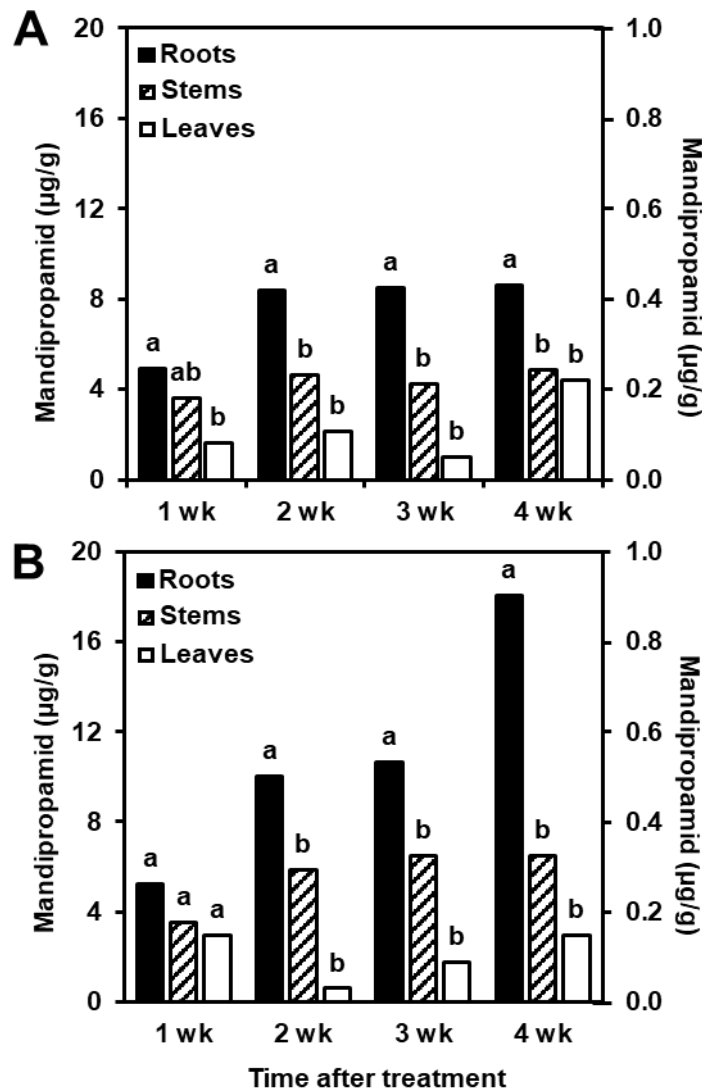


**Fig. 3.2.** Mandipropamid concentrations measured **A**, in a bioassay, and **B**, in the same extracts by high-performance liquid chromatography tandem mass spectrometry (HPLC-MS/MS) in root, stem, and leaf extracts of potted 6- to 7-month-old citrus plants 1, 2, 3, or 4 weeks after soil applications with mandipropamid. The primary vertical axis is used for root extracts, and the secondary vertical axis is used for stem and leaf extracts. Bars followed by the same letter for each sampling time are not significantly different according to a generalized linear mixed model using the PROC GLIMMIX procedure and least square treatment means with the Tukey-Kramer adjustment.

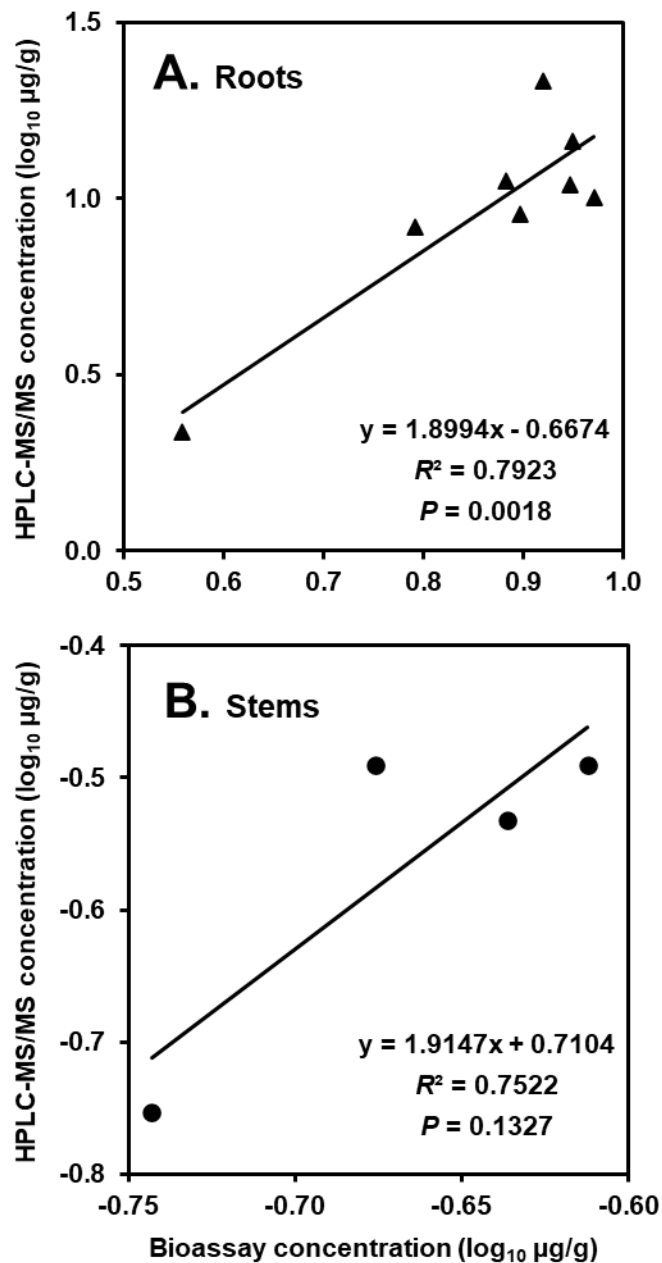


**Fig. 3.3.** Regression of  $\log_{10}$ -transformed concentrations of mandipropamid in **A**, root extracts and **B**, stem extracts determined by high-performance liquid chromatography tandem mass spectrometry (HPLC-MS/MS) on those calculated from bioassays. For the bioassays, fungicide amounts were calculated using the standard curve equation  $y = 0.7522x + 1.8249$ .

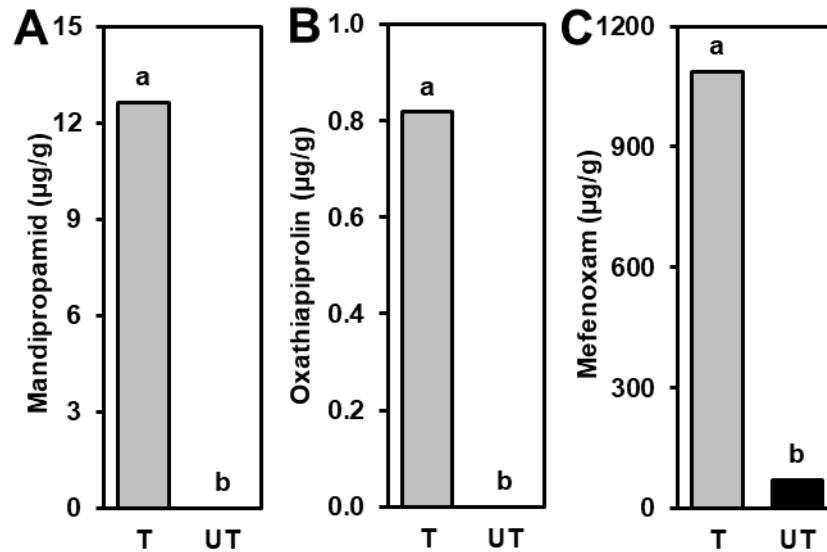


**Fig. 3.4.** Fungicide concentrations in root extracts of 10-month-old split-root-potted citrus plants where soil of one pot of each plant was treated (T) with **A**, mandipropamid, **B**, oxathiapiprolin, or **C**, mefenoxam, and soil in the other pot was not treated (UT). Roots were sampled 4 weeks after fungicide applications. Fungicide amounts were determined based on mean inhibition zones of mycelial growth of *Phytophthora citrophthora* in a bioassay and calculated standard curve equations. Bars followed by the same lowercase letter for each fungicide are not significantly different according to a generalized linear mixed model using the PROC GLIMMIX procedure and least square treatment means with the Tukey-Kramer adjustment.

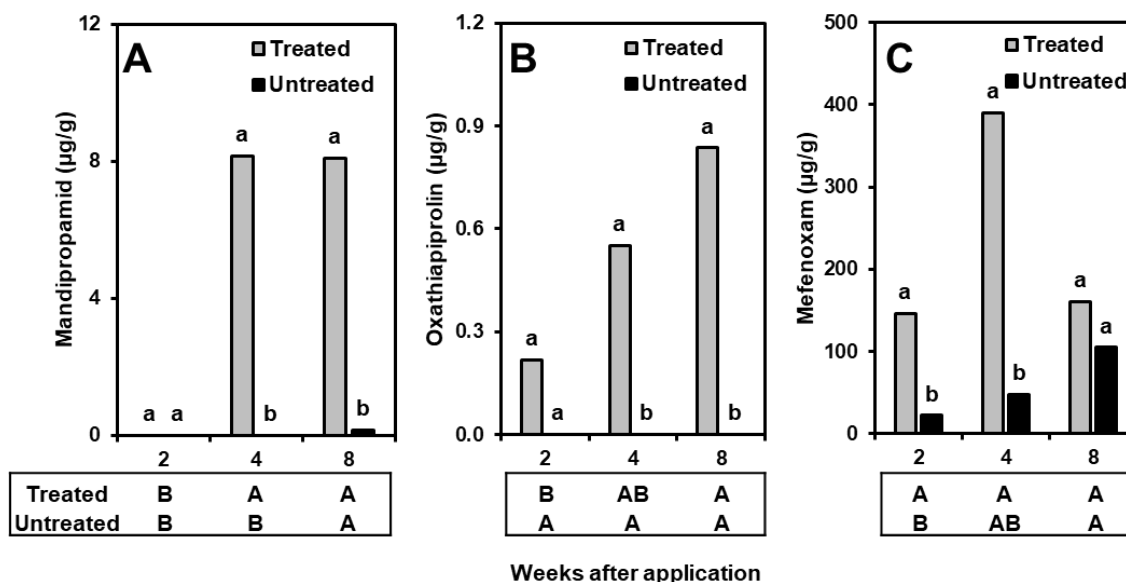


**Fig. 3.5.** Fungicide concentrations in root extracts of citrus trees from a field study where half of each circular basin around the trunk was treated with soil applications of **A**, mandipropamid, **B**, oxathiapiprolin, or **C**, mefenoxam, and the other half was not treated. Roots were sampled 2, 4, and 8 weeks after application. Fungicide amounts were determined based on mean inhibition zones of mycelial growth of *Phytophthora citrophthora* in a bioassay and calculated standard curve equations. Bars followed by the same lowercase letter for each fungicide or by the same uppercase letter for each sampling time in the tables are not significantly different according to a generalized linear mixed model using the PROC GLIMMIX procedure and least square treatment means with the Tukey-Kramer adjustment.

## GENERAL CONCLUSION

Development of integrated management practices for control of plant diseases requires a multi-faceted analysis of the factors affecting the system being considered. These factors are often far too numerous to all be adequately addressed in a single effort, and new factors impacting agricultural systems are constantly being identified. Therefore, the maintenance of integrated management practices involves the ongoing synthesis of current knowledge with recent discoveries and newly developed techniques. The studies comprising this dissertation consider factors pertaining to *Phytophthora* diseases of citrus in California, including population structure and sensitivity to new fungicides of some of the causal organisms, and mobility of a new Oomycota fungicide in citrus plants after soil application. This work is the first to utilize population genomics to characterize the structure and diversity of California populations of *Phytophthora citrophthora* and *P. syringae*. This work is also the first to determine the sensitivity of isolates of both species from fruit with brown rot symptoms from the Inland Empire (IE) and Ventura Co. (VE) in comparison to previously evaluated isolates from the Central Valley (CV) to new (i.e., ethaboxam, fluopicolide, mandipropamid, oxathiapiprolin) and older (i.e., mefenoxam, potassium phosphite) Oomycota-targeted fungicides. This information on fungicide sensitivity was incorporated into population genomic analyses to assess the potential risk for resistance development. Finally, this work is also the first to investigate the systemic properties of mandipropamid in citrus seedlings, and the results provided a better understanding of the protective activity of the fungicide and will help to design the most effective application strategies.

The genomic characterization of *P. citrophthora* and *P. syringae* populations causing citrus brown rot in California supported much of the previous understanding of the lifestyles of these organisms and provided evidence for the influence of these lifestyles on population diversity. *P. citrophthora* is heterothallic, but only one mating type is thought to occur in natural or agricultural environment. Genomic analysis of the sampled populations reflected this, showing high levels of clonality with little variation among individuals and limited mixing between regional populations. In contrast *P. syringae* is homothallic and the genomic data also reflected this. There were comparatively higher levels of diversity indicating sexual reproduction within regional populations. While not exhaustive, the range of analyses performed in this study provided substantial evidence for higher inherent diversity within sampled *P. syringae* populations when compared to *P. citrophthora*. This finding may have contributed to this species becoming as prevalent as *P. citrophthora* as a brown rot pathogen of citrus during the last 40 years.

Another important finding of this study was that citrus isolates of *P. syringae* were clearly differentiated from those from non-citrus tree crop hosts. This was especially noteworthy for isolates from the CV where growing areas of different tree crop hosts often overlap. In rainy winter seasons *P. syringae* can be a serious almond pathogen causing trunk and crotch cankers (i.e., aerial Phytophthora disease), and there has been concern that the extensive almond cultivation contributed to the emergence of *P. syringae* as a major citrus brown rot pathogen. This hypothesis, however, was not supported by the data from a relatively limited sampling of non-citrus isolates, and the source of citrus *P.*

*syringae* inoculum remains unknown. Non-citrus host isolates were genetically diverse, and more sampling is warranted to describe population structures of non-citrus isolates of *P. syringae*. In summary, the distinct lifestyles of the two main species of *Phytophthora* currently causing brown rot of citrus in California were reflected by the population structures observed in this study. The identified genetic diversity of both species indicates that species evolution and development of regional sub-populations are ongoing and that they will continue to adapt to changing environments. Also, it is unlikely that isolates of *P. syringae* affecting citrus originated from other tree crops growing in the CV region.

The comparison of *in vitro* sensitivities of isolates of *P. citrophthora* and *P. syringae* from the IE and VE, regions from which isolates were not evaluated previously, to published sensitivities of CV isolates to new and older Oomycota-targeted fungicides established expanded baseline sensitivities to the new fungicides and updated sensitivity ranges for the older ones. Statistically significant differences in sensitivity among isolates from different geographical regions were observed for fluopicolide, mandipropamid, and oxathiapiprolin for *P. citrophthora* and for ethaboxam and oxathiapiprolin for *P. syringae*. Fungicide toxicity was mostly higher (i.e., lower mean EC<sub>50</sub> values) for CV isolates of both species. Differences in toxicity were mostly in a very narrow range with a less than 2-fold change in mean EC<sub>50</sub> values, and none of the isolates was determined to be resistant. Therefore, the efficacy of field applications with these new fungicides will unlikely be compromised by these slightly higher EC<sub>50</sub> values. The greatest difference was present for toxicity against ethaboxam in isolates of *P. syringae* where CV isolates were 6.8 or 8.2 times more sensitive than those from VE or the IE, respectively, and it



remains to be determined if this difference will affect fungicide performance. Our population genomic analyses indicated that isolates less sensitive to ethaboxam or mandipropamid had slightly different genetic backgrounds, and therefore, reduced sensitivity to each of these fungicides likely emerged multiple times independently. Smaller but significant differences (~1.5x) were observed for toxicity against mandipropamid in *P. citrophthora*. For sensitivity of *P. citrophthora* to mandipropamid and sensitivity of *P. syringae* to ethaboxam, reduced sensitivity phenotypes were found to be strongly correlated with genotypic differences. While resistance to mefenoxam has been observed in other species of *Phytophthora*, and resistance to potassium phosphite has been identified in isolates of *P. citrophthora* and *P. syringae* from the CV, no isolates of either species from the IE or VE were categorized as resistant. Furthermore, sensitivity phenotypes did not appear to correlate with observed genotypic differences.

The information obtained in this study could be used to predict resistance potential for these two *Phytophthora* species in the geographic regions where they were collected. For example, because of often higher EC<sub>50</sub> values in IE and VE isolates of *P. citrophthora* for mandipropamid and of *P. syringae* for ethaboxam, these species are possibly at higher risk for resistance development to these respective fungicides. Population structure analyses indicated that these regional isolates were mostly genetically distinct from CV isolates, and usage of these fungicides may favor selection of resistance if these fungicides are over-used. The sensitivity of isolates of *P. citrophthora* to mandipropamid and of *P. syringae* to ethaboxam should be closely

monitored once these fungicides are in commercial use on citrus especially in the IE and VE regions that are at higher risk.

In the last chapter of this dissertation, the fungicide mandipropamid was found to be taken up by roots and have limited acropetal mobility in citrus plants. For this, mandipropamid concentrations in root, stem, and leaf tissue extracts were determined after soil application to potted citrus seedlings using bioassays and high-performance liquid chromatography-tandem mass spectroscopy (HPLC-MS/MS). Uptake of mandipropamid in comparison with oxathiapiprolin and mfenoxam was evaluated in additional studies. Split-root citrus plants where the root system of a single plant was divided and grown in two separate pots that could be treated and watered independently were cultivated in the greenhouse, and a fungicide solution was added to one of the pots. In additional field studies, one side of the trunk basin of mature trees was treated, while the other side only received water. Fungicide concentrations were then determined by bioassays and HPLC-MS/MS in roots of treated and untreated sides of plants or trees.

The results indicated that mandipropamid was taken up by the roots when applied to the soil of citrus seedlings, and small amounts were also detected in stem and leaf tissues. Concentrations of mandipropamid detected in these tissues were high enough to inhibit growth of *Phytophthora* species causing root rot of citrus in California based on reported mean EC<sub>50</sub> values for mycelial growth inhibition of *P. citrophthora* and *P. nicotianae*. Results from the split-root study demonstrated no basipetal phloem-based mobility of mandipropamid from treated to untreated roots. In the field study with mature trees, very low levels of mandipropamid were detected in untreated roots eight weeks

after application. This was attributed, however, to root system architecture (e.g., roots originating from the treated side of the trunk basin growing into the untreated side) or diffusion of fungicide in the soil with irrigations over the course of the experiment. In contrast, mefenoxam was detected at inhibitory concentrations also in roots of the untreated side starting 2 weeks after application. Uptake of mandipropamid into roots was proportionally higher than for oxathiapiprolin but lower than for mefenoxam. Furthermore, mefenoxam and oxathiapiprolin were detected in roots sooner after application than mandipropamid, indicating a more rapid uptake of the former two fungicides.

Soil applications of mandipropamid have been registered on citrus for management of Phytophthora root rot of nursery container plants, and the findings of uptake and persistence in the roots support this usage. The mode of action of mandipropamid is different from other registered fungicides (i.e., ethaboxam, fluopicolide, oxathiapiprolin, mefenoxam, potassium phosphite), and therefore its use fits well into a resistance management program with a different mode of action applied in nurseries than subsequently in the field. Registration of ethaboxam (FRAC Code 22), fluopicolide (FRAC Code 42), and oxathiapiprolin (FRAC Code 49) will allow rotations and tank mixtures also with mefenoxam (FRAC Code 4) and potassium phosphite (FRAC Code 07/33) in field soil applications to prevent root rot and the selection of resistant strains. Still, the registration of mandipropamid in a premixture with oxathiapiprolin for foliar application in the field will provide the highest level of brown rot management of citrus and be an excellent strategy for preventing the selection of resistant strains.